UNIVERSITÀ
DI SIENA
1240

DEPARTMENT OF BIOTECHNOLOGY, CHEMISTRY AND PHARMACY

Ph.D Program in Chemical and Pharmaceutical Sciences

-XXXV CYCLE-

In search of new antiviral targets: Design and synthesis of new inhibitors of ZIKV Mtase and potential inhibitors of IMPDH

SCIENTIFIC-DISCIPLINARY AREA: **CHIM/08**

Tutor: **Prof. Federico Corelli**

Doctoral candidate: **Martina Gerace**

Academic year: 2021/2022

Abstract

Viral infections are a leading cause of death worldwide. In 2016, WHO declared a public health emergency due to the spread of the Zika virus (ZIKV). In addition, the recent link between this infection and the clustered incidence of microcephaly and other neurological disorders represents a public health emergency of international significance. An effective strategy to address this emergency could be the identification and development of new antiviral agents against the NS5 protein of ZIKV that specifically target the methyltransferase (Mtase) domain. When this enzyme is blocked, the virus cannot cap the RNA and evade restriction by the host's innate immune system, preventing it from replicating. In this work, a new series of antiviral compounds that are easy and reproducible to prepare were designed and synthesized. They were endowed with antiviral activity on ZIKAV-infected cells and the most active of them were screened for their absorption, distribution, metabolism, and excretion (ADME) properties *in vitro*.

In the second part of this work, a new compound, a potential inhibitor of the enzyme IMPDH, was designed and synthesized: IMPDH plays an important role in antiviral and anticancer processes as it catalyzes the rate-limiting step in the de novo biosynthesis of guanine nucleotides and can therefore be considered a strategic target for the development of novel antiviral compounds.

The last part of the thesis explains the work carried out during the stay abroad at RWTH Aachen University, where the synthesis of an S-allenylsulfoximine derivative was studied: thanks to the allenyl group these compounds can be very useful in organic chemistry when it comes to the incorporation of new units and also, thanks to the sulfoximine moiety can also be used in pharmaceutical chemistry by taking advantage of their important properties.

Contents

INDEX OF FIGURES

INDEX OF SCHEMES

INDEX OF TABLES

CDC	Centers for Disease Control and Prevention
DNA	Deoxyribonucleic acid
RNA	Ribonucleic acid
ATP	Adenosine triphosphate
mRNA	Messenger RNA
HIV	Human immunodeficiency virus
ZIKV	Zika Virus
ER	Endoplasmic reticulum
dsRNA	double-stranded RNA
ssRNA	single-stranded RNA
RdRp	RNA-dependent-RNA-Polymerase
MTase	Methyltransferase domain
DENV	Dengue Virus
SAM	S-adenosyl methionine
GTP	Guanosine-5'-triphosphate
WNV	West Nile Virus
EDC	1-Ethyl-3-(3-dimethylaminopropyl)carbodiimide
HOBT	Hydroxybenzotriazole
DIPEA	N,N-Diisopropylethylamine
DCC	N,N'-Dicyclohexylcarbodiimide
DMF	Dimethylformamide
TMEDA	N,N,N',N'-tetramethylethylenediamine
PBS	Phosphate-buffered saline
TLC	Thin layer chromatography
MS	Mass spectra
MTT	3-(4,5-dimethylthiazol-2-yl)-2,5-diphenyltetrazolium bromide
IC_{50}	Half maximal inhibitory concentration .
SAR	Structure-activity relationship
CC_{50}	Cytotoxic concentration
TEA	Triethylamine
THF	Tetrahydrofuran
r.t.	Room temperature
ADME	Absorption, distribution, metabolism excretion
Papp	Passive membrane permeability
PAMPA	Parallel artificial membrane permeabilità
NMR	Nuclear magnetic resonance
DMSO	Dimethylsulfoxide
DCM	Dichloromethane
ACN	Acetonitrile
δ	Chemical shift
XMP	Xantosine monophosphate
IMP	Inosine monophosohate
IMPDH	Inosine 5-monophosphate dehydrogenase enzyme
TOSMIC	Toluenesulfonylmethyl isocyanide
BET	Bromodomain and extra-terminal domain
PIDA	(Diacetoxyiodo)benzene

Chapter 1

INTRODUCTION

1. VIRUSES

According to the CDC (Centers for Disease Control and Prevention), "a parasite is an organism that lives on or in a host organism and feeds at the expense of its host.[1] Viruses are microscopic parasites because their genomes do not encode all the proteins needed for replication. They are typically much smaller than bacteria, ranging in diameter from 20 to 300 nanometers.[2] As obligate intracellular parasites, they are completely dependent on the complicated biochemical machinery of eukaryotic or prokaryotic cells to generate new infectious particles called virions during replication. The main purpose of a virus is to introduce its genome into the host cell to enable its expression (transcription and translation) by the host cell.

When we hear the word "virus," we think of disease-causing pathogens such as the common cold, influenza, chickenpox, human immunodeficiency virus (HIV), SARS-CoV-2, and others. Instead, they also perform many important functions for humans, plants, animals and the environment: for example, some viruses protect the host from other infections. Viruses are also involved in the process of evolution by transferring genes between different species.[3]

1.1 VIRUS REPRODUCTIVE CYCLE

The production of new virions can only occur within a cell The viral replication cycle can cause dramatic biochemical and structural changes in the host cell that can lead to cellular damage. These changes, called cytopathic effects, can alter cell function or even destroy the cell. Some infected cells, such as those infected by the common cold virus known as rhinovirus, die by lysis (bursting) or apoptosis (programmed cell death or "cell suicide"), releasing all of the viruses' progeny at once. Symptoms of viral diseases result from the immune response to the virus, which attempts to control and eliminate the virus from the body, and from cellular damage caused by the virus. Many animal viruses, such as HIV (Human Immunodeficiency Virus), leave infected immune system cells through a process known as budding, in which virions leave the cell one at a time. During the budding process, the cell is not lysed and is not immediately killed. However, damage to the cells that the virus infects may prevent the cells from functioning normally, even if they remain alive for a period of time. Most productive viral

infections follow similar steps in the viral replication cycle: attachment, invasion, uncoating, replication, assembly, and release .[4]

Attachment

A virus attaches to a specific receptor site on the host cell membrane via attachment proteins in the capsid or via glycoproteins embedded in the viral envelope. The specificity of this interaction determines the host (and cells within the host) that can be infected by a particular virus. You can think of it as having multiple keys and multiple locks, with each key fitting only one specific lock.

Entry

The nucleic acid of bacteriophages enters the host cell naked, leaving the capsid outside the cell. Plant and animal viruses can enter by endocytosis, in which the cell membrane surrounds and engulfs the entire virus. Some enveloped viruses enter the cell when the viral envelope fuses directly to the cell membrane. Once the virus is inside the cell, the viral capsid is degraded and the viral nucleic acid is released, which is then available for replication and transcription.

Replication and Assembly

The replication mechanism depends on the viral genome. DNA viruses typically use host cell proteins and enzymes to make additional DNA, which is transcribed into messenger RNA (mRNA) that is then used to direct protein synthesis. RNA viruses generally use the RNA core as a template for the synthesis of viral genomic RNA and mRNA. The viral mRNA instructs the host cell to synthesize viral enzymes and capsid proteins and to assemble new virions. Of course, there are exceptions to this pattern. When a host cell does not provide the enzymes required for viral replication, viral genes provide the information to direct the synthesis of the missing proteins. Retroviruses such as HIV have an RNA genome that must be transcribed into DNA, which is then incorporated into the host cell's genome. In order to convert RNA to DNA, retroviruses must contain genes that encode the virus-specific enzyme reverse transcriptase, which transcribes an RNA template into DNA.[5] Reverse transcription never occurs in uninfected host cells; the required enzyme, reverse transcriptase, is only obtained by expressing viral genes in infected host cells. The

fact that HIV produces some of its own enzymes that are not found in the host has allowed researchers to develop drugs that inhibit these enzymes. These drugs, including the reverse transcriptase inhibitor zidovudine,[6] inhibit HIV replication by reducing the activity of the enzyme without affecting host metabolism. This approach has led to the development of a variety of drugs to treat HIV and has been effective in reducing the number of infectious virions (copies of viral RNA) in the blood to undetectable levels in many HIV-infected individuals.

Egress

The last stage of viral replication is the release of the new virions produced in the host organism. They are then able to infect neighboring cells and repeat the replication cycle. As you have already learned, some viruses are released when the host cell dies, while other viruses can leave infected cells by budding through the membrane without directly killing the cell[7].

1.2 STRUCTURE

Viral particles are designed for effective transfer of the nucleic acid genome from one host cell to another. The simplest virions consist of two basic components: Nucleic acid (single- or double-stranded RNA or DNA) and a protein coat, the capsid, which acts as a shell to protect the viral genome from nucleases and, during infection, binds the virion to specific receptors on the potential host cell. The capsid proteins are encoded by the viral genome. Due to its limited size, the genome encodes only a few structural proteins (in addition to non-structural regulatory proteins involved in virus replication).[8] Capsids are formed as single or double protein shells and consist of only one or a few structural protein species. Therefore, multiple protein copies must self-assemble to form the continuous three-dimensional capsid structure. The self- assembly of the viral capsid follows two basic patterns: helical symmetry, in which the protein subunits and nucleic acid are arranged in a helix, and icosahedral symmetry, in which the protein subunits assemble into a symmetrical shell covering the nucleic acid-containing core[9].

Only a few groups of viruses use DNA. Most viruses hold all their genetic information in single-stranded RNA. There are two types of RNA-based viruses. In most, the genomic RNA is called plus strand because it serves as messenger RNA for direct synthesis (translation) of the viral protein.

However, a few have negative RNA strands. In these cases, the virion has an enzyme called RNA-dependent RNA polymerase (transcriptase) that must first catalyze the production of complementary messenger RNA from the virion's genomic RNA before viral protein synthesis can occur.
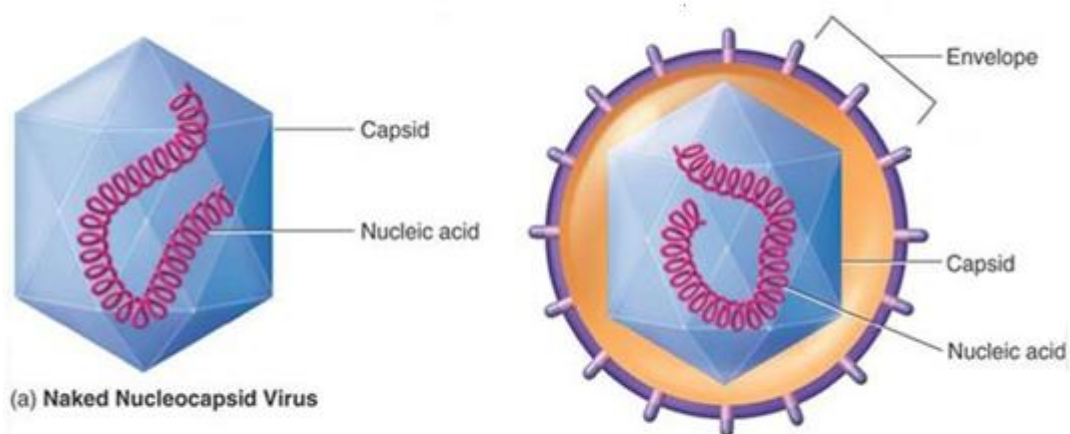
Figure 1. Structure of naked or enveloped viruses

2. VIRAL ENVELOPE

In addition to the capsid and genome, many viruses contain other structural elements that have already been described. Such virus particles have an envelope consisting of a host cell-derived viral membrane, but they differ considerably in size, morphology, and complexity.[10] The envelopes, which protect the genetic material in the virus life cycle as it travels between host cells, form the outermost layer of enveloped viruses and are composed mainly of lipids. The exact composition of the lipids is variable and some proteins, most of which are glycoproteins, are embedded in the membrane: they can help the viruses evade the host immune system.[11] The glycoproteins on the surface of the envelope serve to identify and bind to receptor sites on the host membrane. The viral envelope then fuses with the host membrane, allowing the capsid and viral genome to enter and infect the host.

There are many differences between enveloped and naked viruses. First, the envelope structure gives the virus the ability to enter the host cell by fusion and exit by budding without compromising the integrity of the cell. Naked viruses exit the cell by lysis of the cell membrane,

causing cell death. Egress via the cellular machinery and avoidance of cellular damage allows signals from the immune response to be prevented, thus increasing the spread of the virus.

In addition, the membrane envelope is able to hide structurally restricted capsid antigens from circulating antibodies: envelope proteins on the surface of a virus are structurally more flexible than capsid proteins because they are not part of a rigid capsid structure; therefore, enveloped viruses are better able to escape a neutralizing immune response than their non-enveloped counterparts. These structures also determine the stability properties of the virus particle, such as resistance to chemical or physical inactivation. Envelope membranes are sensitive to desiccation, alcohols, heat and detergents, which limit the survival of virus particles outside host cells.[12]

So why do some viruses have a membrane envelope and others do not? Plants, fungi, protists, algae, and bacteria have a cell wall as a robust layer surrounding the cell membrane. The cell wall has a number of functions: It acts as a selective filter, is involved in maintaining cell shape, and also provides structural support to resist internal osmotic pressure. Therefore, the cell wall provides a rigid and strong barrier to the entry and exit of viruses. Viruses cannot enter by endocytosis or exit by budding. In contrast, animal cells have no cell walls and are surrounded by a lipid bilayer that allows virus entry by endocytosis and exit by budding. Thus, enveloped viruses infect cells without cell walls, whereas naked viruses can infect cells with and without cell walls, although most of their hosts are equipped with walls. These observations suggest that the envelope structure is the result of an adaptation that allows viruses to infect animal cells, while non-enveloped viruses are the result of an adaptation to the evolution of the cell wall.[13]

Another observation that underscores how the envelope membrane is the result of evolution is that the common denominator of organisms with cell walls is the lack of an adaptive immune system, which, in contrast, is an essential feature of animal organisms. Through the adaptive immune system, animal organisms are able to protect themselves from a particular imagined pathogen and have virtually unlimited ability to recognize pathogens, whereas innate immunity recognizes pathogens in a generic manner. In this context, enveloped viruses can exploit the ability to adapt to different cell types by expressing multiple viral receptors than on a single capsid. The appropriation of a host membrane is also useful for masquerading as a normal cell and being invisible to the immune system.[14]

Examples of enveloped viruses include ones that cause notorious diseases in humans, such as COVID-19, Influenza, Hepatitis B and C, Hemorrhagic Fever (Ebola Virus Disease) and Zika Fever (ZIka Virus Disease).

3. ZIKA VIRUS

Zika virus (ZIKV) belongs to the Flaviviridae family of viruses and was first isolated from a primate in the Zika forest in Uganda in 1947.[15] This virus is similar to other viruses in the Flaviviridae family, including yellow fever virus, dengue virus, and West Nile virus, which cause febrile illness and skin rashes. It is transmitted to humans through the bite of Aedes aegypti mosquitoes. However, there is also a risk of infection through sexual activity and blood transfusions.[16]
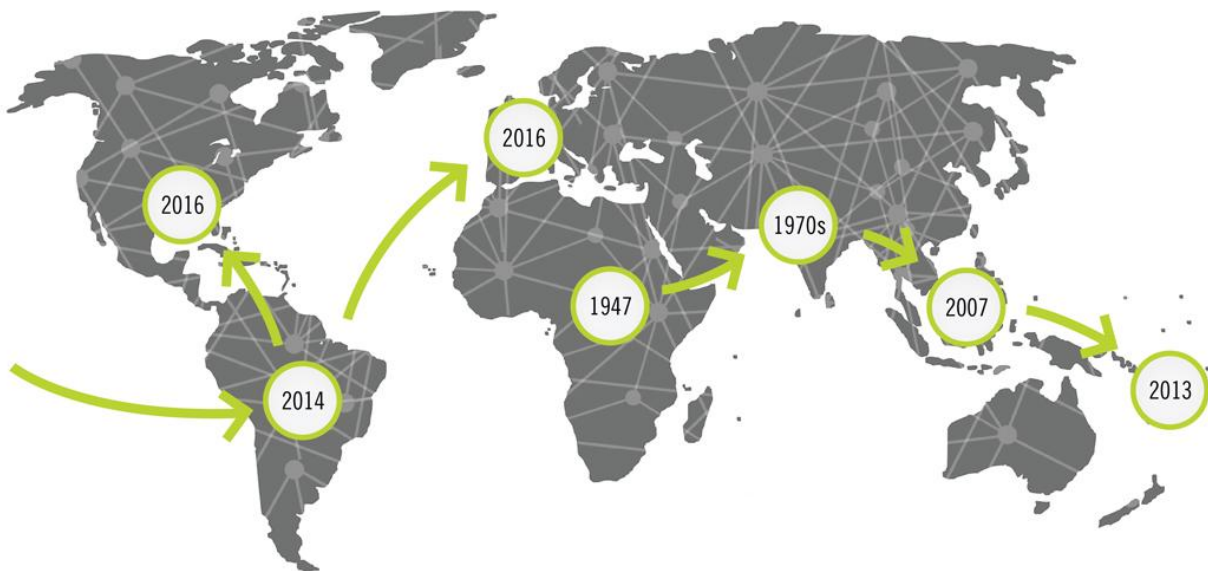
Figure 2. Spread of Zika Virus all over the world

As shown in Figure 2, ZIKV spread to India, Pakistan, and Indonesia in 1970, then to Micronesia in 2007, and finally to the United States in 2016. That year, the World Health Organization declared that "the recent association of Zika infections with the clustered occurrence of microcephaly and other neurological disorders represents a public health emergency of international concern".[17]

Although ZIKV typically causes only mild or no symptoms in adults, ZIKV infection in pregnancy during the 2015-2016 outbreak resulted in a spectrum of disease in infants, including birth defects and neurodevelopmental disorders identified in childhood.[18] Congenital ZIKV syndrome is a pattern of birth defects that includes severe microcephaly (Figure 3a), thinning of the cerebral cortex with subcortical calcifications, macular scars and retinal spots, congenital contractures, and

hypertension. Infants with congenital ZIKV syndrome may develop seizures, hearing and visual disturbances (uveitis), feeding difficulties, and gross motor abnormalities, including Guillain-Barré syndromes (Figure 3b and 3c).[19]
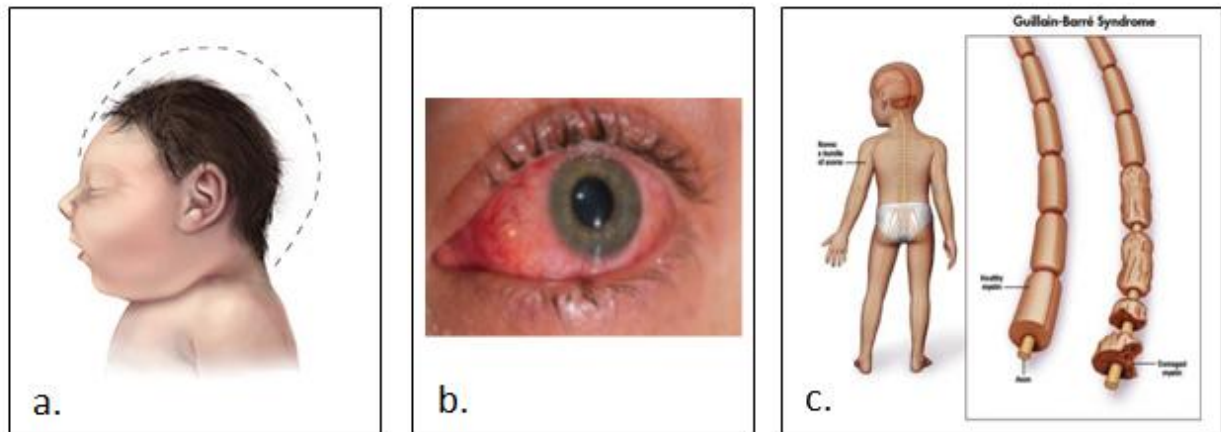
Figure 3. Consequence of Zika Virus infection: microcephaly, uveitis and Guillan-Barrè syndroms

Guillain-Barré syndrome is a rare autoimmune disease characterized by progressive damage to nerve cells, resulting in muscle weakness and sometimes paralysis. It can lead to death because the respiratory muscles of the autonomic nervous system are affected. The causal effect of infectious agents on the induction of autoimmunity can be attributed to the similarity between foreign antigens and autoepitopes causing cross-reactivity, also known as molecular mimicry.[20]

3.1 ZIKA REPRODUCTIVE CYCLE
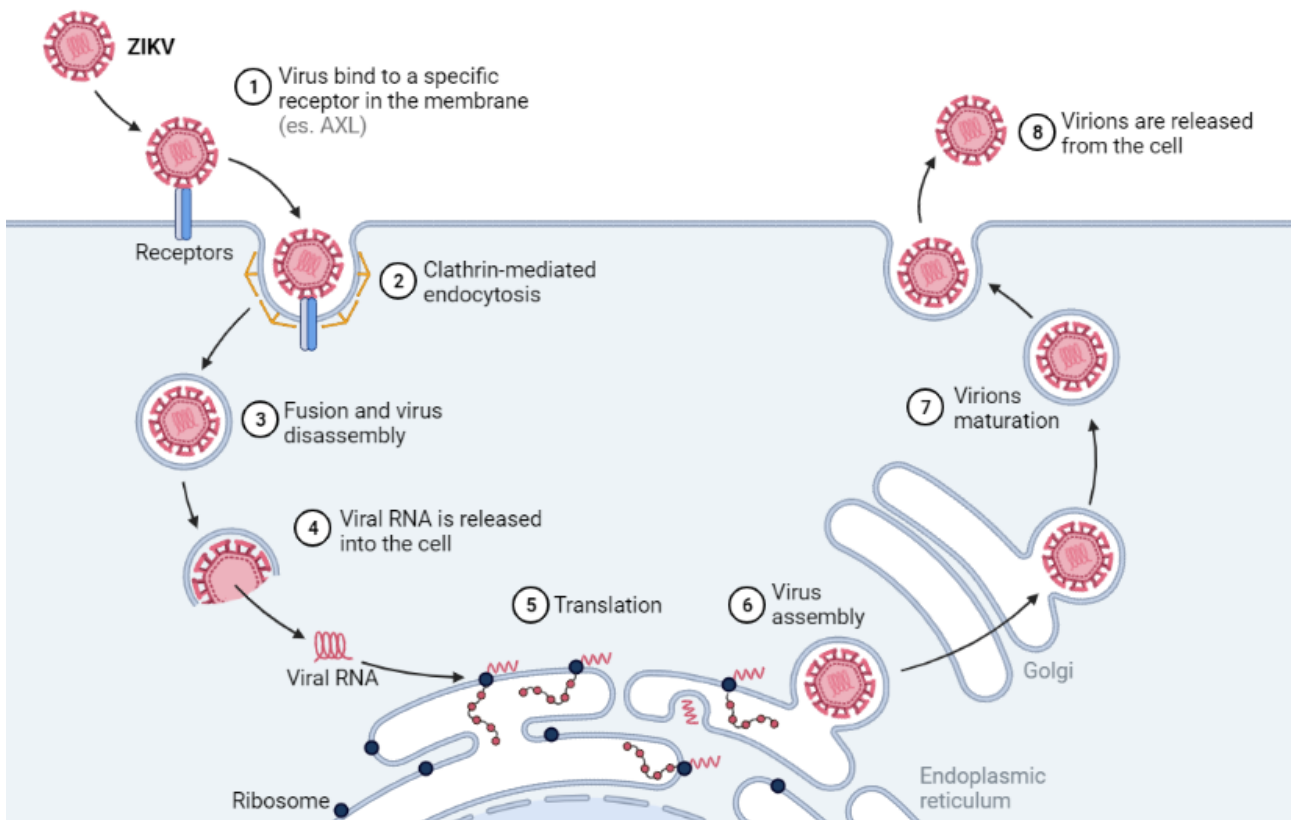
Figure 4. ZikV reproductive cycle

The replication cycle of ZIKV (Figure 4) begins with binding of the virion to the host cell membrane via an envelope protein, clathrin, which promotes endocytosis. After endocytosis, the viral membrane fuses with the endosomal membrane and single-stranded RNA (ssRNA) is unloaded into the host cell cytoplasm. Translation then begins and a polyprotein is cleaved that is involved in the formation of three structural and seven non-structural proteins. The structural proteins are glycoprotein E, protein C, and protein M. The nonstructural proteins NS2A, NS2B, NS3, NS4A, NS4B and NS5 are involved in the formation of a complex at the cytoplasmic level that ensures replication, translation, and post-processing. The nonstructural protein NS1 is involved not only in replication but also in subsequent infection.[21] Replication occurs in the next step in the cytoplasmic viral factories of the endoplasmic reticulum (ER) and generates double-stranded RNA (dsRNA). This dsRNA is transcribed to form additional ssRNAs that assemble into new virions

within the ER. These virions are then transferred to the Golgi apparatus and eventually released into the extracellular spaces where they cause infection of new cells.[22]

3.2 PHARMACEUTICAL TREATMENT

There is no specific treatment or antiviral drug for ZIKV infection. Current treatment recommendations are based on a limited body of evidence. Treatment of symptoms with acetaminophen for fever and pain, an antihistamine for itchy rash, and plenty of fluids is recommended. Treatment with acetylsalicylic acid and nonsteroidal anti-inflammatory drugs is discouraged because of the reported increased risk of hemorrhagic syndrome with other flaviviruse.[23] A proven approach to treating ZIKV infection is drug-repurposing with azithromycin,[24] chloroquine, niclosamide, mefloquine, sertraline, which have demonstrated activity in reducing cell proliferation in vitro.[25]

Potential new drugs are:

- Inhibitors of viral entry into the cell by blocking human receptors used in pathogen recognition;[26]

- Inhibitors of viral endosome-membrane fusion, by acting on intravesicular pH variation;[26]

- RNA-dependent-RNA-Polymerase (RdRp) inhibitors; [27]

- NS2B/NS3 protease inhibitors;[28]

- Novel inhibitors of virion assembly;[26]

- Inhibitors of the methyltransferase (MTase) domain of the NS5 protein.[29]

3.3 NS5 PROTEIN

Viral NS5 protein is the largest (~100 kDa) and most conserved ZIKV protein, with 94% sequence identity between the two major ZIKV lineages: Asian and African. NS5 consists of two domains, an N-terminal methyltransferase domain (Mtase) and an RNA-dependent RNA polymerase (RdRP) domain at the C-terminal end. It fulfils three essential roles in the viral life cycle: genome

replication, interferon suppression, and capping. In addition, recent evidence suggests that it may also play a role in modulating cellular spliceosome activity.[30]
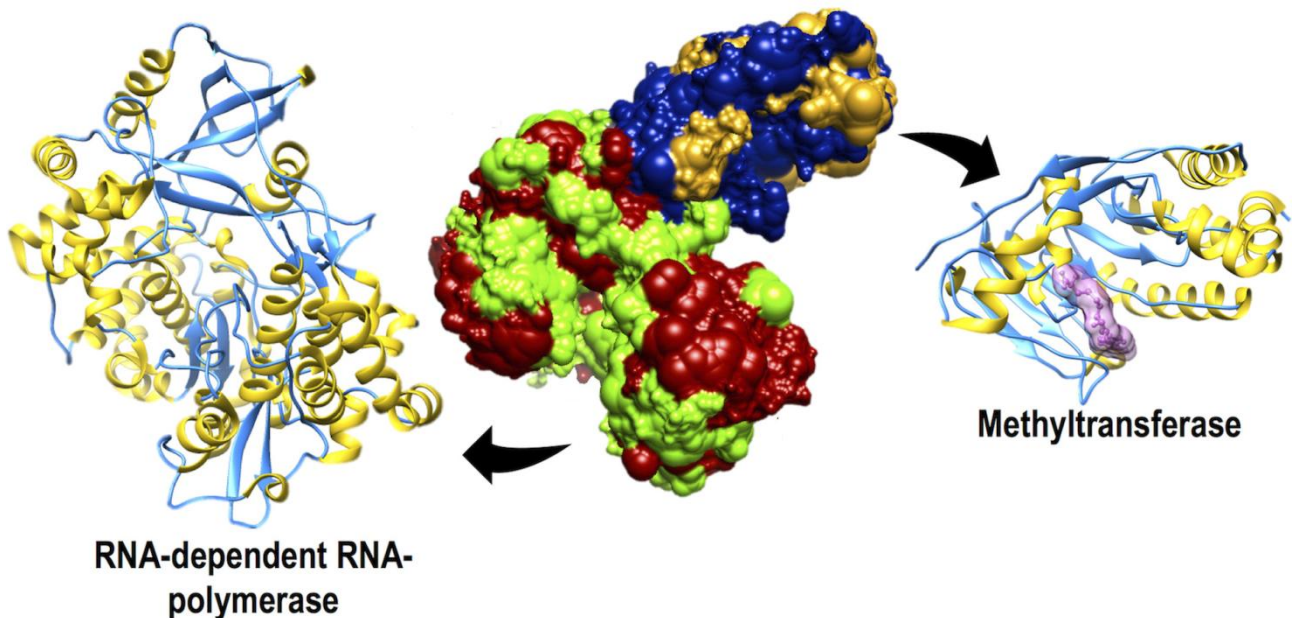
Figure 5. Structure of protein NS5 and its two subdomains, methyltransferase (Mtase) and RdRp

Genome replication

RdRP domain of ZIKV NS5 generates positive- and negative-sense copies of the RNA genome via a de novo mechanism: it uses RNA as a template, but does not require a primer to elongate nascent RNA.[31] It is likely that additional viral factors are also involved in facilitating ZIKV RNA replication as observed in other flaviviruses. For example, ZIKV NS3 encodes a helicase domain essential to unwind the double-stranded (ds) RNA intermediate formed during genome synthesis.[32]

Interferon suppression

Type I interferons (IFN-α and -β) play a crucial role in fighting viral infections. To establish infection, flaviviruses have evolved various immune evasion mechanisms to suppress the IFN type I antiviral responses. Of particular note, both the DENV and ZIKV NS5 proteins inhibit type I interferon responses by binding to and targeting the host transcription 2 signal transducer and activator (STAT2) for proteasome dependent degradation.[33]

Capping

The methyltransferase activity of the N-terminal Mtase domain of NS5 is required for the final 5' capping steps using S-adenosyl-methionine (SAM) as the methyl donor.[34] Based on in vitro evidence, the Mtase domain mediates methylation of the N7 atom of cap guanine and the 2'-O atom of adenine ribose (the first nucleotide of the viral genome) by a two-step reaction.[35] In addition, the N-terminal Mtase serves as a guanylyltransferase, which uses GTP as a substrate to form a covalent NS5-GMP intermediate, followed by transfer of the GMP from NS5 to the end of an acceptor RNA transcript. In particular, formation of the NS5-GMP intermediate can be stimulated by the NS3 helicase.[32]

Due to its importance, Mtase is a very attractive target for the development of new antiviral drugs. Both the N-7-methylguanosine and 2'-O-methyladenosine activities of Mtase have been shown to be essential for viral replication.[36,37] Crystal structure studies revealed that the Mtase core domain consists of SAM -binding pocket, cap- binding site and positive RNA-binding site. Both the SAM binding pocket and the cap binding site of the Mtase have been shown to be essential, making the ZIKV Mtase an attractive target for the design of ZIKV inhibitors.[38] The Mtase activity maximal at pH 8-9 consists of two different methylations, as already mentioned. N-methylation at N7 of guanosine is critical to ensure genome stability and allow recognition of the viral genome by the eukaryotic translation initiation factor eIF4. The O-methylation at 2'-OH of adenosine ribose is involved in masking the virus to the immune system as it prevents recognition of the pathogen by cellular sensors and subsequent activation of the immune response with release of interferons. Experimental tests have shown that blocking only O-methylation leads to an attenuated viral phenotype, while lack of N-methylation leads to instability of the viral genome and thus virus death.[39] Another interesting thing about the MTase domain is that it has a hydrophobic pocket near the SAM binding site: this is absent in human RNA methyltransferase (hRNMT), providing an opportunity for selective inhibition (Figure 6).[40]
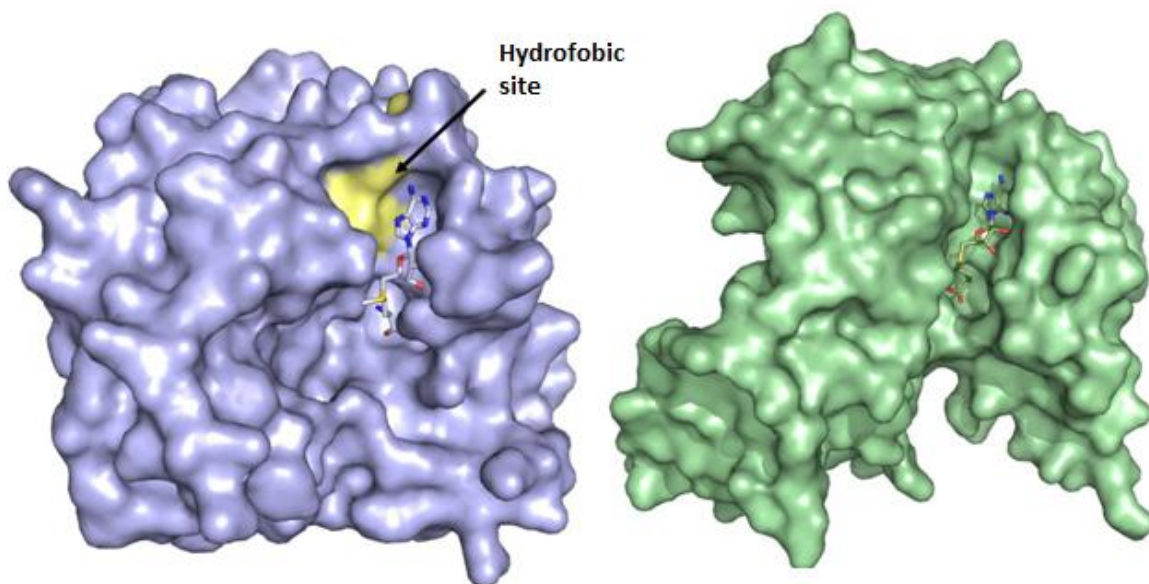
Figure 6. Zika Virus' Mtase (left) and human Mtase (right)

3.4. MTASE INHIBITORS

Inhibitors of ZIKV Mtase can be divided into three types: competitive with RNA, competitive with SAM, and allosteric.

Competitive with RNA

The cap-RNA binding site is one of the two subdomains of the Mtase domain of the NS5 protein, in which it binds viral single-stranded RNA, which is then the substrate for the capping mechanism. This binding site in the Mtase of Zika virus is characterized by a hydrophobic portion formed by alanine and leucine, which have a shorter side chain than the arginine and lysine residues normally found in other Flaviviruses (dengue, West Nile,...) and cause a more open conformation of the site. Inhibitors active at this site are aurintricarboxylic acid,[41,42] nucleosides such as ribavirin triphosphate,[43] compound 10, and 35 (Figure 7).[44]

The RNA cap site tends to be shallow and solvent-exposed, making it difficult to find molecules that interact firmly with this site.
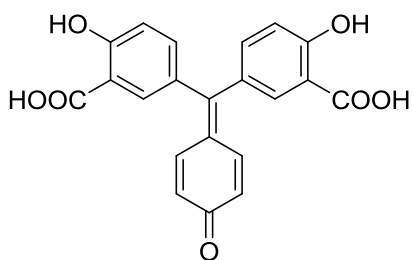
Aurintricarboxilic acid
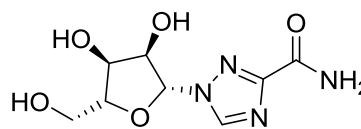
Ribavirin
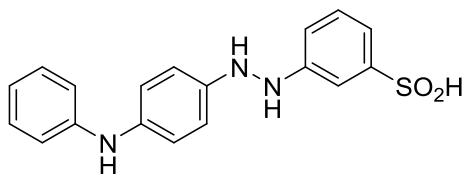
10
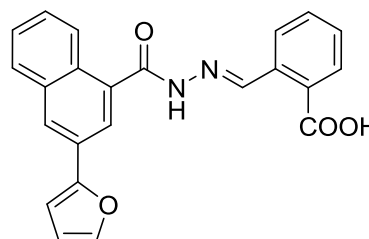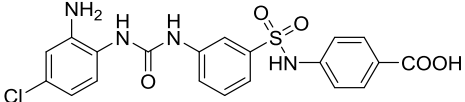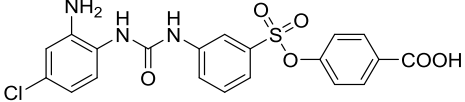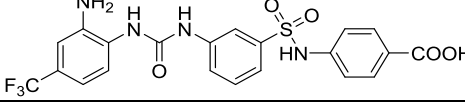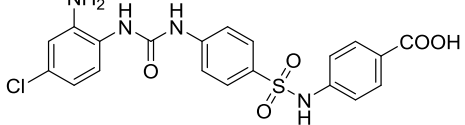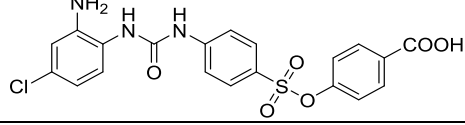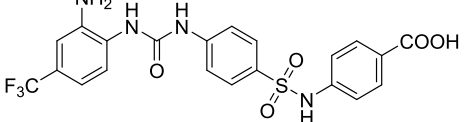
35

Figure 7. Inhibitors of ZikV Mtase competitive with RNA

Allosteric inhibitors

Structural and biochemical analyses indicate that the Mtase of ZIKV shares common structural and functional features with the Mtase of DENV. Therefore, allosteric inhibitors that we can find in the literature were identified as active against West Nile virus (WNV) and DENV and then tested on the Mtase of ZIKV, where they were found to be more active in inhibiting O-methylation than N-methylation (Table 1).[39] These inhibitors were obtained using a computational fragment-based approach.[45] Biological activity is around 100 µM, with better efficacy for WNV than for DENV, although in some cases they show promising activity toward the MTase of ZIKV.

Table 1. Allosteric inhibitors of ZikV Mtase

Structure	ZikV IC50 (µM)	DenV IC50 (µM)	WNV IC50 (µM)
	221 ± 19	452 ± 38	182 ± 7
	33.0 ± 2.7	369 ± 14	120 ± 11
	24.0 ± 1.2	91 ±8	51 ± 2
	87.0 ± 9.7	435 ± 26	299 ± 13
	31.0 ± 6.7	368 ± 11	190 ± 9
	67.0 ± 5.1±	110 ± 11	71 ± 5

Competitive with SAM
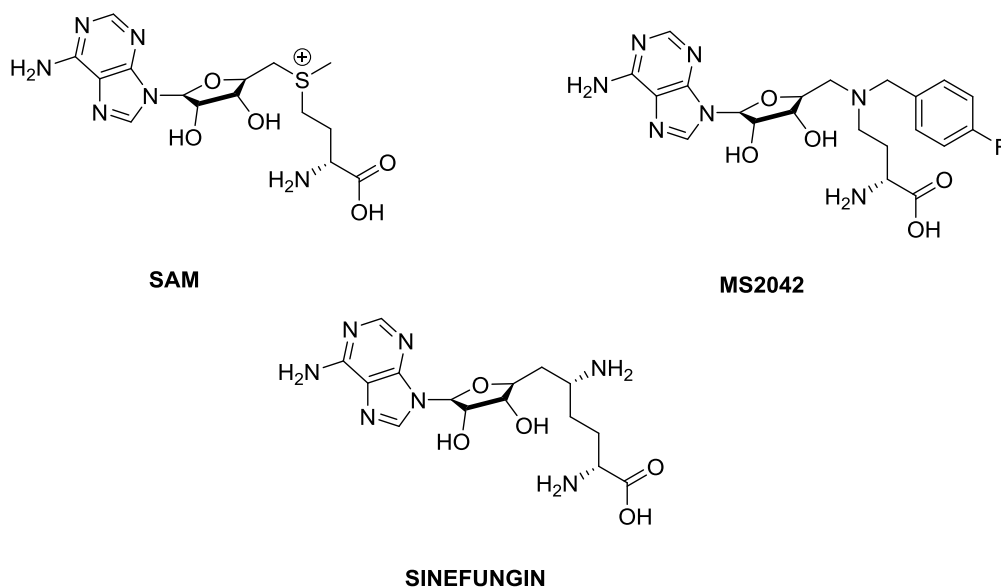
Figure 8. Structure of inhibitors of ZIKV Mtase compettitive with SAM

In 2017, Rinku Jain et al, designed MS2042 (Figure 8) an analogue of S-adenosylmethionine, on the basis of recent high resolution structures of the ZIKV NS5-MTase bound to SAM alone (NS5-MTase$_{SAM}$), or to both SAM and the 5'cap mimic 7-methyl guanosine diphosphate (7-MeGpp, NS5-MTase$_{SAM,7-MeGpp}$). MS2042 was found to be active on ZIKV MTase. The 4-fluorophenyl group of MS2042 extends into a shallow cavity adjacent to the SAM binding pocket (Figure 9).[46]
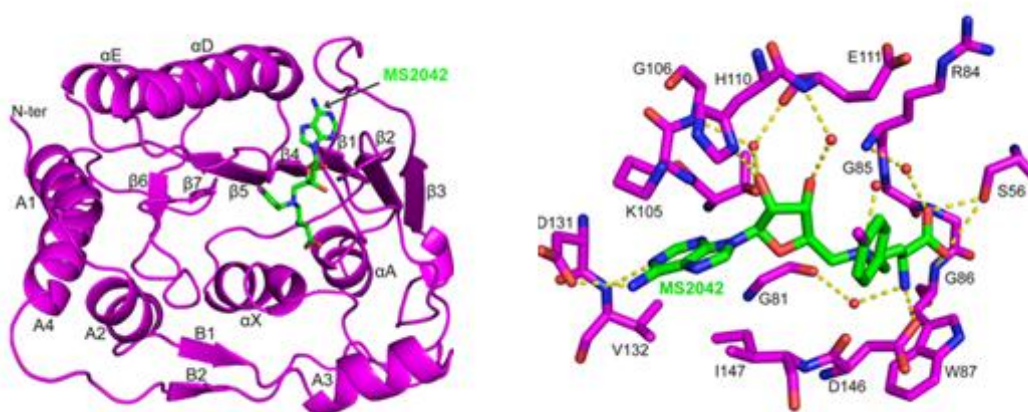
Figure 9. Left: Structure of ZIKAV NS5-MTase; **Right**: Interaction of MS2042 with NS5-MTase

There are no specific hydrogen bonds with any amino acids and the fluorine atom protrudes into the solvent. Most of the contacts between the 4-fluorophenyl group and NS5-Mtase are van der Waals interactions. Most importantly, the shallow cavity containing the 4-fluorophenyl group is

the presumed binding site of the base and the 2'-OH group of adenosine when the RNA binds a flavivirus NS5 methyltransferase.[46]

Hercik et al. reported the crystal structure of Zika virus methyltransferase in complex with the pan-methyltransferase inhibitor sinefungin,[47] an adenosine derivative originally isolated from *Streptomyces griseoleus* by Eli Lilly and Co. as a potential antifungal antibiotic.[48] It is a competitive inhibitor of the natural substrate of numerous Mtases (SAM)[49] and was therefore an interesting starting point for the development of new competitive inhibitors of this fundamental enzyme involved in the Zika virus replication cycle.[47] The activity of sinefungin was promising (4.03 µM), but its limitation was its high cytotoxicity, which makes its administration as a drug impossible, so it is often used as a positive control in enzyme inhibition assays.[38]

Finding inhibitors of Mtase that compete with SAM seems to be a difficult task. The inhibitors described in the literature have shown that it is difficult to find compounds with good toxicity and activity profiles.[50] Based on the literature reports, the main problems in finding analogues of the cofactor as inhibitors are the following:

- Selectivity for the viral enzyme, limiting cytotoxicity;
- High stability of the physiological cofactor at the binding site, which is characterised by a high number of interactions.

In Professor Botta's research group, the enzyme methyltransferase of ZIKV has been studied for years, with particular emphasis on the mode of binding of the cofactor to obtain enzymatic inhibitors competitive with S-adenosylmethionine.

After the in-depth study of the SAM binding mode, a protocol for a virtual screening was developed, consisting of two different approaches.

The first approach consists of performing molecular dynamics of the cofactor at the binding site, from which a pharmacophore model was created for the most populated cluster. The created pharmacophore was used for an initial screening in which molecules with at least 3 features

among the mandatory features and at least 1 feature among the optional features were selected. From the subsequent consensus docking, 3 molecules were selected.

The second approach was developed using the Mtase enzyme crystal (PDB 5M5B), from which a second drug model was obtained, and a second screening was performed. The resulting molecules were subjected to a docking procedure.

A total of 13 molecules were selected from the two approaches, purchased, and biologically evaluated by enzyme inhibition assay: the most active was GP1 with an IC_{50} of 53 µM and a CC_{50} >100 µM (Figure 10).

Starting from GP1 and studing the interactions the molecule does with the binding site usind molecular docking and dynamics, another library of compounds was investigated, looking for possible modifications and different scaffolds to increase activity. Structural semplifications/complications of the phthalimide ring were evaluated and among all the molecules tested, **GP15** proved to be the hit, as it showed an antienzymatic activity of 29 µM.
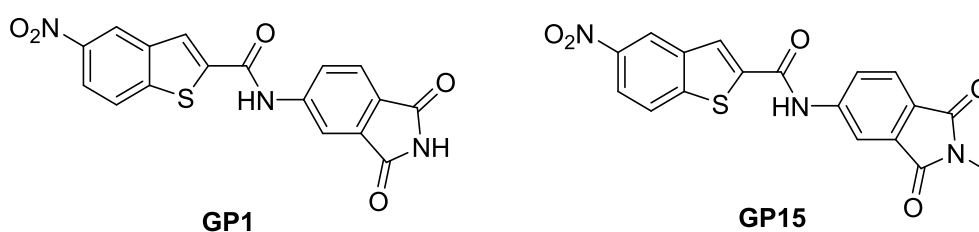
Figure 10. Structure of hit compounds GP1 and GP15

In addition, **GP15** was also tested for its cytotoxic effect, but proved to be non-toxic (CC_{50} > 100 µM), so it is a good starting point for further modifications: its limit is in its solubility (< 0.01 mg/mL in water).

AIM OF THE WORK
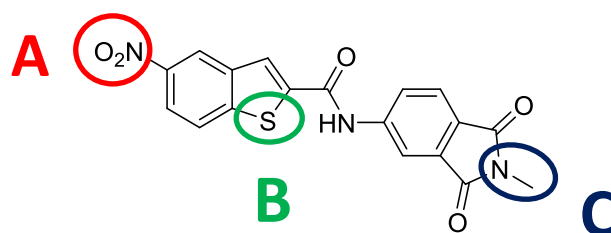
Synthesis of derivatives of GP15

In vitro enzymatic and antiviral assays
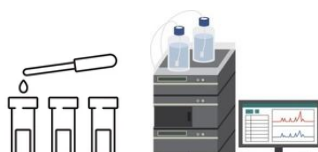
In vitro permeability and stability

The project aimed to investigate the structure-activity relationship through three types of modifications (A, B, and C) to the scaffold of the hit compound. Several derivatives of GP15 were prepared in paralel to increase the activity and solubility. In addition, some derivatives were synthesized with pyrrole and thiophene instead of benzothiophene and some others in which the phthalimide ring was replaced to avoid the difficulty in handling this moiety. The synthesized compounds were tested for their antiviral activity against ZIKV and for their cytotoxicity in

noninfected cells. Most of the active compounds were tested in vitro for their permeability and stability.

CHEMISTRY

1. Modifications in part A

Starting from **GP15**, the first modification was the replacement of the nitro group: it is well known that drugs containing nitro groups can cause serious toxicity,[48] so it was replaced by different units, some smaller, others larger.
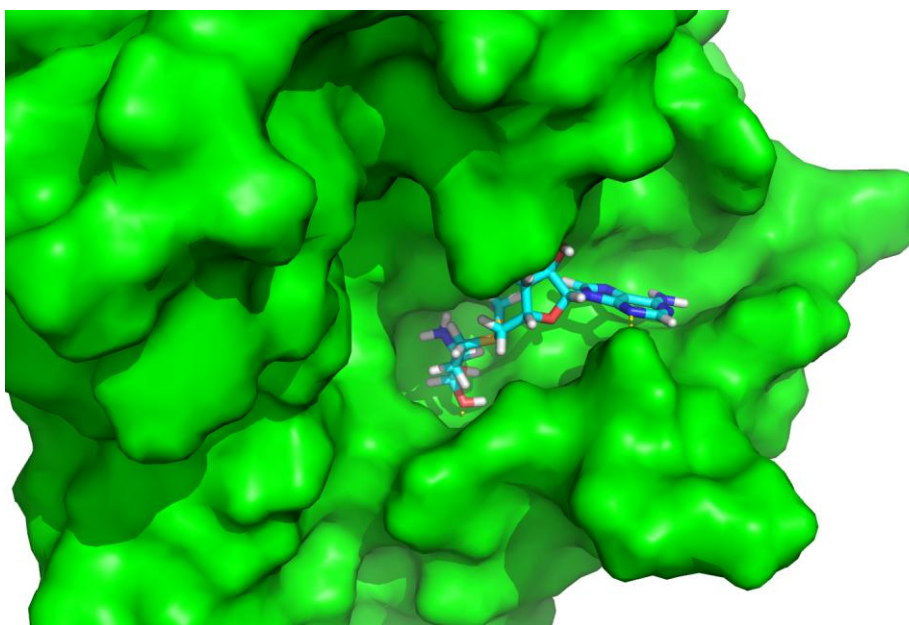
Figure 11. Binding mode of SAM in Mtase domain

Figure 11 shows the binding mode between S-adenosil methionine and the Mtase enzyme: these molecules, competitive with SAM, bind in the same space but **GP15** is smaller than SAM, so it explore just a little part of the enzyme pocket. Replacing the nitro group with a bulkier substituent led to exploration of new areas and other interactions.

Several derivatives were synthesized (Figure 12).

GP15

GP45: R= 5-Br
GP47: R= 5-CN
GP49: R= 5-Ph
GP50: R= 5-(4-CN-Ph)
GP51: R= 7-F
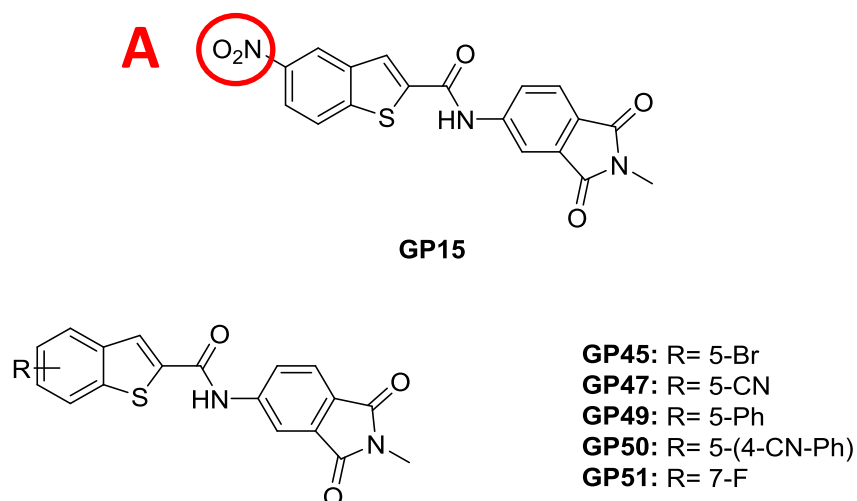
Figure 12. Compounds with modification in part A

The synthesis of these benzothiophene derivatives is shown in Scheme 1.

Starting from the reaction between the suitable 2-chlorobenzaldehydes and ethyl thioglycolate (**1**), the benzothiophenes **2a**, **2b**, and **2c** were obtained, which were subsequently hydrolyzed to give the carboxylic acids **3a**, **3b**, and **3c**. For the other part of the molecules, 4-nitrophthalic anhydride was reacted with methylamine in dry THF at 40 °C for 30 minutes. Then the solvent was removed at vacuum and the crude was stirred at 190 °C for 2 hours to give compound **4**, which was reduced with hydrogen and palladium on carbon to give compound **5** (Scheme 1).
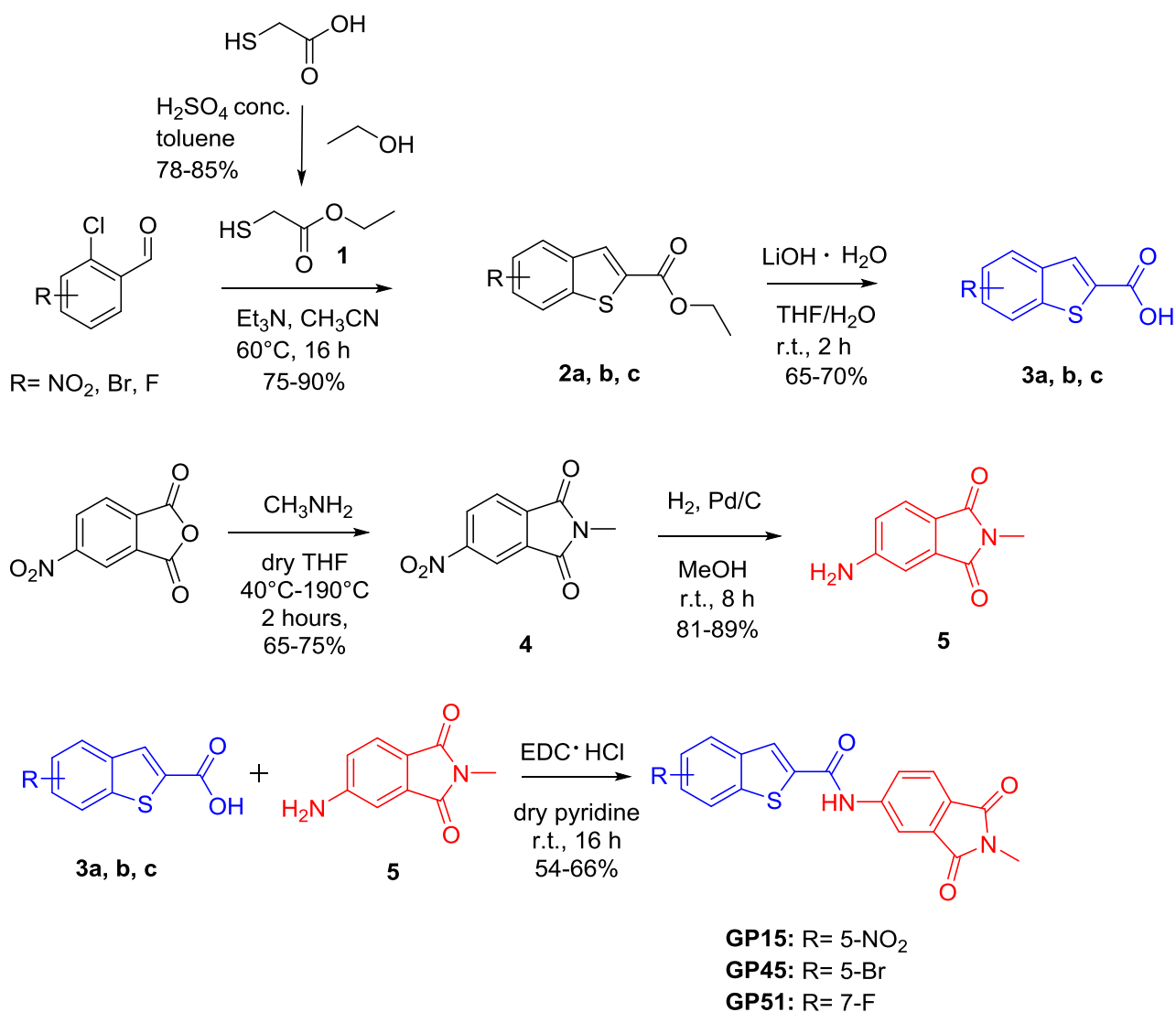
Scheme 1. Synthesis of benzothiophene derivatives

The coupling between compound **3a**, **3b**, **3c** and compound **5** proved to be difficult. Table 2 summarizes all experimental conditions tested. Reaction with common coupling reagents such as EDC, HOBT and DIPEA or DCC in DCM/DMF proved unsuccessful even when the temperature was increased.

The use of thionyl chloride to activate carboxylic acids also did not give the expected results. Finally, reaction with pyridine as solvent and EDC as coupling reagent gave the desired products with a yield of 62-66%.

Table 2. Coupling experiments between compounds **3 a- c** and compound **5**

Entry	3a/3b/3c (eq)	5 (eq)	Coupling Reagents	Time, °C	Solvent	Yield (%)
1	1	1.2	EDC HCl HOBT, DIPEA	12 h, r.t.	dry DCM/ dry DMF	-
2	1	1.2	EDC HCl HOBT, DIPEA	12 h, reflux	dry DCM/ dry DMF	8%
3	1	1.2	DCC, DIPEA	12 h, reflux	dry DCM	-
4	1	1.2	SOCl₂	15 h, reflux	dry DCM	-
5	1	1.2	1)SOCl₂ 2) TEA	15 h, reflux	dry DCM	-
6	1	1	EDC HCl	3 h, r.t.	dry pyridine	66%

To prepare **GP47**, 4-bromo-2-chlorobenzaldehyde was used to install the cyano group with CuCN in refluxing acetonitrile. Then, the coupling reaction was carried out in the same way and the desired compound was obtained (Scheme 2).
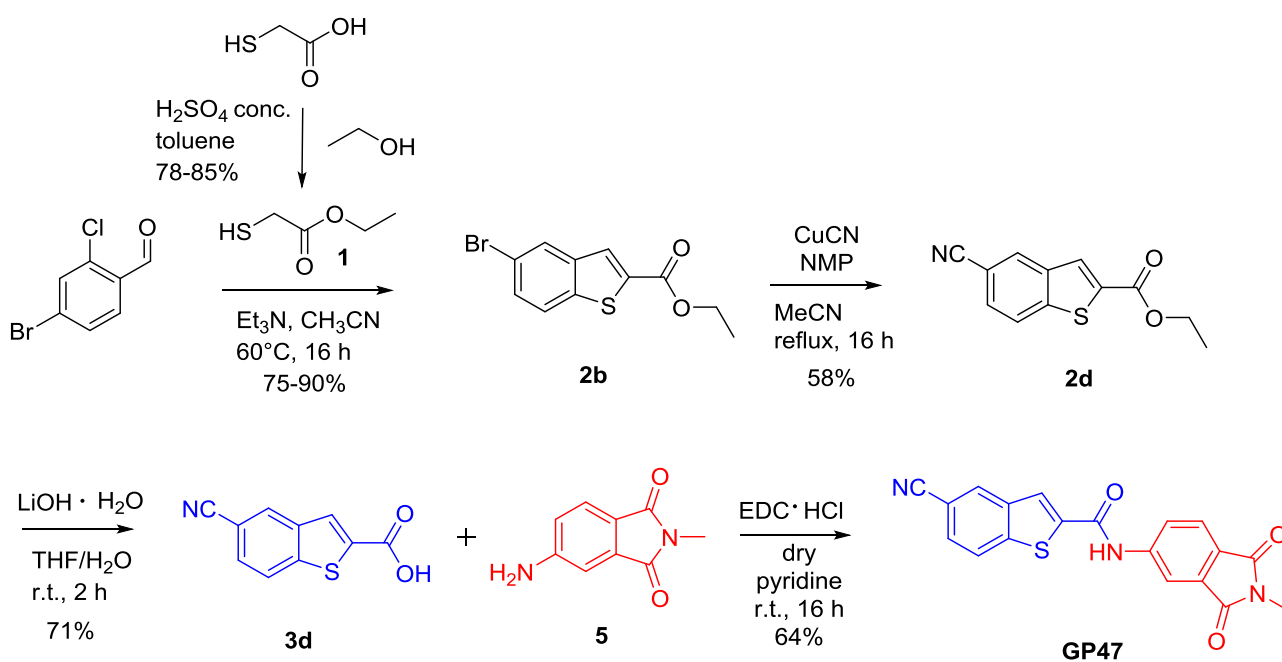
Scheme 2. Synthetic strategy for the synthesis of **GP47**

To prepare benzofurane compounds with bulkier substituents, **GP45** was subjected to a Suzuki reaction with phenylboronic acid or 4-cyanophenylboronic acid in the presence of tetrakis(triphenylphosphine)palladium(0), Na_2CO_3, and LiCl in a mixture of 1,4-dioxane and H_2O to give **GP49** and **GP50**.
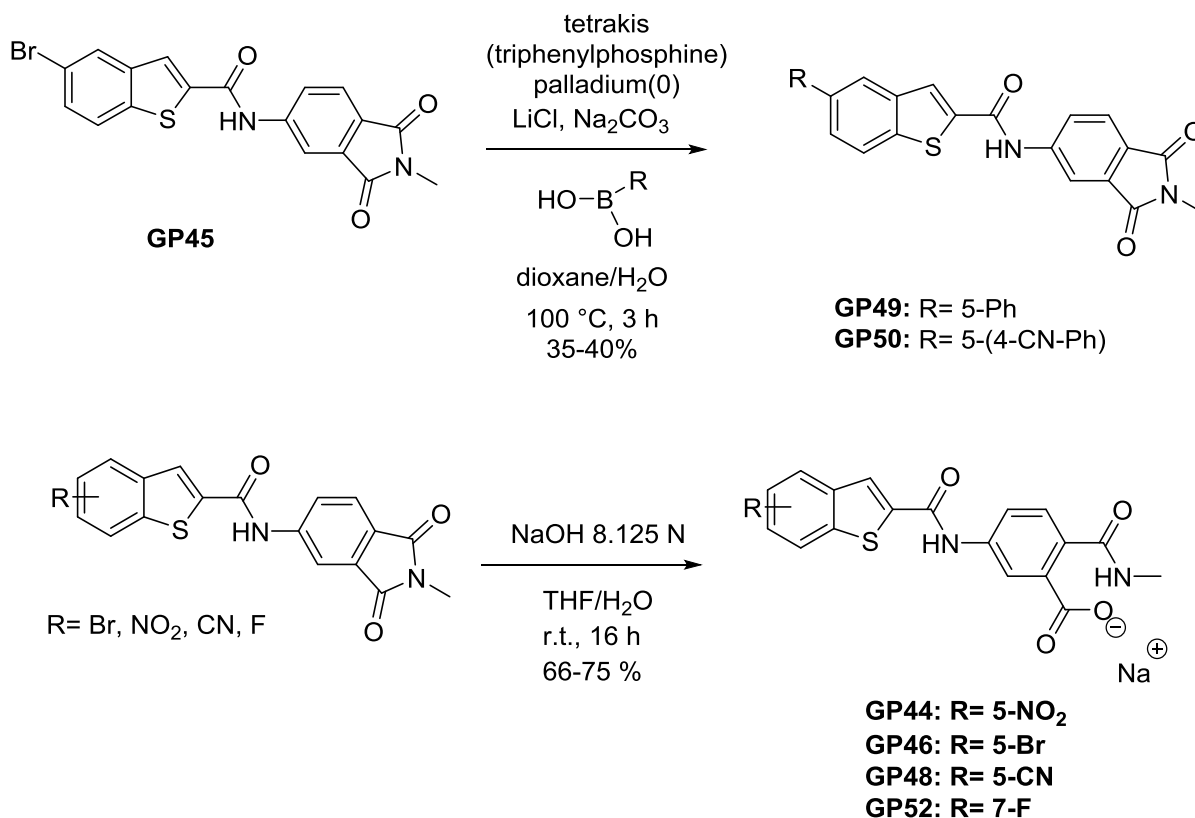
Scheme 3. Synthesis of **GP44**, **GP46**, **GP48, GP49**, **GP50**, **GP52**.

To increase the solubility of the **GP** compounds and to investigate their ability to establish further interactions within the MTase binding site, some molecules were reacted with a solution of NaOH to open the phthalimide ring and salt the newly formed carboxyl group (Scheme 3). To accurately salt the molecules, a NaOH solution was prepared and titrated three times with a 1 N solution of oxalic acid dihydrate to determine the exact normality. This NaOH solution was then reacted with the phthalimido derivatives to generate sodium salts.

2. Modifications in part B

Another modification of the hit compound **GP15** was to replace the benzothiophene heterocycle with indole to increase solubility and also to investigate other interactions that the residue might have with amino acids in the binding site.

GP15

GP53: R_1= 6-F, R_2= Methoxymethyl
GP54: R_1= 6-Br, R_2= Methoxymethyl
GP55: R_1= 6-Br, R_2= H
GP56: R_1= 6-F, R_2= H
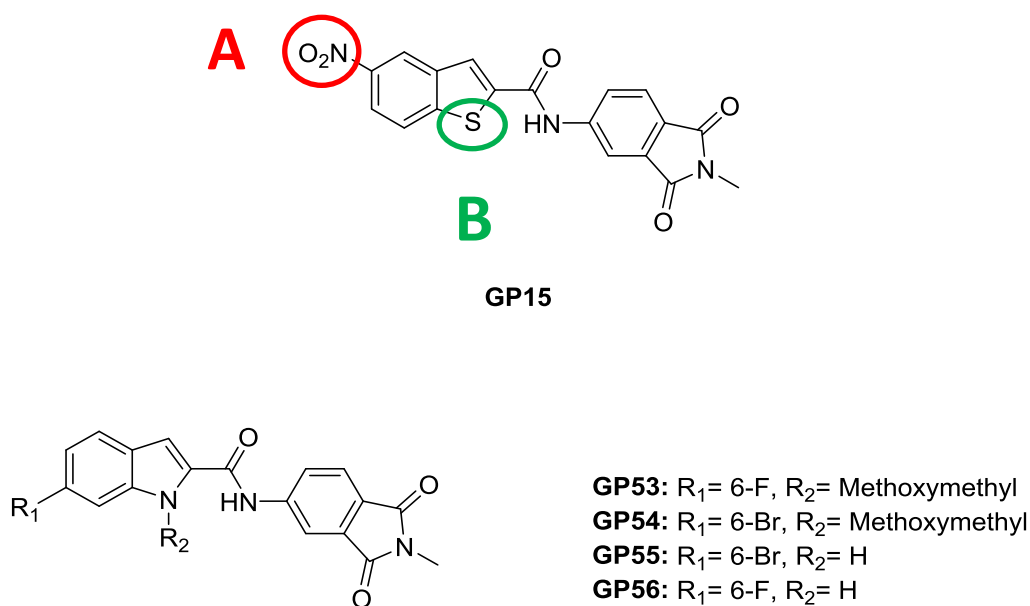
Figure 13. Structure of compounds with modifications in part B

The indole derivatives were prepared according to the synthesis strategy shown in Scheme 4. Starting from the suitable para-substituted aldehyde, compounds **7a** and **7b** were obtained by reaction with ethyl azidoacetate **6** in MeCN at low temperature.
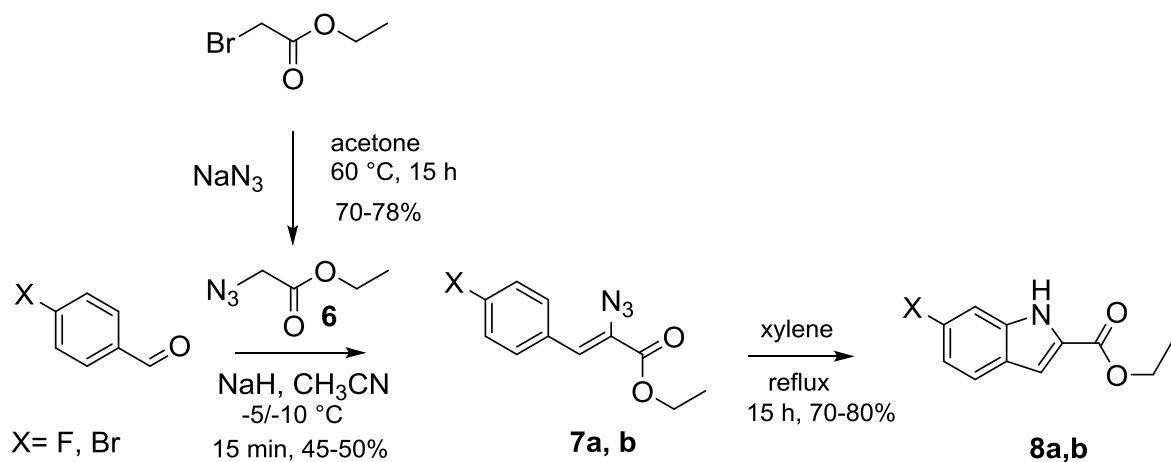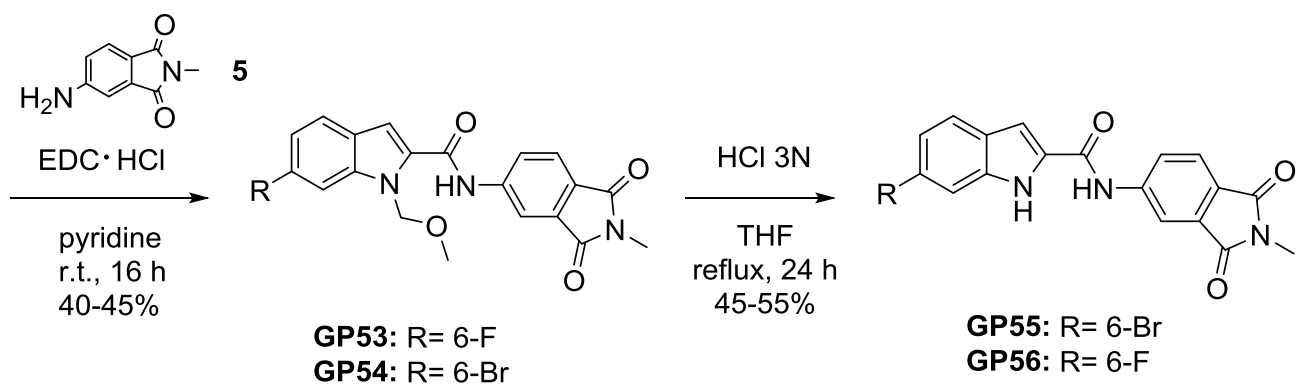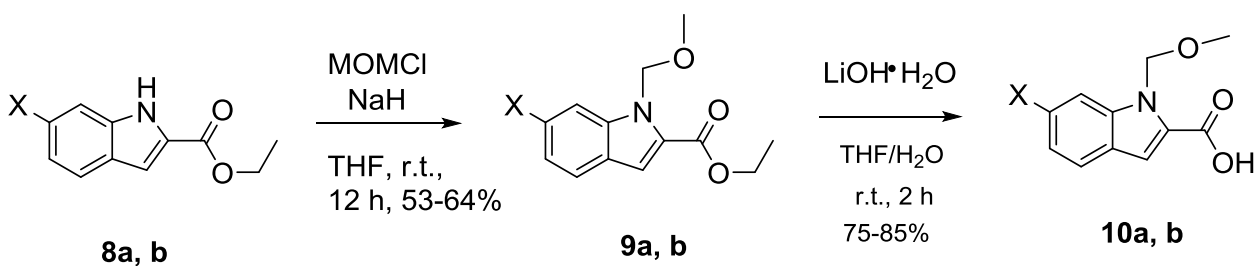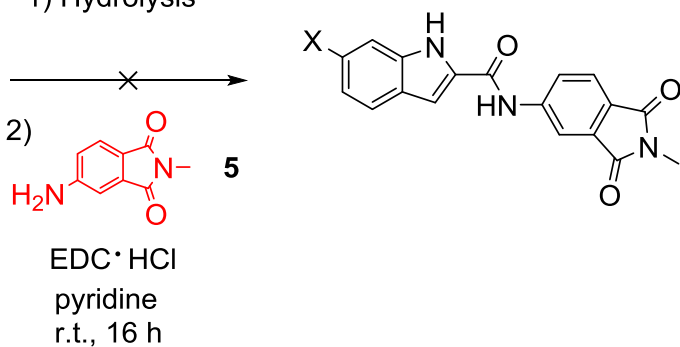
Scheme 4. Synthesis of **GP53**, **GP54**, **GP55** and **GP56**

Subsequently, compounds **7a** and **7b** were dissolved in xylene and heated under reflux to give indoles **8a** and **8b**, which were first hydrolyzed directly and then treated with compound **5** and EDC in pyridine, using the same procedure as for the benzothiophene compounds. However, this approach did not work with indoles and the desired compounds were never obtained in this way. Assuming that the obstacle was perhaps the presence of an acidic hydrogen on the nitrogen of the indole, compounds **8a** and **8b** were protected as methoxymethyl ethers (compounds **9a** and **9b**) and then the esters were hydrolyzed to give the carboxylic acids **10a** and **10b**. Now the coupling with compound **5** was successful and **GP53** and **GP54** were obtained and purified. Removal of the protecting group in acidic medium provided **GP55** and **GP56**.

3. Modification in part C

The last change of the hit compound concerned part C.

GP15

GP57: R= 5-Br; R_1=H; R_2=CH$_3$
GP58: R= 7-F; R_1=H; R_2=CH$_3$
GP59: R= 5-Br; R_1=CH(CH$_3$)$_2$; R_2=H
GP60: R= 7-F; R_1=CH(CH$_3$)$_2$; R_2=H
GP66: R= 5-CN; R_1=H; R_2=CH$_3$
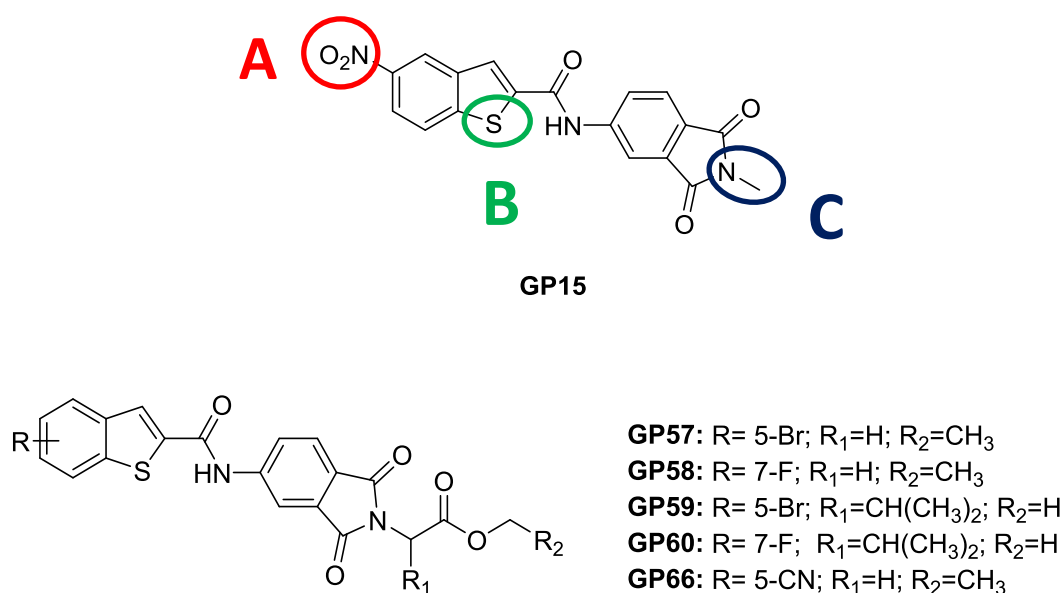
Figure 14. Structure of compounds with modifications in part C

To explore another part of the binding site and to see if other interaction between the molecules and the enzyme can be found, the methyl group was eventually replaced by amino acids, in particular glycine ethyl ester and valine methyl ester. Hydrolysis of the esters was not possible

because the basic/acidic environment required for conversion to an acid also led to breakage of the amide bond of the phthalimide ring.

For the synthesis of compounds shown in Figure 13, 4-nitrophthalic anhydride was reacted with glycine methyl ester or valine methyl ester using acetic acid as solvent at 120 °C. Nitro group was then reduced with H_2 and Palladium on carbon at room temperature. The procedure to form final compounds is the same adopted in the other cases: **GP57**, **GP58**, **GP59**, **GP60** and **GP66** were synthesised.

GP57: R= 5-Br; R_1=H; R_2=CH$_3$
GP58: R= 7-F; R_1=H; R_2=CH$_3$
GP59: R= 5-Br; R_1=CH(CH$_3$)$_2$; R_2=H
GP60: R= 7-F; R_1=CH(CH$_3$)$_2$; R_2=H
GP66: R= 5-CN; R_1=H; R_2=CH$_3$
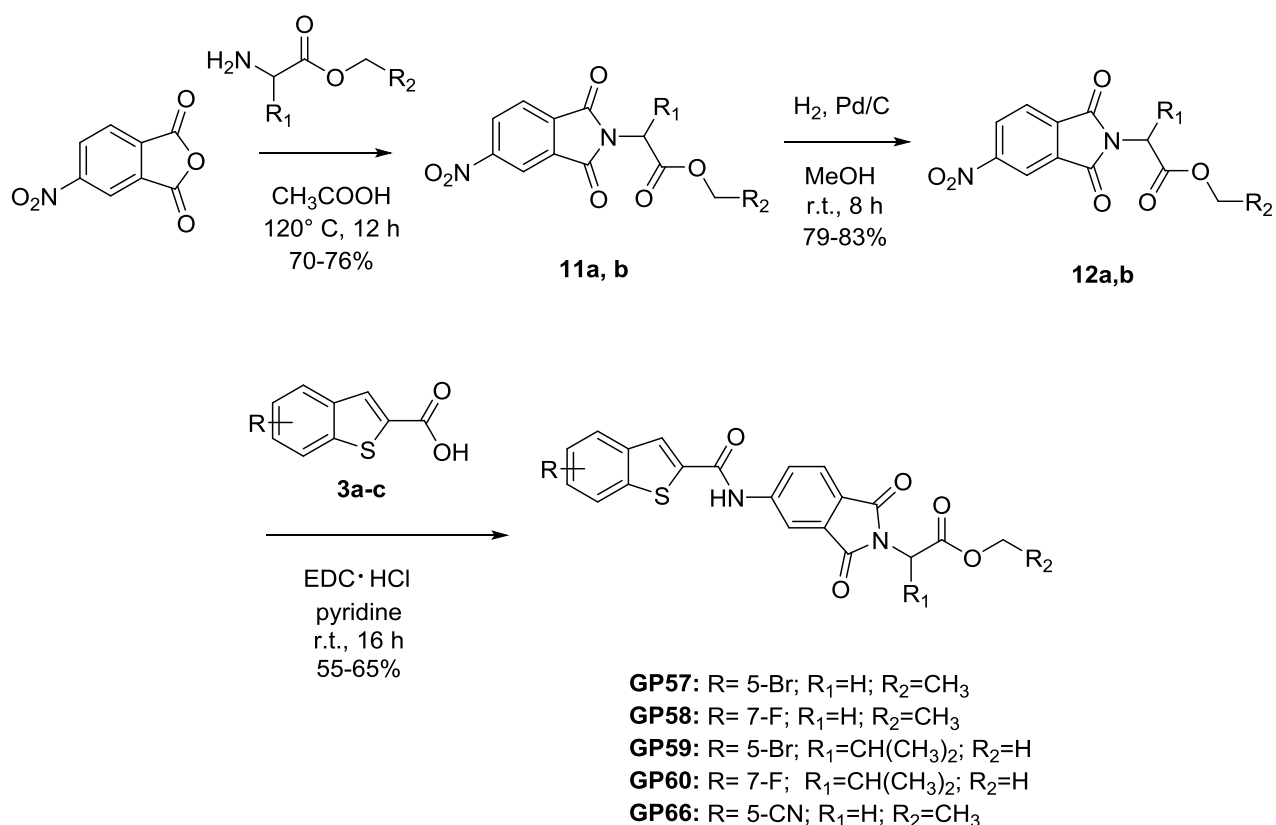
Scheme 5. Synthesis of compounds with modification in part C

4. Phenylpyrimidine-2,4-dione compounds

GP63: R= 7-F, R_1= H
GP62: R= 5-Br, R_1= H
GP64: R= 5-Br, R_1= $CH_2COOCH_2CH_3$
GP67: R= 5-Br, R_1= CH_2COOH
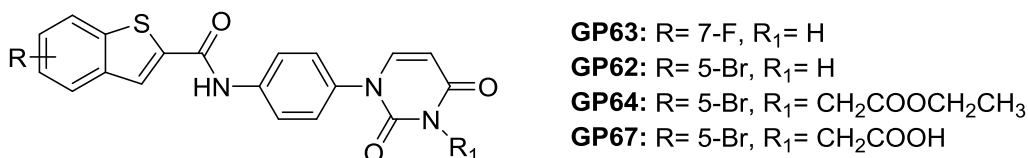
Figure 15. Structure of phenylpyrimidine-2,4-dione compounds

To avoid the difficulties in dealing with the phthalimide ring, which is not stable at basic pH, it was replaced by a phenylpyrimidine-2,4-dione unit and the compounds shown in Figure 14 were synthesized. Starting from uracil, it was treated with 4-aminophenylboronic acid in the presence of copper(II) acetate monohydrate and tetramethylethylenediamine (TMEDA) in a mixture of MeOH and water as solvent. Normally, the coupling reaction of N-heterocycles with arylboronic acids is carried out under anhydrous conditions.[51] Surprisingly, the coupling reaction of the nucleobase with phenylboronic acid catalyzed by $Cu(OAc)_2$ with dry methanol as reaction solvent and in the presence of molecular sieves gave only traces of the coupling product even after 24 hours. In contrast, when $Cu(OAc)_2$ was replaced by $Cu(OAc)_2$-H_2O, the yield of the coupling product was significantly increased in the absence of molecular sieves.[52] For our compounds, uracil was reacted with nitrophenylboronic acid and then, the product was reduced with H_2 and palladium on carbon to obtain the synthon **14** (Scheme 6).

GP62 and **GP63** were obtained from the reaction between the corresponding benzothiophene carboxylic acid and synthon **14** using the same procedure as for the preparation of other amido derivatives.
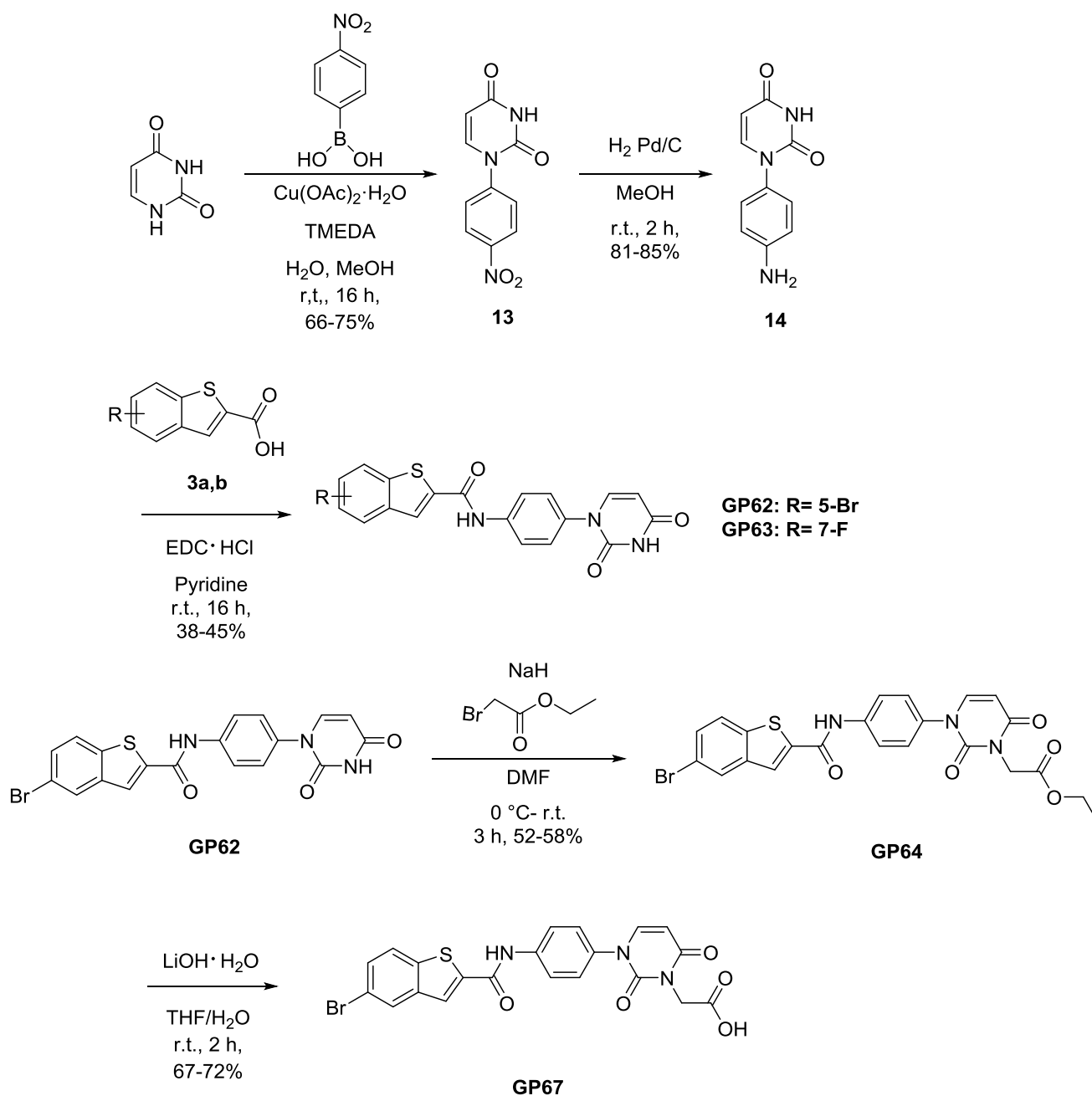
Scheme 6. Synthesis of **GP62**, **GP63**, **GP64**, **GP67**

GP62 was then treated with sodium hydride and ethyl bromoacetate to give the N-substituted pyrimidine-2,4-dione compound **GP64**. The ethyl ester was finally hydrolyzed with lithium hydroxide monohydrate to give **GP67** (scheme 6).

5. Thiophene- and pyrrole-based compounds

As a final modification, the substitution of pyrrole and thiophene for benzothiophene and indole was investigated to determine if a smaller group would increase affinity for the enzyme pocket and thus activity. Three compounds **GP69-71** were synthesised, as shown in Figure 15.

GP69: R=2-Cl; X= S
GP70: R= H; X= NCH_2OCH_3
GP71: R= H; X= S
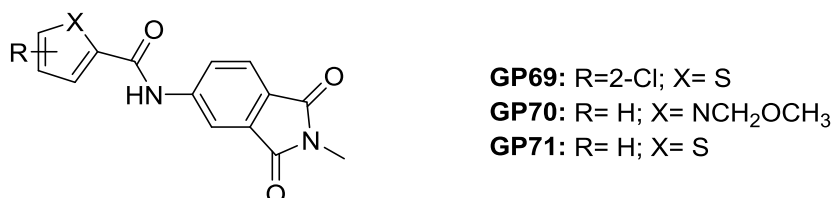
Figure 15. Structure of pyrrole- and thiophene-based molecules

For the synthesis of **GP69** and **GP71**, the suitable thiophene carboxylic acid was reacted with compound **5** under the same conditions already used for the coupling reaction (Scheme 7).

Compound **GP70** was obtained by first protecting methyl 2-pyrrolecarboxylate with MOM in THF and then hydrolyzing **16** to carboxylic acid **17**. Coupling between **17** and **5** was now possible with EDC hydrochloride in pyridine (Scheme 7).
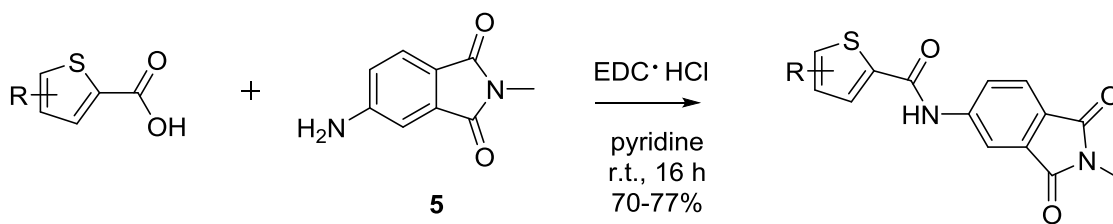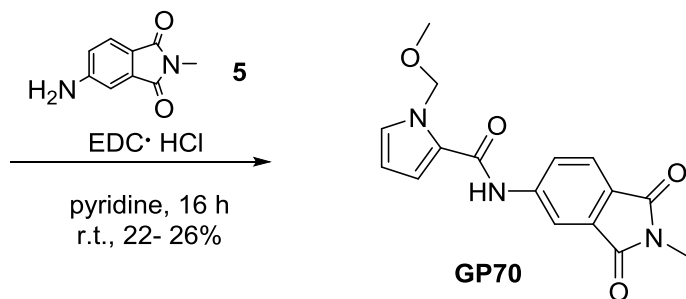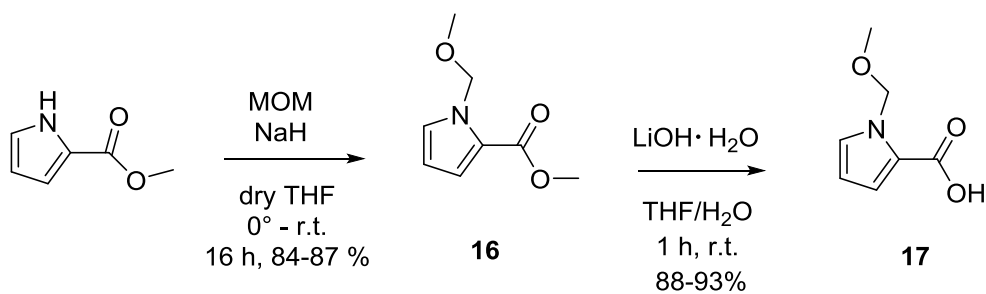
Scheme 7. Synthesis of **GP69-71**

RESULTS

1. Enzymatic assay

All molecules obtained were tested in enzymatic assays to determine if they had comparable activity to the hit compound **GP15**. The enzymatic assays were performed by Etienne Decroly and Priscila Sutto-Ortiz at the Laboratoire Architecture et Fonction des Macromolécules Biologiques of the University of Aix-Marseille.

The test consisted of a filter-binding experiment. The molecules were incubated at 30 °C for 30 minutes with the enzyme MTase from ZIKV to see if the amount of free enzyme decreased, indicating that the molecules bind and inhibit MTase. The reaction was performed in buffer Tris-HCl 40 mM pH 8.0, DTT 1 mM, ZIKV MTase 500 nM, RNA GpppAC4 0.7 µM, SAM 1.9 µM, 3H SAM 0.1 µM.

The following Tables show the results of the enzymatic test.

First of all, enzymatic test shows that bulky substituents on the benzothiophene ring decreased the activity of the molecule (Table 3), while insert a cyano group or a halogen such as bromine or fluorine seems to maintain a similar activity. Derivatives with open phthalimide ring (Table 4) were not active, meaning that intact phthalimide ring is fundamental for the activity. Replacing the methyl group on the nitrogen of the phthalimide with bulky substituents (Table 5) did not prove beneficial, and almost all of these derivatives lost activity. The best modification within the series is represented by the glycyl derivative **GP66**, although its IC_{50} decreased threefold, despite the predicted better solubility in water. When the phthalimide ring is replaced by a pyrimidine analogue (Table 6), the molecules were found to be less active than the other derivatives (IC_{50}s > 100 µM) and finally, replacing the benzothiophene ring with thiophene or pyrrole (Table 7) had a negative effect on the activity.
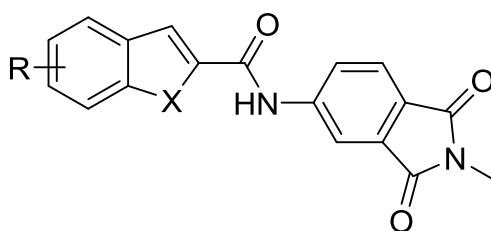
Table 3. Results of enzymatic assay for GP compounds with modification in part A

Compound	R	X	IC$_{50}$
GP15	5-NO$_2$	S	29
GP45	5-Br	S	124
GP51	7-F	S	51
GP47	5-CN	S	28
GP53	6-F	NCH$_2$OCH$_3$	130
GP54	6-Br	NCH$_2$OCH$_3$	33.5
GP55	6-Br	NH	43
GP56	6-F	NH	31
GP49	5-Ph	S	-
GP50	5-CN-Ph	S	-
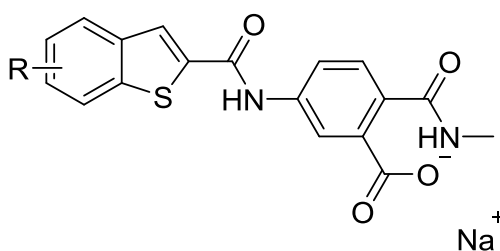
Table 4. Results of enzymatic assay for GP sodium salts

Compound	R	IC$_{50}$
GP46	5-Br	173
GP52	5-F	-
GP48	5-CN	108
GP44	5-NO$_2$	224
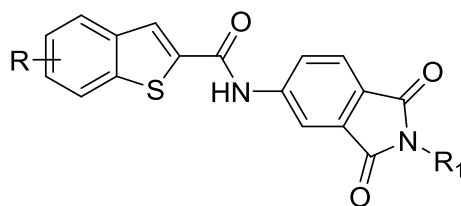
Table 5. Results of enzymatic assay for GP compounds with modification in part C

Compound	R	R_1	IC_{50}
GP57	5-Br	$CH_2COOCH_2CH_3$	na
GP59	5-Br	$CH(CHC_2H_6)COOCH_2CH_3$	na
GP58	7-F	$CH_2COOCH_2CH_3$	150
GP60	7-F	$CH(CHC_2H_6)COOCH_2CH_3$	na
GP66	5-CN	$CH_2COOCH_2CH_3$	63
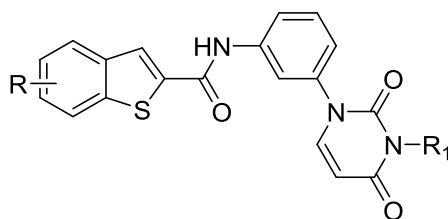
Table 6. Results of enzymatic assay of phenylpyrimidine-2,4-dione compounds

Compound	R	R_1	IC_{50}
GP62	5-Br	H	123
GP63	7-F	H	na
GP64	5-Br	$CH_2COOCH_2CH_3$	102
GP67	5-Br	CH_2COOH	103
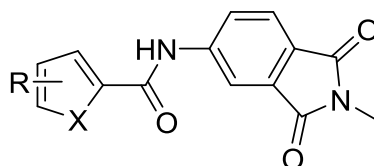
Table 7. Results of enzymatic assay for pyrrole- and thiophene-based compounds

Compound	X	R	IC_{50}
GP70	NCH_2OCH_3	H	101
GP69	S	H	na
GP71	S	5-Cl	na

na = not active (IC$_{50}$ > 250 μM)

To summarize all the results, SAR can be briefly proposed for these compounds (Figure 15).

The R group should not be bulky; the cyano group seems to be the best. Even if benzothiophene is replaced by indole, the activity does not increase but remains comparable to that of the hit compound. However, it should be kept in mind that indole derivatives are more difficult to purify than benzothiophene derivatives. In the phthalimide ring, the structure must remain closed to maintain activity, and the best substituent for the phthalimide nitrogen proved to be the methyl group.
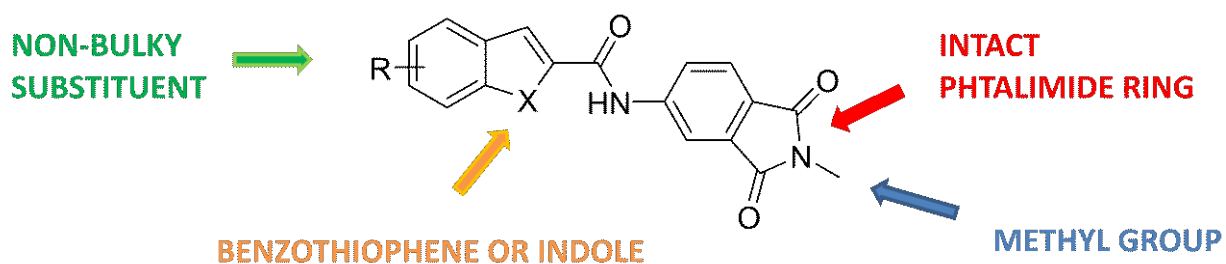
Figure 16. SAR study of GP compounds
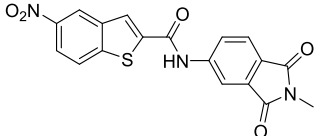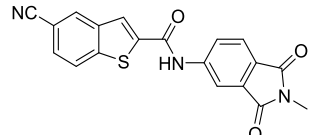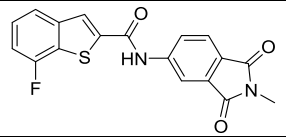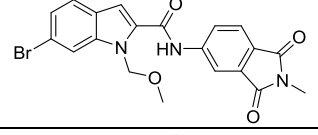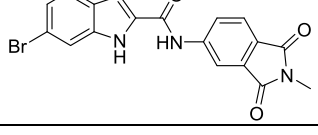
2. Antiviral assay

The four top candidates and the hit compound **GP15** were tested in vitro for antiviral activity and cytotoxicity.

As for cytotoxicity, the molecules were tested at concentrations of 0.01-100 micromolar on uninfected Vero E6 cells. Then, the 3-(4,5-dimethylthiazol-2-yl)-2,5-diphenyltetrazolium bromide (MTT) assay was used to complete the reduction assay. In this assay, the amount of product formation resulting from cellular enzymatic actions, automatically read by absorbance at 595 nm, is directly proportional to live cells. As shown in table 8, the CC$_{50}$ values for all molecules are >100, which means that they are not at all toxic to cells.

To investigate antiviral activity, the molecules were tested at various concentrations (0.01-100 micromolar) in virus inhibition experiments with ZIKV at a multiplicity of infection (MOI) of 0.1 on Vero E6 cells in 6-well plates, with reduction in plaque formation 3 days post infection assessed as the end point. In these experiments, performed in triplicate, the inhibitory activities expressed as mean inhibitory concentration 50% (IC_{50}) were determined. As we can see from the results, **GP47** showed an IC_{50} value of 4.2 µM, better than 28.6 µM of the hit compound and seems to be the most promising molecule. **GP51** and **GP55** showed higher values, while **GP54** showed similar activity to **GP15**.

Table 8. Results of antiviral assay on the most promising GP compunds

NAME	STRUTTURA	CC_{50}	IC_{50}
GP15		>100	28.6
GP47		>100	4.2
GP51		>100	51
GP54		>100	33.5
GP55		>100	61.8

IN VITRO PERMEABILITY AND STABILITY ASSAYS

Permeability assay
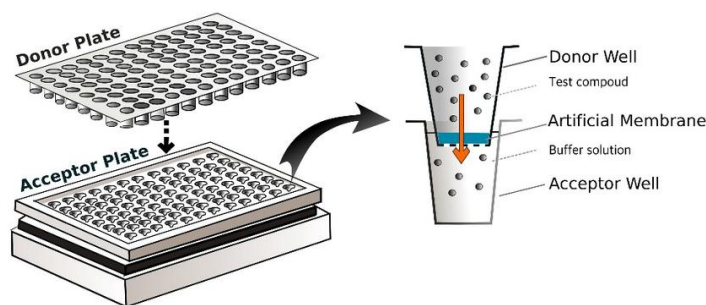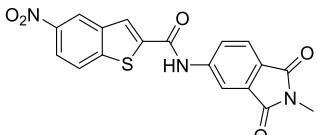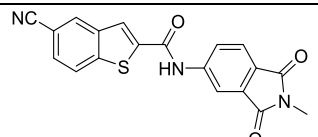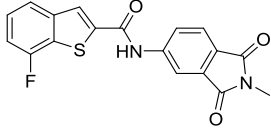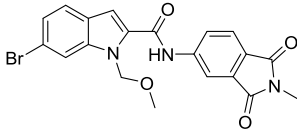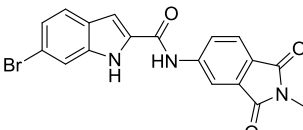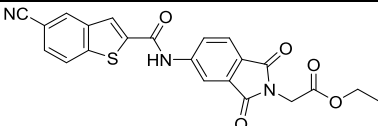
Figure 17. Graphical representation of PAMPA assay

Permeability was studied using the Parallel Artificial Membrane Permeability Assay (PAMPA) (Figure 16). This type of approach provides information on permeability by passive diffusion, which is not affected by other mechanisms such as active transport or metabolism. Passive diffusion is an important factor in determining transport through the gastrointestinal tract, penetration of the blood-brain barrier, and transport across cell membranes. Results were obtained in terms of Papp, expressed as 10^{-6} cm/sec, and percent membrane retention values.

Table 9. Results of PAMPA assay

NAME	STRUTTURA	P_{app} x 10^{-6} (cm/sec)	%RM
GP15		1.68	24.5
GP47		3.56	0
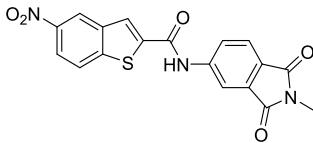
GP51		4.47	0
GP54		2.28	93.4
GP55		0.92	0
GP66		1.82	0
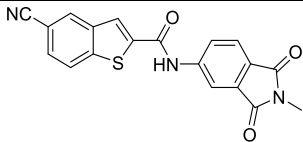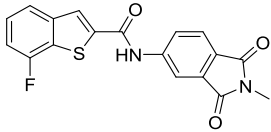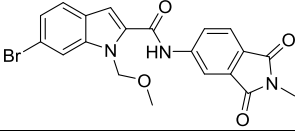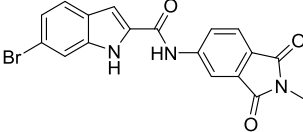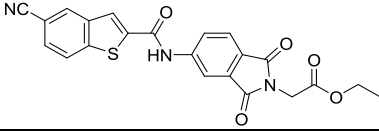
All compounds except **GP55** showed good Papp values (Table 9), better than the hit compound **GP15**, and a low percentage of membrane retention, except **GP54**.

Stability assay

Known concentrations of the compounds were mixed with human plasma and HEPES buffer and stirred. Samples were collected at different time points, denatured, and mixed with known concentrations of the internal standard to be analysed. Stability in methanol and PBS was also evaluated. As can be seen in Table 10, stability for all molecules was >99% after 24 hours in plasma, methanol and PBS.

Table 10. Results of stability assay

NAME	STRUTTURA	Stab. in plasma 24h	Stab. in MeOH 24h	Stab in PBS (pH 7.4) 24h
GP15		>99%	>99%	>99%

GP47		>99%	>99%	>99%
GP51		>99%	>99%	>99%
GP54		>99%	>99%	>99%
GP55		>99%	>99%	>99%
GP66		>99%	>99%	>99%

CONCLUSIONS

The preparation of GP compounds is a simple and effective synthesis, allowing good amounts of product to be obtained in a short time. At first, compounds appeared promising by analyzing them with Swissadme, which gave an indication regarding their pharmacokinetic behaviour: the studies carried out have confirmed that the pharmacokinetic properties are very good. The limit of these compounds still remains the solubility. The real solubility has not been calculated, but compounds still have too many unsaturations and lipophilic groups that lower the solubility: it is enough to think that to purify most of these are cristallyzed from methanol, and unfortunately, the strategy of opening phthalimide to create sodium salts proved to be unsuccessful. The most promising compound is **GP47**: the nitro group has been eliminated, the antiviral activity (4.2 μM) increased and pharmacokinetic data are also better than the hit compound.

However, the enzyme pocket remains unexplored thinking about the size of the SAM molecule compared with **GP47**: in future, it would be interesting to study what modifications can be made to **GP47** to increase its affinity for the binding site and to increase its solubility.

EXPERIMENTAL SECTION

Synthesis

Reagents were purchased from commercial suppliers (e.g., Sigma-Aldrich). All commercially available chemicals were used as purchased and without further purification. ACN was dried over calcium hydride, DCM was dried over sodium hydride, THF and dioxane were dried over Na/benzophenone before use, while DMF was purchased already anhydrous. The anhydrous reactions were carried out under a positive pressure of dry N_2. TLC was performed using Merck TLC plates on silica gel 60 F_{254}. Chromatographic purifications were performed on columns packed with Merk 60 silica gel, 23-400 mesh, for flash technique. ^{1}H NMR and ^{13}C NMR spectra were recorded at 400 MHz or 100 MHz using a Brucker Avance DPX400. Chemical shifts are given relative to tetramethylsilane at 0.00 ppm. Mass spectra (MS) were recorded using an Agilent 1100 LC / MSD VL system (G1946C) with a flow rate of 0.4 mL/min and a binary solvent system of 95:5 methanol/water. UV detection was performed at 254 nm. MS was recorded in positive and negative modes over the mass range 50-1500. The following ion source parameters were used: drying gas flow rate, 9 mL/min; nebulizer pressure, 40 psig; drying gas temperature, 350 °C.

HPLC analyses

HPLC analyses were performed using an Agilent 1100 LC / MSD VL system (G1946C) (Agilent Technologies, Palo Alto, CA) consisting of a vacuum solvent degassing unit, a high-pressure binary gradient pump, an 1100 Series UV detector, and an 1100 MSD model VL benchtop mass spectrometer. The Agilent 1100 Series Mass Spectra Detection (MSD) single quadrupole instrument was equipped with the orthogonal spray API-ES (Agilent Technologies, Palo Alto, CA). The following ion source parameters were used: drying gas flow rate, 9 mL/min; nebulizer pressure, 40 psig; drying gas temperature, 350° C. UV detection was monitored at 254 nm. Determination of LC-ESI-MS was performed by running the MSD in negative ion mode. Spectra were acquired over the scan range m/z 100-1500 with a step size of 0.1 us. LC Analyses were performed by HPLC using a Polaris C18 column (150 x 4.6 mm, 5 µm particle size) at a flow rate of 0.4 mL-min-1 with a mobile phase gradient consisting of MeOH and 1% HCOOH-H2O [t = 0: 0%

MeOH, t = 20 min: 98% MeOH, t = 25 min: 0% MeOH] and an injection volume of 20 μL. Purity analysis was performed using an Agilent 1260 Infinity HPLC-DAD in conjunction with an Agilent 6130 MSD. The Agilent 1260 Infinity HPLC-DAD system consists of a solvent degasser, an injection valve with a volume of 1 to 100 μL, a binary pump system, a UV detector, a diode array, a thermostated housing for a column, and an autosampler. The instrument is connected to an Agilent 6130 single quadrupole MSD analyzer. Analysis was performed at a flow rate of 0.4 mL-min-1 using a Phenomenex Kinetecs C18 column (30 x 2.1 mm, 2.6 μm particle size). Chromatograms were recorded at 240 and 290 nm using a gradient with ACN/MeOH 1: 1 mobile phase and H2O/ammonium acetate 0.1% v/v.

1. BENZOTIOPHENE COMPOUNDS
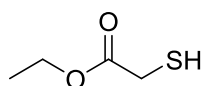
Ethyl 2-Mercaptoacetate (**1**)

To a solution of mercaptoacetic acid (1.52 g, 14.33 mmol) and ethanol (919 μL, 15.76 mmol) in toluene (5 mL) was added concentrated H_2SO_4 (4 drops), and the reaction mixture was stirred for 2 h under reflux with a Dean-Stark trap. After cooling, H_2O was added and the reaction mixture was extracted with EtOAc (3 x 25 mL). The organic layers were combined and washed three times with water, then washed with brine and dried over Na_2SO_4. The product obtained by evaporation of the solvent was used directly for the next step, without further purification.

Colourless oil. Yield: 78-85%.^{1}H NMR (400 MHz, chloroform-*d*): δ (ppm) 4.18 (q, *J* = 7.2 Hz, 2H), 3.35 – 3.20 (m, 2H), 1.99 (t, *J* = 8.2 Hz, 1H), 1.27 (t, *J* = 7.1 Hz, 3H); MS: (ESI) m/z 119.1 [M–H]⁻.

General procedure for the synthesis of intermediates 2a-d

The appropriate benzaldehyde (1 mmol) was dissolved in anhydrous CH_3CN (20 mL). To this was added triethylamine (2.5 mmol) and compound 1 (1.1 mmol) and the solution was stirred at 60 °C for 14 h. Then the reaction mixture was evaporated under reduced pressure, diluted with water

and extracted with EtOAc (3x20 mL). After washing with brine, the organic layer was dried over Na$_2$SO$_4$ and evaporated. The crude product was purified by flash chromatography on silica gel with an appropriate eluent.
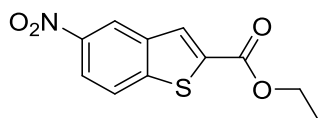
Ethyl 5-Nitrobenzothiophene-2-carboxylate (**2a**)

Eluent: PE/EtOAc (95:5). Yellow solid. Yield 75-80%. ^{1}H NMR (400 MHz, DMSO-d_6): δ (ppm) 9.03 (d, J = 6.8 Hz, 1H), 8.41 − 8.32 (m, 3H), 4.43 (q, J = 6.9, 2H), 1.39 (t, J = 7.1 Hz, 3H); MS: (ESI) m/z 250.3 [M−H]$^-$.
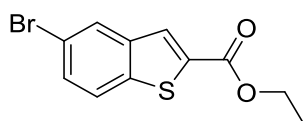
Ethyl 5-Bromobenzothiophene-2-carboxylate (**2b**)

Eluent: PE/EtOAc (98:2 to 95:5). White solid. Yield: 75%-83%. ^{1}H NMR (400 MHz, chloroform-d): δ (ppm) 8.11 − 7.96 (m, 2H), 7.76 (d, J = 8.6 Hz, 1H), 7.58 (d, J = 8.7 Hz, 1H), 4.45 (q, J = 7.1 Hz, 2H), 1.45 (t, J = 7.3 Hz, 3H); MS: (ESI) m/z 284.3 [M−H]$^-$
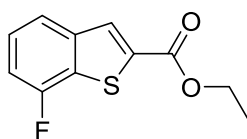
Ethyl 7-Fluorobenzothiophene-2-carboxylate (**2c**)

Eluent: PE/EtOAc (95:5). White solid. Yield: 82-90%; ^{1}H NMR (400 MHz, chloroform-*d*): δ (ppm) 8.32 (s, 1H), 8.21 (m, 2H), 7.89 (t, *J* = 5.1 Hz, 1H), 4.52 (q, *J* = 6.8 Hz, 2H), 1.51 (t, *J* = 7.0 Hz, 3H). MS: (ESI) m/z 221.9 [M–H]$^-$
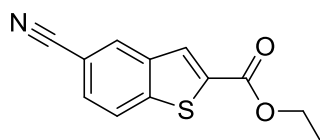
Ethyl 5-Cyanobenzothiophene-2-carboxylate (**2d**)

Compound **2b** (375 mg, 1.40 mmol) was dissolved in anhydrous NMP (10 mL), to which CuCN (188 mg, 2.10 mmol) was added. The reaction mixture was stirred under N_2 atmosphere at 190-200 °C for 20 h and then taken up with water and extracted with $CHCl_3$ (3x25 mL). The combined organic layers were washed with water and brine, dried over Na_2SO_4 and evaporated. The crude product was purified by flash chromatography on silica gel.

Eluent: PE/EtOAc (9:1). Brown solid. Yield: 65-68%. ^{1}H NMR (400 MHz, chloroform-*d*): δ (ppm) 8.30 (s, 1H), 8.12 (s, 1H), 8.00 (d, *J* = 8.2 Hz, 1H), 7.76 (d, *J* = 7.7 Hz, 1H), 4.53 (q, *J* = 4.4 Hz, 2H), 1.53 (t, *J* = 1.4 Hz, 3H); MS: (ESI) m/z 230.1 [M–H]$^-$.

General procedure for the synthesis of intermediates 3a-d

To a solution of appropriate esters **2a-d** (1 mmol) in THF (5 mL) was added H_2O (5 mL) and lithium hydroxide monohydrate (4 mmol), and the reaction mixture was stirred at room temperature for 2 h. Then THF was removed under reduced pressure and the crude product was taken up in water, acidified to pH=2 with 2 N HCl and extracted with DCM (3 x 30 mL). The organic layers were combined, washed with brine and dried over Na_2SO_4. After evaporation of the solvent, compounds **3a-d** were obtained without further purification.
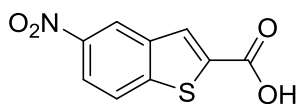
5-Nitrobenzothiophene-2-carboxylic acid (**3a**)

Brown solid. Yield: 65-70%. ^{1}H NMR (400 MHz, DMSO-d_6): δ (ppm) 8.97 (d, J = 2.0 Hz, 1H), 8.36 – 8.26 (m, 3H); MS: (ESI) m/z 222.1 [M–H]$^-$
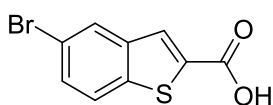
5-Bromobenzothiophene-2-carboxylic acid (**3b**)

White solid. Yield: 66-69%; ^{1}H NMR (400 MHz, DMSO-d_6): δ (ppm) 8.28 (s, 1H), 8.10 (s, 1H), 8.05 (d, J = 8.3 Hz, 1H), 7.67 (d, J = 8.6, 1H); MS: (ESI) m/z 255.2 [M–H]$^-$
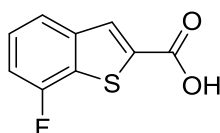
7-Fluorobenzothiophene-2-carboxylic acid (**3c**)

White solid. Yield: 75-80%. ^{1}H NMR (400 MHz, methanol-d_4): δ (ppm) 8.09 (s, 1H), 7.76 (d, J = 8.0 Hz, 1H), 7.44 (t, J = 8.0 Hz, 1H), 7.28 – 7.18 (m, 1H); MS: (ESI) m/z 195.0 [M–H]$^-$
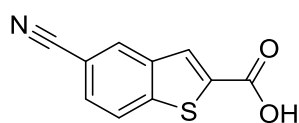
5-Cyanobenzothiophene-2-carboxylic acid (**3d**)

White solid. Yield: 78-80%. ^{1}H NMR (400 MHz, DMSO-d_6): δ (ppm) 8.57 (s, 1H), 8.32 (d, J = 8.5 Hz, 1H), 8.20 (s, 1H), 7.88 (d, J = 8.5, 1H); MS: (ESI) m/z 202.0 [M–H]$^-$
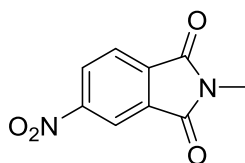
2-Methyl-5-nitroisoindoline-1,3-dione (**4**)

4-Nitrophthalic anhydride (1.93 g, 10 mmol) was dissolved in anhydrous THF (15 mL) and a 2 M solution of methylamine in THF (5.5 mL, 11 mmol) was added. The reaction mixture was stirred under N2 atmosphere at 40 °C for 1 hour, then the solvent was removed under reduced pressure and the corresponding brown solid was heated at 190 °C for 15 h. After cooling, the crude product was purified by flash chromatography on silica gel.

Eluent: hexane/EtOAc (1:1). White solid. Yield: 65-75%. ^{1}H NMR (400 MHz, chloroform-d): δ (ppm) 8.70 (s, 1H), 8.63 (d, J = 8.1 Hz, 1H), 8.08 (d, J = 8.2 Hz, 1H), 3.29 (s, 3H); MS: (ESI) m/z 207.9 [M+H]$^+$

General procedure for the synthesis of intermediates 11a-b

4-Nitrophtalic anhydride (1 mmol) was dissolved in 10 mL of acetic acid and to this solution was added the appropriate amine (1.1 mmol) and the reaction mixture was stirred under reflux for 24 h. Then the reaction mixture was diluted with water and extracted with EtOAc (3x20 mL), the organic layers were combined, washed with brine, dried over Na_2SO_4 and evaporated. The crude product obtained was purified by flash chromatography on silica gel using appropriate eluents.
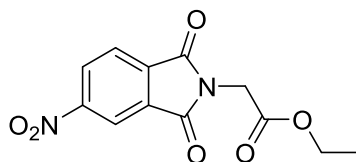
Ethyl 2-(5-Nitro-1,3-dioxoisoindolin-2-yl)acetate (**11a**)

Eluent: PE/EtOAc (7:3). White solid. Yield: 70-75%. ^{1}H NMR (400 MHz, chloroform-*d*): δ (ppm) 8.72 (d, *J* = 7.1 Hz, 1H), 8.47 (s, 1H), 8.06 (d, *J* = 7.1 Hz, 1H), 4.69 (s, 2H), 4.32 (q, *J* = 5.2 Hz, 2H), 1.25 (t, *J* = 5.1 Hz, 3H); MS: (ESI) m/z 277.1 [M–H]⁻
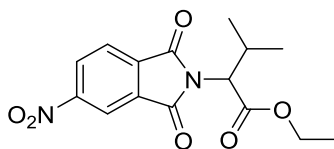
Ethyl 3-Methyl-2-(5-nitro-1,3-dioxoisoindolin-2-yl)butanoate (**11b**)

Eluent: PE/EtOAc (8:2). White solid (yield 72-74%). ^{1}H NMR (400 MHz, chloroform-*d*): δ (ppm) 8.76 (d, *J* = 8.3 Hz, 1H), 8.50 (s, 1H), 8.11 (d, *J* = 8.3 Hz, 1H), 5.15 (d, *J* = 1.9 Hz, 1H), 4.24 (q, *J* = 5.1 Hz, 2H), 3.02 (t, *J* = 2.4 Hz, 1H), 1.21 (t, *J* = 5.1 Hz, 3H), 1.06 (d, *J* = 2.4 Hz, 6H); MS: (ESI) m/z 291.2 [M–H]⁻

General procedure for synthesis of intermediates 5, 12a-b

To a solution of compounds **4/11a/11b** (1 mmol) in MeOH (50 mL) was added Pd/C (0.1 mmol) and the reaction mixture was stirred for 2 h under H_2 atmosphere. Then the catalyst was filtered off over a Celite pad and the solution was evaporated to give compounds **5, 12a-b**.
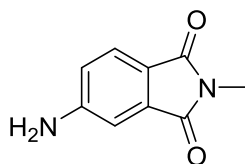
5-Amino-2-methylisoindoline-1,3-dione (**5**)

Yellow solid. Yield: 81-89%. ^{1}H NMR (400 MHz, DMSO-d_6): δ (ppm) 7.48 (d, J = 8.0 Hz, 1H), 6.93 (s, 1H), 6.79 (d, J = 8.2 Hz, 1H), 6.43 (s, 2H), 2.96 (s, 3H); MS: (ESI) m/z 177.8 [M+H]$^+$
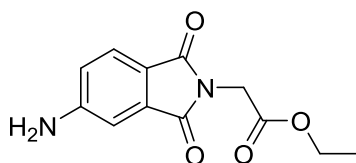
Ethyl 2-(5-Amino-1,3-dioxoisoindolin-2-yl)acetate (**12a**)

Light green solid. Yield: 79-81%. ^{1}H NMR (400 MHz, methanol-d_4): δ (ppm) 7.53 (d, J = 8.2 Hz, 1H), 7.02 (s, 1H), 6.86 (d, J = 8.2 Hz, 1H), 4.44 (s, 2H), 4.29 (q, J = 7.1 Hz, 2H), 1.26 (t, J = 7.1 Hz, 3H). MS: (ESI) m/z 271.2 [M+Na]$^+$
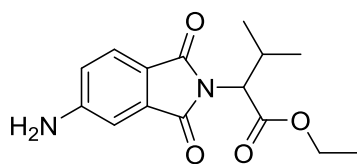
Ethyl 2-(5-Amino-1,3-dioxoisoindolin-2-yl)-3-methylbutanoate (**12b**)

Orange solid. Yield: 79-83%. ^{1}H NMR (400 MHz, DMSO-$d6$): δ (ppm) 7.55 (d, J = 7.8 Hz, 1H), 7.15 (s, 1H), 6.98 (d, J = 7.7 Hz, 1H), 6.48 (s, 2H), 5.34 (d, J = 4.2 Hz, 1H), 4.25 (q, J = 5.8 Hz, 2H), 3.08 (d, J = 4.2 Hz, 1H), 1.45 (t, J = 5.8 Hz, 3H), 1.19 (d, J = 4.1 Hz, 6H); MS: (ESI) m/z 263.1 [M+H]$^+$

General procedure for the synthesis of GP15, GP45, GP47, GP51, GP57, GP58 GP59, GP60, GP66

Compounds **3a-d** (0.89 mmol) were dissolved in anhydrous pyridine (10 mL) and EDC hydrochloride (1.34 mmol) was added to this solution. The reaction mixture was stirred at room temperature under N_2 atmosphere for 10 minutes. Then compound **5**, **12a-b** (0.89 mmol) was added and the solution was stirred at room temperature under N_2 atmosphere. After 16 h, the solvent was removed in air, then the crude product was taken up with water and extracted with EtOAc (3x25 mL). The organic layers were washed three times with water to remove the residue of pyridine, then with brine and dried over Na_2SO_4. After evaporation of the solvent, the crude product was purified by flash chromatography on silica gel with an appropriate eluent.
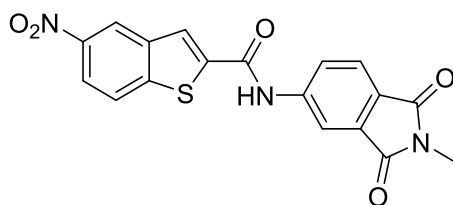
N-(2-Methyl-1,3-dioxoisoindolin-5-yl)-5-nitrobenzothiophene-2-carboxamide (**GP15**)

Eluent: PE/EtOAc (6:4) and crystallization from MeOH. White solid. Yield: 62-64%. ^{1}H NMR (400 MHz, DMSO-d_6): δ (ppm) 11.24 (s, 1H), 9.01 (d, *J* = 2.2 Hz, 1H), 8.60 (s, 1H), 8.42 − 8.30 (m, 3H), 8.13 (d, *J* = 8.4 Hz, 1H), 7.91 (d, *J* = 8.2 Hz, 1H), 3.05 (s, 3H); ^{13}C NMR (101 MHz, DMSO-d_6): δ (ppm) 188.3¸ 160.5, 151.7, 146.8, 144.1, 142.5, 133.9, 129.1, 127.5, 125.1, 123.6, 119.5, 119.2, 118.9, 117.3; MS: (ESI) m/z 282.3 [M–H]⁻
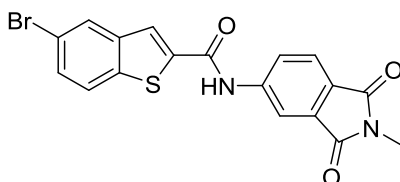
5-Bromo-*N*-(2-methyl-1,3-dioxoisoindolin-5-yl)benzothiophene-2-carboxamide (**GP45**)

Eluent PE/EtOAc (7:3) and crystallization from EtOH. Light brown solid. Yield: 62-64%. ^{1}H NMR (400 MHz, DMSO-d_6): δ (ppm) 11.10 (s, 1H), 8.37 (s, 1H), 8.32 (d, *J* = 4.7 Hz, 2H), 8.15 − 8.07 (m, 2H), 7.89 (d, *J* = 8.2 Hz, 1H), 7.67 (d, *J* = 8.0, 1H), 3.05 (s, 4H); ^{13}C NMR (101 MHz, DMSO-d_6): δ (ppm)

168.2, 160.9, 144.3, 141.3, 140.0, 133.6, 129.9, 128.2, 126.2, 125.4, 124.5, 118.8, 114.2, 24.1; MS: (ESI) m/z 413.6 [M–H]⁻

5-Cyano-*N*-(2-methyl-1,3-dioxoisoindolin-5-yl)benzothiophene-2-carboxamide (**GP47**)

Eluent: PE/EtOAc (6:4) and crystallization from MeOH. Light yellow solid. Yield: 54-58%. ^{1}H NMR (400 MHz, DMSO-*d*$_6$): δ (ppm) 11.15 (s, 1H), 8.67 (s, 1H), 8.50 (s, 1H), 8.35 – 8.31 (m, 2H), 8.12 (d, *J* = 8.2 Hz, 1H), 7.91 – 7.85 (m, 2H), 3.05 (s, 3H); ^{13}C NMR (101 MHz, DMSO-*d*$_6$): δ (ppm) 168.5, 167.7, 161.3, 145.3, 140.9, 135.8, 132.9, 132.4, 128.9, 128.0, 126.2, 125.1, 123.0, 123.5, 118.7, 113.7, 111.6, 26.2. MS: (ESI) m/z 360.2 [M–H]⁻
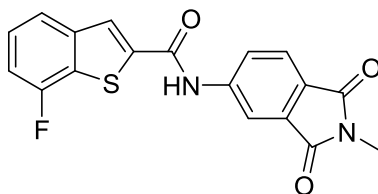
7-Fluoro-*N*-(2-methyl-1,3-dioxoisoindolin-5-yl)benzothiophene-2-carboxamide (**GP51**)

Eluent: PE/EtOAc (75:25) and crystallization from MeOH. Light yellow solid. Yield 60-66%. ^{1}H NMR (400 MHz, DMSO-*d*$_6$): δ (ppm) 11.09 (s, 1H), 8.47 (s, 1H), 8.30 (d, *J* = 1.8 Hz, 1H), 8.08 (t, *J* = 1.9 Hz, 1H), 7.88 (m, 2H), 7.51 (d, *J* = 7.9 Hz, 1H), 7.39 (d, *J* = 7.9 Hz, 1H), 3.01 (s, 3H); ^{13}C NMR (101 MHz, DMSO-*d*$_6$): δ (ppm) 168.0, 163.5, 158.3, 155.8, 144.2, 142.5, 140.8, 136.6, 133.6, 130.8, 128.4, 127.0, 124.5, 122.6, 114.2, 112.3, 24.2; MS: (ESI) m/z 354.36 [M–H]⁻
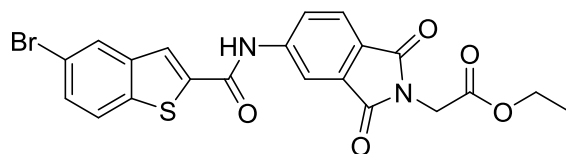
Ethyl 2-(5-(5-Bromobenzothiophene-2-carboxamido)-1,3-dioxoisoindolin-2-yl)acetate (**GP57**)

Eluent: PE/EtOAc (7:3) and crystallization from MeOH. White solid. Yield: 60-65%. ^{1}H NMR (400 MHz, DMSO-d_6): δ (ppm) 11.14 (s, 1H), 8.39 − 8.32 (m, 2H), 8.29 (d, J = 2.0 Hz, 1H), 8.14 (d, J = 1.9 Hz, 1H), 8.04 (d, J = 8.7 Hz, 1H), 7.93 (d, J = 8.2 Hz, 1H), 7.63 (d, J = 8.7 Hz, 1H), 4.38 (s, 2H), 4.13 (q, J = 7.1 Hz, 2H), 1.18 (t, J = 7.1 Hz, 3H); ^{13}C NMR (101 MHz, DMSO-d_6): δ (ppm) 168.0, 167.4, 167.3, 159.3, 143.2, 142.1, 137.0, 132.8, 131.8, 128.3, 127.4, 127.3, 126.3, 126.2, 125.2, 124.7, 122.5, 113.7, 60.8, 40.3, 14.1; MS: (ESI) m/z 485.2 [M−H]$^-$
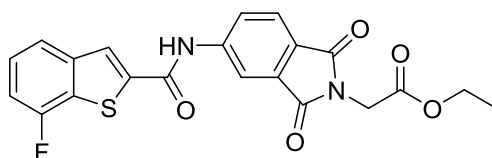
Ethyl 2-(5-(7-Fluorobenzothiophene-2-carboxamido)-1,3-dioxoisoindolin-2-yl)acetate (**GP58**)

Eluent: PE/EtOAc (6:4) and crystallization from MeOH. White solid. Yield: 55-60%. ^{1}H NMR (400 MHz, DMSO-d_6): δ (ppm) 11.05 (s, 1H), 8.44 (s, 1H), 8.32 (s, 1H), 8.09 (d, J = 8.1 Hz, 1H), 7.86 (m, 2H), 7.48 (d, J = 8.8 Hz, 1H), 7.34 (d, J = 9.0 Hz, 1H), 4.36 (s, 2H), 4.13 (q, J = 7.1 Hz, 2H), 1.17 (t, J = 7.1 Hz, 3H). ^{13}C NMR (101 MHz, DMSO-d_6): δ (ppm) 168.0, 167.2, 167.0, 160.8, 155.8, 144.7, 142.6, 140.7, 133.1, 127.5, 126.1, 125.1, 122.5, 114.5, 112.2, 61.8, 14.4; MS: (ESI) m/z 425.1 [M−H]$^-$
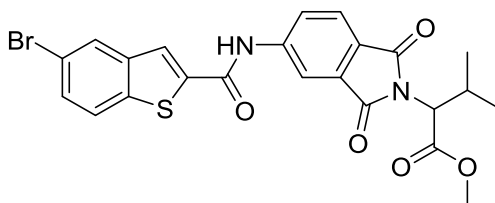
Methyl 2-(5-(5-Bromobenzothiophene-2-carboxamido)-1,3-dioxoisoindolin-2-yl)-3-methylbutanoate (**GP59**)

Eluent: PE/EtOAc (8:2). White solid. Yield: 58-62%. ^{1}H NMR (400 MHz, DMSO-d_6): δ (ppm) 11.09 (s, 1H), 8.36 − 8.28 (m, 2H), 8.25 (d, J = 1.9 Hz, 1H), 8.13 (dd, J = 8.2, 1.9 Hz, 1H), 8.00 (d, J = 8.7 Hz,

1H), 7.95 − 7.87 (m, 1H), 7.59 (d, J = 8.7 Hz, 1H), 4.54 (d, J = 7.7 Hz, 1H), 3.59 (s, 3H), 2.61 − 2.47 (m, 1H), 1.02 (d, J = 6.7 Hz, 3H), 0.80 (d, J = 6.8 Hz, 3H); ^{13}C NMR (101 MHz, DMSO-d_6): δ (ppm) 169.2, 167.5, 167.3, 161.0, 144.9, 141.4, 141.1, 140.0, 132.7, 129.9, 128.2, 126.3, 125.6, 125.3, 125.1, 118.8, 114.7, 57.1, 52.7, 28.6, 20.9, 19.4; MS: (ESI) m/z 513.2 [M−H]$^-$

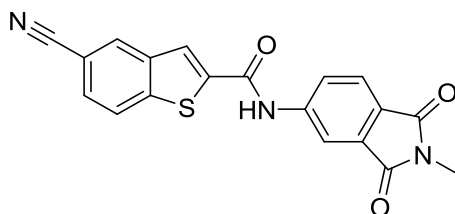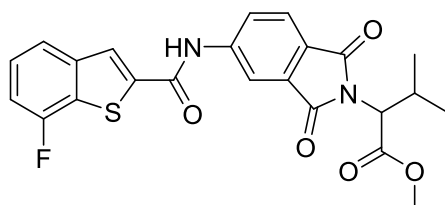Methyl 2-(5-(7-Fluorobenzothiophene-2-carboxamido)-1,3-dioxoisoindolin-2-yl)-3-methylbutanoate (**GP60**)

Eluent: PE/EtOAc (8:2) and crystallization from MeOH. White solid. Yield: 58-63%. ^{1}H NMR (400 MHz, DMSO-d_6): δ (ppm) 11.13 (s, 1H), 8.48 (d, J = 3.6 Hz, 1H), 8.34 (d, J = 1.9 Hz, 1H), 8.13 (d, J =1.9 Hz, 1H), 7.90 (t, J = 8.2 Hz, 2H), 7.50 (td, J = 8.0, 5.1 Hz, 1H), 7.37 (dd, J = 10.2, 7.9 Hz, 1H), 4.55 (d, J = 7.7 Hz, 1H), 3.59 (s, 3H), 2.55 (t, J = 6.8 Hz, 1H), 1.03 (d, J = 6.6 Hz, 3H), 0.80 (d, J = 6.8 Hz, 3H); ^{13}C NMR (101 MHz, DMSO-d_6): δ (ppm) 169.3, 167.5, 167.3, 160.9, 158.3, 155.9, 144.9, 142.7, 140.7, 132.7, 127.7, 127.6, 127.5, 125.7, 125.3, 125.2, 122.6, 114.7, 112.4, 112.2, 57.1, 52.7, 28.6, 20.9, 19.3; MS (ESI) m/z 453.1 [M−H]$^-$
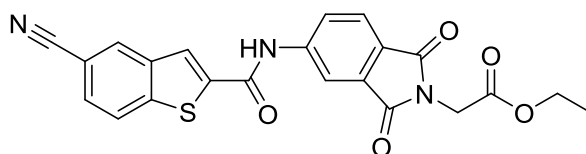
Ethyl 2-(5-(5-Cyanobenzothiophene-2-carboxamido)-1,3-dioxoisoindolin-2-yl)acetate (**GP66**)

Eluent: PE/EtOAc (8:2 to 7:3). Light brown solid. Yield: 56-60%. ^{1}H NMR (400 MHz, DMSO-d_6): δ (ppm) 11.18 (s, 1H), 8.68 − 8.61 (m, 1H), 8.48 (s, 1H), 8.36 (d, J = 1.8 Hz, 1H), 8.29 (d, J = 8.5 Hz, 1H), 8.14 (d, J = 8.2 H, 1H), 7.93 (d, J = 8.2 Hz, 1H), 7.83 (d, J = 8.4 Hz, 1H), 4.38 (s, 2H), 4.13 (q, J = 7.1 Hz, 2H), 1.18 (t, J = 7.1 Hz, 3H). ^{13}C NMR (101 MHz, DMSO-d_6): δ (ppm) 168.0, 167.3, 167.0,

160.8, 144.7, 142.2, 139.3, 133.2, 131.0, 128.8, 126.8, 126.3, 125.2, 125.1, 124.9, 119.4, 114.6, 108.4, 61.8, 14.4; MS: (ESI) m/z 432.0 [M–H]⁻

General procedure for the synthesis of GP44, GP46, GP48, GP52

To a suspension of compounds **GP15**, **GP45**, **GP47** and **GP66** (1 mmol) in THF/H_2O 1:1 (10 mL) was added lithium hydroxide monohydrate (1.2 mmol) and the reaction mixture was stirred at room temperature for 1 hour. After completion of the reaction, THF was removed under reduced pressure and the reaction mixture was taken up with water. The solution was acidified to pH = 2 with 2 N HCl and then extracted with DCM (3x20 mL). The organic layers were washed with brine, dried over Na_2SO_4 and evaporated to afford the desired compounds without further purification.
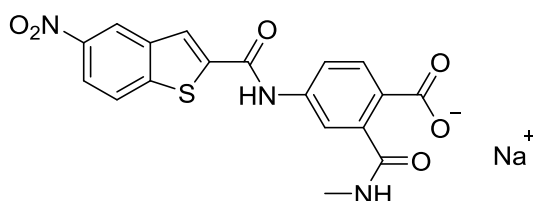
2-(Methylcarbamoyl)-4-(5-nitrobenzothiophene-2-carboxamido)benzoate (**GP44**)

White solid. Yield 66-70%. ¹H NMR (400 MHz, DMSO-d_6): δ (ppm) 11.06 (d, *J* = 4.3 Hz, 1H), 9.00 (q, *J* = 4.0 Hz, 1H), 8.63 (s, 1H), 8.44 − 8.31 (m, 2H), 8.11 (d, *J* = 3.4 Hz, 1H), 7.99 − 7.82 (m, 2H), 7.57 (d, *J* = 8.3 Hz, 1H), 2.76 (s, 3H); ¹³C NMR (101 MHz, DMSO-d_6): δ (ppm) 166.6, 163.3, 158.1, 155.1, 143.9, 141.9, 141.4, 135.4, 132.7, 129.9, 129.7, 128.7, 124.8, 122.4, 120.9, 119.4, 108.5, 26.4; MS: (ESI) m/z 397.1 [M–H]⁻
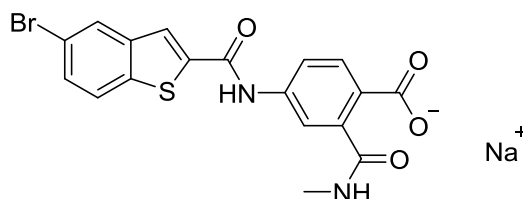
4-(5-Bromobenzothiophene-2-carboxamido)-2-(methylcarbamoyl)benzoate (**GP46**)

White solid. Yield: 68-75%. ^{1}H NMR (400 MHz, DMSO-d_6): δ (ppm) 10.99 (s, 1H), 8.97 (d, J = 6.5 Hz, 1H), 8.59 (s, 1H), 8.35 (d, J = 8.8 Hz, 1H), 8.28 (d, J = 9.0 Hz, 1H), 8.07 (s, 1H), 7.94 (d, J = 8.9 Hz, 1H), 7.53 (d, J = 8.4 Hz, 1H), 2.72 (s, 3H); ^{13}C NMR (101 MHz, DMSO-d_6): δ (ppm) 169.5, 168.8, 168.5, 167.4, 160.7, 142.0, 141.7, 139.9, 133.7, 132.8, 131.2, 129.7, 128.8, 125.9, 122.1, 120.9, 118.7, 29.4; MS: (ESI) m/z 431.0 [M–H]$^-$
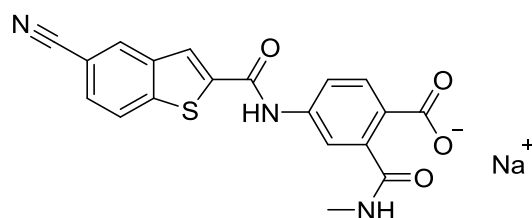
4-(5-Cyanobenzothiophene-2-carboxamido)-2-(methylcarbamoyl)benzoate (**GP48**)

White solid. Yield: 65-68%. ^{1}H NMR (400 MHz, DMSO-d_6): δ (ppm) 12.95 (s, 1H), 10.92 (d, J = 4.5 Hz, 1H), 8.64 (t, J = 2.6 Hz, 1H), 8.48 (s, 1H), 8.30 (t, J = 10.0 Hz, 2H), 8.13 (d, J = 2.2 Hz, 1H), 7.97 (dd, J = 8.4, 2.2 Hz, 1H), 7.85 (dd, J = 8.3, 1.9 Hz, 1H), 7.46 (d, J = 8.4 Hz, 1H), 2.71 (s, 3H); ^{13}C NMR (101 MHz, DMSO-d_6): δ (ppm) 168.6, 160.4, 145.0, 142.8, 139.4, 133.9, 132.9, 130.9, 128.7, 124.8, 121.5, 120.7, 119.4, 108.3, 26.5; MS: (ESI) m/z 378.4 [M–H]$^-$
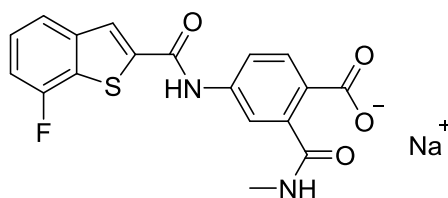
4-(7-Fluorobenzothiophene-2-carboxamido)-2-(methylcarbamoyl)benzoate (**GP52**)

White solid. Yield: 66-71%. ^{1}H NMR (400 MHz, DMSO-d_6): δ (ppm) 10.78 (s, 1H), 8.53 (d, J = 2.6 Hz, 1H), 8.00 (d, J = 2.5 Hz, 1H), 7.90 − 7.81 (m, 2H), 7.61 (d, J = 8.2 Hz, 1H), 7.51 (d, J = 8.0 Hz, 1H),

7.42 – 7.35 (m, 2H), 2.72 (s, 3H); ^{13}C NMR (101 MHz, DMSO-d_6): δ (ppm) 168.4, 168.0, 160.8, 155.3, 151.3, 140.0, 139.6, 138.2, 138.1, 134.0, 131.0, 130.6, 130.5, 130.3, 126.8, 126.7, 126.7, 122.2, 122.1, 121.7, 116.2, 112.3, 112.1, 26.2; MS: (ESI) m/z 371.2 [M–H]$^−$

General procedure for the synthesis of GP49 and GP50

GP45 (0.08 mmol) was dissolved in a mixture of 1,4-dioxane/H$_2$O (2:1). Na$_2$CO$_3$ (0.2 mmol), LiCl (0.5 mmol), tetrakis((triphenylphosphine)-palladium(0)) (0.05 mmol) and the appropriate boronic acid (0.13 mmol) were added and the reaction mixture was stirred at 100 °C for 3 h. After cooling, the reaction mixture was diluted with water and extracted with EtOAc (3x25 mL). The organic layer was washed with brine, dried over Na$_2$SO$_4$ and evaporated. The crude product was purified by flash chromatography.
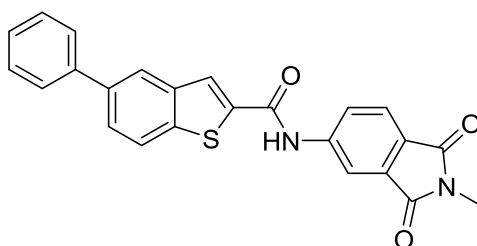
N-(2-Methyl-1,3-dioxoisoindolin-5-yl)-5-phenylbenzothiophene-2-carboxamide (**GP49**)

Eluent: PE/EtOAc (6:4) and crystallization from MeOH. White solid. Yield: 35-38%. ^{1}H NMR (400 MHz, DMSO-d_6): δ (ppm) 11.09 (s, 1H), 8.44 (s, 1H), 8.33 (d, *J* = 1.9 Hz, 1H), 8.28 (d, *J* = 2.0 Hz, 1H), 8.12 (m, 2H), 7.86- 7.81 (m, 2H), 7.76 (d, *J* = 7.5 Hz, 2H), 7.51 (t, *J* = 7.5 Hz, 2H), 7.41 (d, *J* = 7.7 Hz, 1H), 3.02 (s, 3H); ^{13}C NMR (101 MHz, DMSO-d_6): δ (ppm) 169.4, 168.7, 168.4, 160.4, 145.0, 142.8, 139.5, 139.4, 133.8, 132.8, 130.9, 128.9, 128.6, 126.2, 124.8, 122.2, 120.9, 119.4, 108.3, 26.5; MS: (ESI) m/z 411.1 [M–H]$^−$
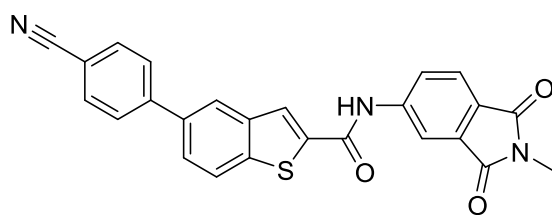
5-(4-Cyanophenyl)-*N*-(2-methyl-1,3-dioxoisoindolin-5-yl)benzothiophene-2-carboxamide (**GP50**)

Eluent: PE/EtOAc (7:3) and crystallization from MeOH. Light yellow solid. Yield 38-40%. ^{1}H NMR (400 MHz, DMSO-d_6): δ (ppm) 11.13 (s, 1H), 8.48 (s, 1H), 8.41 (d, *J* = 1.8 Hz, 1H), 8.34 (d, *J* = 1.9 Hz, 1H), 8.21 (d, *J* = 8.5 Hz, 1H), 8.13 (d, *J* = 8.2 Hz, 1H), 8.02 – 7.95 (m, 4H), 7.91 – 7.86 (m, 2H), 3.02 (s, 3H); ^{13}C NMR (101 MHz, DMSO-d_6): δ (ppm) 168.1, 161.2, 134.6, 133.4, 132.5, 131.9, 129.2, 126.1, 124.4, 118.2, 115.4, 114.3, 46.1, 24.3; MS: (ESI) m/z 436.2 [M–H]$^{-}$

2. INDOLE COMPOUNDS
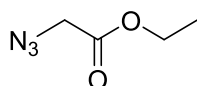
Ethyl 2-Azidoacetate (**6**)

To a solution of ethyl bromoacetate (4.5 g, 27.05 mmol) in acetone (30 mL) at 0 °C, a solution of sodium azide (4.3 g, 67.7 mmol) in H_2O (25 mL) was added dropwise in 30 minutes. The solution was stirred at room temperature for 1 hour and then at 50 °C for 15 h. The reaction mixture was then extracted with Et_2O (3x30 mL), the organic layers were combined, washed with a solution of saturated $NaHCO_3$, then with brine, dried over Na_2SO_4, and evaporated. Compound **6** was obtained without further purification.

Colourless oil. Yield: 70-78%. ^{1}H NMR (400 MHz, chloroform-*d*): δ (ppm) 4.29 (q, *J* = 7.1 Hz, 2H), 1.34 (t, *J* = 7.1 Hz, 3H); MS: (ESI) 130.1 [M+H]$^{+}$

General procedure for the synthesis of intermediate 7a-b

To a suspension of NaH (6.76 mmol) in anhydrous CH_3CN (50 mL) cooled to -10 °C, compound **6** was added and the reaction mixture was stirred at -10 °C for 10 min. Then, the appropriate benzadehyde (2.70 mmol) was added dropwise and the solution was stirred at 0 °C for 15 min. Water was then added slowly and the reaction mixture was extracted with Et_2O (3x30 mL), washed with brine, dried over Na_2SO_4 and evaporated at reduced pressure. The crude product was purified by flash chromatography.
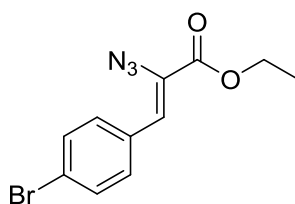
Ethyl 2-Azido-3-(4-bromophenyl)acrylate (**7a**)

Eluent: PE/EtOAc (9:1). White solid. Yield: 45-48%. ^{1}H NMR (400 MHz, chloroform-*d*): δ (ppm) 7.82 (d, *J* = 9.5 Hz, 2H), 7.61 (d, *J* = 9.5 Hz, 2H), 6.86 (s, 1H), 4.49 (q, *J* = 7.5 Hz, 2H), 1.44 (t, *J* = 7.4, Hz, 3H); MS: (ESI) m/z 293.9 [M–H]⁻
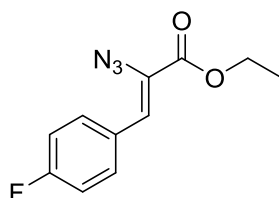
Ethyl 2-Azido-3-(4-fluorophenyl)acrylate (**7b**)

Eluent: PE/EtOAc (95:5). White solid. Yield: 48-50%. ^{1}H NMR (400 MHz, chloroform-*d*): δ (ppm) 7.86 (d, *J* = 8.7 Hz, 2H), 7.10 (d, *J* = 8.7 Hz, 2H), 6.90 (s, 1H), 4.41 (q, *J* = 7.1 Hz, 2H), 1.49 (t, *J* = 7.0 Hz, 3H); MS: (ESI) m/z 234.1 [M–H]⁻

General procedure for the synthesis of intermediates 8a-b

Intermediates **7a-b** (1 mmol) were dissolved in anhydrous xylene (5 mL) and the solution was stirred at reflux for 15 h. Then the solvent was removed under reduced pressure and the crude product was purified by flash chromatography.
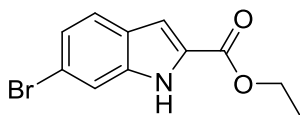
Ethyl 6-Bromo-1*H*-indole-2-carboxylate (**8a**)

Eluent: PE/EtOAc (95:5). White solid. Yield: 70-75%. ^{1}H NMR (400 MHz, chloroform-*d*): δ (ppm) 9.07 (s, 1H), 7.65 (s, 1H), 7.58 (d, *J* = 8.4 Hz, 1H), 7.32 (s, 1H), 7.22 (m, 1H), 4.57 (q, *J* = 7.6 Hz, 2H), 1.45 (t, *J* = 7.5 Hz, 3H); MS: (ESI) m/z 266.9 [M–H]$^{-}$
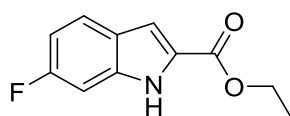
Ethyl 6-Fluoro-1*H*-indole-2-carboxylate (**8b**)

Eluent: PE/EtOAc (9:1). White solid. Yield: 73-80%. ^{1}H NMR (400 MHz, chloroform-*d*): δ (ppm) 9.12 (s, 1H), 7.65 (d, *J* = 8.7 Hz, 1H), 7.20 – 7.07 (m, 1H), 7.00 (m, 2H), 4.55 (q, *J* = 7.3 Hz, 2H), 1.53 (t, *J* = 7.3 Hz, 3H); MS: (ESI) m/z 208.0 [M–H]$^{-}$

General procedure for the synthesis of intermediates 9a-b

To a solution of compound **8a-b** (1 mmol) in anhydrous THF (20 mL) cooled to 0 °C, NaH (2.5 mmol) was added and the reaction mixture was stirred at 0 °C for 10 min. Then, chloromethyl methyl ether (1.2 mmol) was added dropwise and the solution was stirred for 15 h under N_2 atmosphere. The solvent was then removed under reduced pressure and the residue was taken up with water, extracted with DCM (3 x 30 mL), washed with a saturated solution of $NaHCO_3$, then dried over Na_2SO_4 and evaporated.
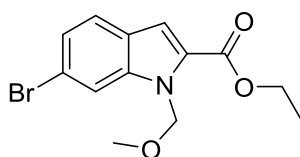
Ethyl 6-Bromo-1-(methoxymethyl)-1*H*-indole-2-carboxylate (**9a**)

No further purification. White solid. Yield 61-66%. ^{1}H NMR (400 MHz, chloroform-*d*): δ (ppm) 8.35 (s, 1H), 8.12 (d, *J* = 8.4 Hz, 1H), 7.89 (d, *J* = 8.4 Hz, 1H), 7.34 (s, 1H), 5.96 (s, 2H), 4.40 (q, *J* = 6.4 Hz, 2H), 3.34 (s, 3H), 1.29 (t, *J* = 6.4 Hz, 3H); MS: (ESI) m/z 310.3 [M–H]$^-$
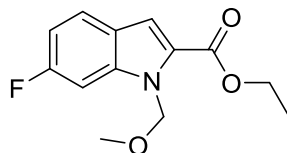
Ethyl 6-Fluoro-1-(methoxymethyl)-1*H*-indole-2-carboxylate (**9b**)

Eluent: PE/EtOAc (95:5). Yellow solid. Yield: 53-60%. ^{1}H NMR (400 MHz, chloroform-*d*): δ (ppm) 8.42 (s, 1H), 8.19 (d, *J* = 8.4 Hz, 1H), 7.99 (d, *J* = 8.4 Hz, 1H), 7.36 (s, 1H), 5.90 (s, 2H), 4.43 (q, *J* = 5.8 Hz, 2H), 3.30 (s, 3H), 1.36 (t, *J* = 5.8 Hz, 3H); MS: (ESI) m/z 250 [M–H]$^-$

General procedure for the synthesis of compounds 10a-b

To a solution of esters **9a-b** (1.00 mmol) in THF (5 mL) was added H_2O (5 mL) and lithium hydroxide monohydrate (4.00 mmol), and the reaction mixture was stirred at room temperature for 2 h. Then THF was removed under reduced pressure and the crude product was taken up with water, acidified to pH = 2 with 2 N HCl and extracted with DCM (3 x 30 mL). The organic layers were combined, washed with brine and dried over Na_2SO_4. After evaporation, compounds **10a-b** were obtained without further purification.
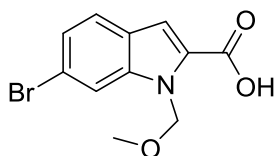
6-Bromo-1-(methoxymethyl)-1*H*-indole-2-carboxylic acid (**10a**)

White solid. Yield: 80-85%. ^{1}H NMR (400 MHz, methanol-*d*$_4$): δ (ppm) 8.44 (s, 1H), 8.02 (s, 1H), 7.89 (d, *J* = 6.5 Hz, 1H), 7.66 (d, *J* = 6.5 Hz, 1H), 5.91 (s, 2H), 3.29 (s, 3H). MS: (ESI) 282.2 [M–H]$^-$
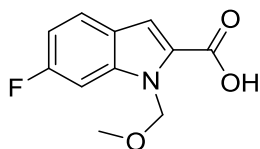
6-Fluoro-1-(methoxymethyl)-1*H*-indole-2-carboxylic acid (**10b**)

White solid. Yield: 75-82%. ^{1}H NMR (400 MHz, methanol-d_4): δ (ppm) 8.51 (s, 1H), 8.12 (s, 1H), 7.75 (m, 1H), 7.69 (m, 1H), 5.96 (s, 2H), 3.31 (s, 3H). MS: (ESI) 222.4 [M–H]$^-$

General procedure for the synthesis of GP53 and GP54

Compounds **10a-b** (1 mmol) were dissolved in anhydrous pyridine (10 mL) and EDC hydrochloride (1.5 mmol) was added to this solution. The reaction mixture was stirred for 10 min, then compound **5** (1 mmol) was added and the solution was stirred at 40 °C under N_2 atmosphere for 15 h. Then the pyridine was removed with an air stream, the residue was taken up with water and extracted with EtOAc, the organic layers were washed with 0.1 N HCl, then with brine to remove the pyridine residue, and finally dried over Na_2SO_4. After evaporation, the crude product was purified by flash chromatography.
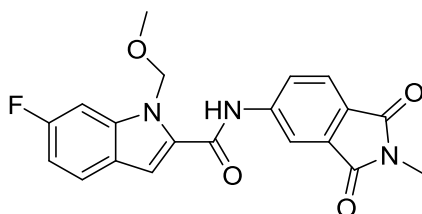
6-Fluoro-1-(methoxymethyl)-*N*-(2-methyl-1,3-dioxoisoindolin-5-yl)-1*H*-indole-2-carboxamide (**GP53**)

Eluent: PE/EtOAc (7:3). Light yellow solid. Yield: 45-48%. ^{1}H NMR (400 MHz, DMSO-d_6): δ (ppm) 10.92 (s, 1H), 8.34 (s, 1H), 8.09 (d, *J* = 7.7 Hz, 1H), 7.99 (s, 1H), 7.86 (d, *J* = 10.3 Hz, 1H), 7.71 (d, *J* = 7.7 Hz, 1H), 7.49 (s, 1H), 7.32 (d, *J* = 10.3 Hz, 1H), 5.92 (s, 2H), 3.15 (s, 3H), 3.03 (s, 3H); ^{13}C NMR (101 MHz, DMSO-d_6): δ (ppm) 168.2, 162.4, 160.8, 144.7, 139.9, 133.6, 132.3, 131.6, 126.4, 124.4, 124.2, 122.8, 114.0, 110.9, 109.4, 98.2, 74.7, 55.9, 2.2; MS (ESI): m/z 380.1 [M–H]$^-$
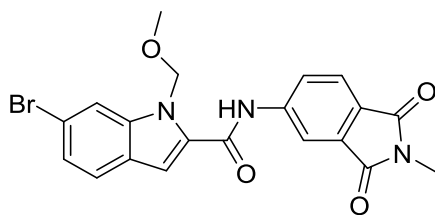
6-Bromo-1-(methoxymethyl)-*N*-(2-methyl-1,3-dioxoisoindolin-5-yl)-1*H*-indole-2-carboxamide (**GP54**)

Eluent: PE/EtOAc (8:2) and crystallization from MeOH. Light yellow solid. Yield: 45-50%. ^{1}H NMR (400 MHz, DMSO-d_6): δ (ppm) 10.98 (s, 1H), 8.33 (s, 1H), 8.09 (d, *J* = 9.1 Hz, 1H), 7.85 (d, *J* = 12.2 Hz, 1H), 7.79 (m, 1H), 7.57 (d, *J* = 9.1 Hz, 1H), 7.50 (s, 1H), 7.07(m, 1H), 5.93 (s, 2H), 3.15 (s, 3H), 3.02 (s, 3H); ^{13}C NMR (101 MHz, DMSO-d_6): δ (ppm) 168.5, 160.8, 144.5, 140.2, 133.6, 132.3, 126.5, 124.9, 124.4, 114.7, 114.0, 109.2, 74.9, 55.9, 24.1; MS: (ESI) m/z 441.2 [M–H]$^-$

General procedure for the synthesis GP55 and GP56

GP53 and **GP54** (1 mmol) were suspended in THF (5 mL) and to this was added 3 N HCl (3 mL). The reaction mixture was stirred at room temperature for 24 h and then at 100 °C for 48 h until the starting procedure was completed. The solvent was then removed under reduced pressure and the residue was taken up with water and extracted with EtOAc (3 x 15 mL). The organic layers were combined, washed with brine, dried over Na_2SO_4 and evaporated. The compounds were obtained without further purification.
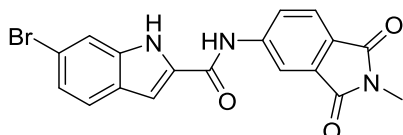
6-Bromo-*N*-(2-methyl-1,3-dioxoisoindolin-5-yl)-1*H*-indole-2-carboxamide (**GP55**)

White solid. Yield: 45-52%. ^{1}H NMR (400 MHz, DMSO-d_6): δ (ppm) 12.01 (s, 1H), 10.78 (s, 1H), 8.37 (s, 1H), 8.14 (d, *J* = 8.3 Hz, 1H), 7.87 (d, *J* = 8.2 Hz, 1H), 7.69 (d, *J* = 8.6 Hz, 1H), 7.63 (s, 1H), 7.51 (s, 1H), 7.24 (d, *J* = 8.6 Hz, 1H), 3.02 (s, 3H); ^{13}C NMR (101 MHz, DMSO-d_6): δ (ppm) 168.2, 160.3,

144.7, 138.2, 133.6, 132.0, 126.3, 125.5, 117.5, 115.3, 114.0, 105.4, 24.1; MS: (ESI) m/z 395.8 [M–H]⁻
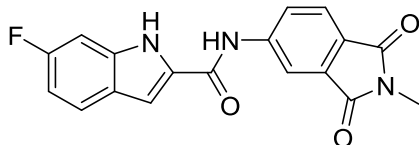
6-Fluoro-*N*-(2-methyl-1,3-dioxoisoindolin-5-yl)-1*H*-indole-2-carboxamide (**GP56**)

Light yellow solid. Yield: 48-55%. ^{1}H NMR (400 MHz, DMSO-d_6): δ (ppm) 11.98 (s, 1H), 10.81 (s, 1H), 8.39 (s, 1H), 8.17 (d, *J* = 8.2 Hz, 1H), 7.86 (d, *J* = 8.2 Hz, 1H), 7.74 (m, 1H), 7.55 (s, 1H), 7.18 (d, *J* = 8.6 Hz, 1H), 7.00 (d, *J* = 8.5 Hz, 1H), 3.02 (s, 3H); ^{13}C NMR (101 MHz, DMSO-d_6): δ (ppm) 168.6, 165.9, 162.3, 161.3, 159.4, 143.2, 136.9, 136.8, 131.9, 131.2, 128.9, 125.1, 125.1, 124.9, 124.2, 124.1, 123.0, 113.8, 111.6, 110.4, 109.4, 97.4, 97.4, 24.6; MS: (ESI) m/z 336.3 [M–H]⁻

3. PHENYLPYRIMIDINE-2,4-DIONE COMPOUNDS
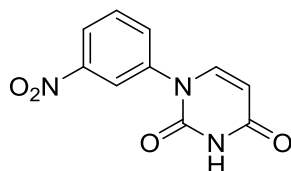
1-(Nitrophenyl)pyrimidine-2,4-dione (**13**)

Uracil (50 mg, 0.45 mmol) was vigorously stirred in 40 mL MeOH and 10 mL H_2O until it dissolved. Then nitrophenylboronic acid (150 mg, 0.9 mmol), TMEDA (104 mg, 0.9 mmol) and Cu(OAc)$_2$ hydrate (90 mg, 0.45 mmol) were added and the reaction mixture was stirred in air at room temperature for 15 h. The blue solution was evaporated under reduced pressure and then taken up with DCM, washed with water (3 x 20 mL), dried over Na_2SO_4 and evaporated. The residue was purified by flash chromatography on silica gel.

Eluent: DCM/MeOH (9:1) and crystallization from EtOAc. White solid. Yield: 66-75%. ^{1}H NMR (400 MHz, methanol-d_4): δ (ppm) 10.32 (s, 1H), 8.40 (d, *J* = 5.1 Hz, 1H), 7.89 (d, *J* = 6.4 Hz, 1H), 7.76 (t, *J* = 6.4 Hz, 1H), 7.58 (d, *J* = 6.3 Hz, 1H), 5.85 (d, *J* = 5.1 Hz, 1H); MS: (ESI) m/z 232.1 [M–H]⁻
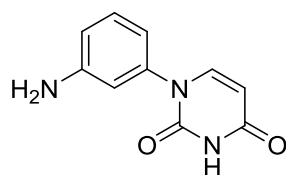
1-(3-Aminophenyl)pyrimidine-2,4-dione (**14**)

To a solution of compound **13** (30 mg, 0.13 mmol) in 5 mL methanol was added palladium on carbon (1.37 mg, 0.1 mmol), and the solution was stirred for 2 h under H_2 atmosphere. The catalyst was then filtered off over a Celite pad and the solution was evaporated under reduced pressure. The crude product was purified by flash chromatography on silica gel.

Eluent: DMC/MeOH (95:5). Yellow solid. Yield: 81-85%. ^{1}H NMR (400 MHz, DMSO-d_6): δ (ppm) 11.05 (s, 1H), 8.48 (d, *J* = 6.3 Hz, 1H), 7.89 (m, 2H), 7.76 (t, *J* = 6.4 Hz, 1H), 7.58 (d, *J* = 6.3 Hz, 1H), 6.12 (s, 2H), 5.85 (d, *J* = 5.1 Hz, 1H); MS: (ESI) m/z 204.1 [M+H]$^+$, 226.3 [M+Na]$^+$

General procedure for the synthesis of GP62 and GP63

Compound **3a** or **3b** (1 mmol) was dissolved in anhydrous pyridine (8 mL) and EDC hydrochloride (1.5 mmol) was added to this solution. The reaction mixture was stirred for 10 minutes, then compound **5** (1 mmol) was added and the solution was stirred under N_2 atmosphere for 15 h at room temperature. Then the pyridine was removed with an air stream, the residue was taken up with water and extracted with EtOAc, the organic layers were washed with 0.1 N HCl, then with brine to remove the pyridine residue, and finally dried over Na_2SO_4. After evaporation, the crude product was purified by flash chromatography.
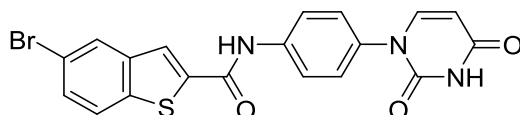
5-Bromo-*N*-(4-(2,4-dioxo-3,4-dihydropyrimidin-1-yl)phenyl)benzothiophene-2-carboxamide (**GP62**)

Eluent: PE/EtOAc (98:2). Yellow solid. Yield: 38-40%. ^{1}H NMR (400 MHz, DMSO-d_6): δ (ppm) 11.26 (s, 1H), 10.71 (s, 1H), 8.29 (s, 1H), 8.25 (d, *J* = 1.9 Hz, 1H), 8.01 (d, *J* = 2.0 Hz, 1H), 7.76 – 7.69 (m, 1H), 7.65 – 7.56 (m, 2H), 7.52 (d, *J* = 7.6 Hz, 1H), 7.43 (t, *J* = 8.0 Hz, 1H), 7.01 – 6.94 (m, 1H), 5.67 (d,

J = 7.7 Hz, 1H). ^{13}C NMR (101 MHz, DMSO-d_6): δ (ppm) 163.6, 160.4, 151.8, 142.3, 141.9, 141.3, 139.8, 139.4, 136.2, 129.6, 129.6, 128.1, 125.5, 125.3, 124.9, 121.0, 120.4, 118.7. MS: (ESI) m/z = 442.1 [M–H]$^-$
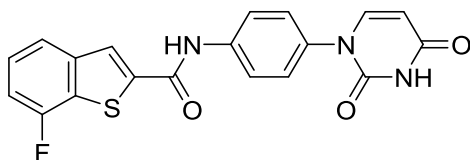
N-(4-(2,4-Dioxo-3,4-dihydropyrimidin-1(2*H*)-yl)phenyl)-7-fluorobenzothiophene-2-carboxamide (**GP63**)

Eluent: PE/EtOAc (95:5). Yellow solid. Yield: 42-45%. ^{1}H NMR (400 MHz, DMSO-d_6): δ (ppm) 11.22 (s, 1H), 10.71 (s, 1H), 8.45 (d, *J* = 3.6 Hz, 1H), 7.88 (d, *J* = 8.0 Hz, 1H), 7.82 – 7.75 (m, 2H), 7.50 (m, 2H), 7.37 (d, *J* = 7.7 Hz, 1H), 7.23 – 7.16 (m, 2H), 5.66 (d, *J* = 7.7 Hz, 1H). ^{13}C NMR (101 MHz, DMSO-d_6): δ (ppm) 166.0, 163.3, 154.9, 153.8, 151.6, 145.7, 138.7, 137.4, 135.4, 134.3, 132.6, 131.6, 130.2, 130.1, 128.8, 126.7, 126.5, 126.2, 125.0, 122.7, 122.2, 122.0, 112.2, 112.1, 101.6; MS: (ESI) m/z = 380.01 [M–H]$^-$
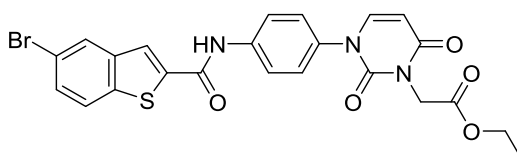
Ethyl 2-(3-(4-(5-Bromobenzothiophene-2-carboxamido)phenyl)-2,6-dioxo-3,6-dihydropyrimidin-1(2*H*)-yl)acetate (**GP64**)

GP62 (20 mg, 0.05 mmol) was dissolved in dry DMF (8 mL) and NaH (1.08 mg, 0.05 mmol) was added at 0 °C. The mixture was stirred at r.t. for 10 minutes, then ethyl bromoacetate (4.47 µL, 0.06 mmol) was added and the solution was stirred at reflux for 3 h. The mixture was then extracted with DCM (3 x 30 mL), the organic layers were combined, washed with brine, dried over Na$_2$SO$_4$ and evaporated. The crude product was purified by flash chromatography on silica gel.

Eluent: DCM/MeOH (98:2) and crystallization from MeOH. White solid. Yield= 52-58%. ^{1}H NMR (400 MHz, DMSO-d_6): δ (ppm) 10.73 (s, 1H), 8.29 (d, *J* = 1.7 Hz, 2H), 8.25 (d, *J* = 1.9 Hz, 1H), 8.01 (d, *J* = 8.6 Hz, 1H), 7.81 – 7.73 (m, 2H), 7.65 – 7.57 (m, 2H), 7.44 (t, *J* = 8.1 Hz, 2H), 6.95 (d, *J* = 7.9 Hz, 1H), 5.87 (d, *J* = 7.9 Hz, 1H), 4.60 (s, 2H), 3.68 (m, 2H), 2.46 (t, *J* = 1.8 Hz, 3H). ^{13}C NMR (101 MHz, DMSO-d_6): δ (ppm) 168.9, 162.8, 160.4, 151.5, 145.6, 142.2, 141.3, 139.8, 136.0, 129.7, 129.6, 128.1, 125.5, 124.7, 120.7, 118.7, 101.3, 52.8, 50.0. MS: (ESI) m/z 526.2 [M–H]$^-$, 561.3 [M+Cl]$^-$
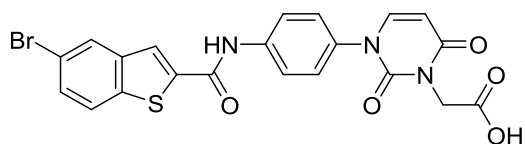
2-(3-(4-(5-Bromobenzothiophene-2-carboxamido)phenyl)-2,6-dioxo-3,6-dihydropyrimidin-1(2*H*)-yl)acetic acid (**GP67**)

GP64 (60 mg, 0.11 mmol) was dissolved in THF/H$_2$O 1:1 (8 mL) and LiOH·H$_2$O (5.7 mg, 0.13 mmol) was added. The suspension was stirred at room temperature for 2 h and then the solvent was removed under reduced pressure. The residue was extracted with DCM (3 x 20 mL), washed with brine, dried over Na$_2$SO$_4$ and evaporated. **GP67** was obtained without further purification.

White solid. Yield: 67-72%. ^{1}H NMR (400 MHz, DMSO-d_6): δ (ppm) 10.72 (s, 1H), 8.29 (d, *J* = 1.7 Hz, 1H), 8.25 (d, *J* = 1.9 Hz, 1H), 8.02 (d, *J* = 8.7 Hz, 1H), 7.79 – 7.74 (m, 2H), 7.64 – 7.58 (m, 2H), 7.44 (t, *J* = 8.1 Hz, 1H), 6.95 (d, *J* = 7.9 Hz, 1H), 5.84 (d, *J* = 7.9 Hz, 1H), 4.47 (s, 2H), 3.29 (s, 1H); ^{13}C NMR (101 MHz, DMSO-d_6): δ (ppm) 169.8, 163.0, 162.9, 160.4, 151.5, 145.8, 142.5, 139.8, 136.1, 129.7, 128.1, 125.4, 124.7, 120.6, 118.7, 101.0, 50.7; MS: (ESI) m/z 498.2 [M–H]$^-$

4. PYRROLE- AND THIOPHENE-BASED COMPOUNDS
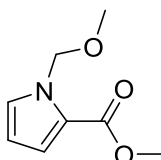
Methyl 1-(Methoxymethyl)-1*H*-pyrrole-2-carboxylate (**16**)

Methyl pyrrole-2-carboxylate (200 mg, 1.6 mmol) was dissolved in anhydrous THF (10 mL) with stirring at 0 °C, to which NaH (96 mg, 4 mmol) was added. The mixture was stirred at 0 °C for 10 min, then chloromethyl methyl ether (150 μL, 1.92 mmol) was added dropwise. The solution was stirred at room temperature for 24 h under N$_2$ atmosphere. THF was then removed under reduced pressure and the crude product was extracted with DCM (3 x 30 mL), washed with brine, dried over Na$_2$SO$_4$ and evaporated. Compound **16** was obtained without further purification.

Colourless oil. Yield: 84-87%. ^{1}H NMR (400 MHz, chloroform-*d*): δ (ppm) 7.35 (d, *J* = 6.3 Hz, 1H), 7.15 (d, *J* = 4.3 Hz, 1H), 6.47 (m, 1H), 5.45 (s, 2H), 3.66 (s, 3H), 3.30 (s, 3H); MS: (ESI) m/z 193.1 [M+Na]$^+$
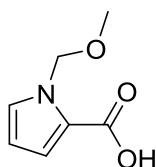
1-(Methoxymethyl)-1*H*-pyrrole-2-carboxylic acid (**17**)

To a solution of ester **16** (140 mg, 0.83 mmol) in THF (5 mL) was added H_2O (5 mL) and lithium hydroxide monohydrate (42 mg, 1 mmol), and the reaction mixture was stirred at room temperature for 2 h. Then THF was removed under reduced pressure and the crude product was taken up with water, acidified to pH = 2 with 2 N HCl, and extracted with DCM (3x30 mL). The organic layers were combined, washed with brine and dried over Na_2SO_4. After evaporation, compound **17** was obtained without further purification.

White solid. Yield: 88-93%. ^{1}H NMR (400 MHz, methanol-d_4): δ (ppm) 7.58 (d, *J* = 6.3 Hz, 1H), 7.33 (d, *J* = 4.3 Hz, 1H), 6.75 (m, 1H), 5.55 (s, 2H), 3.22 (s, 3H); MS: (ESI) m/z 154.1 [M–H]⁻

General procedure for the synthesis of GP69, GP70 and GP71

Compound **17** or thiophene-2-carboxylic acid or 2-chlorothiophene-5-carboxylic acid (0.89 mmol) was dissolved in anhydrous pyridine (10 mL) and to this solution was added EDC hydrochloride (1.34 mmol). The reaction mixture was stirred at room temperature under N_2 atmosphere for 10 minutes and then compound **5** (0.89 mmol) was added to the solution, which was stirred at room temperature under N_2 atmosphere for 16 h. The solvent was removed in air, then the crude product was taken up with water and extracted with EtOAc (3x25 mL). The organic layers were washed three times with water to remove the residue of pyridine, then with brine and dried over Na_2SO_4. After evaporation, the crude product was purified by crystallization or preparative LC.
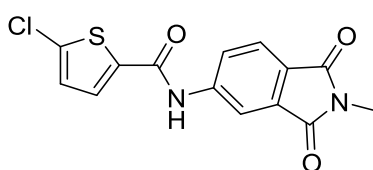
5-Chloro-*N*-(2-methyl-1,3-dioxoisoindolin-5-yl)thiophene-2-carboxamide (**GP69**)

Crystallization from MeOH. White solid. Yield: 70-74%. ^{1}H NMR (400 MHz, DMSO-d_6): δ (ppm) 10.68 (s, 1H), 8.18 (d, J = 1.9 Hz, 1H), 7.99 (d, J = 1.9 Hz, 1H), 7.91 (d, J = 4.1 Hz, 1H), 7.81 – 7.75 (m, 1H), 7.25 (d, J = 4.1 Hz, 1H), 2.97 (s, 3H); ^{13}C NMR (101 MHz, DMSO-d_6): δ (ppm) 168.1, 168.0, 159.7, 144.2, 138.5, 135.3, 133.6, 130.5, 128.9, 126.6, 124.5, 124.4, 114.6, 24.1; MS: (ESI) 318.9 [M–H]$^-$
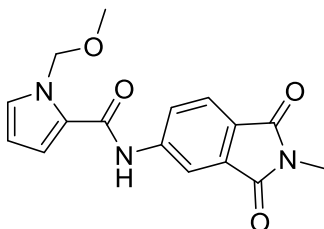
1-(Methoxymethyl)-*N*-(2-methyl-1,3-dioxoisoindolin-5-yl)-1*H*-pyrrole-2-carboxamide (**GP70**)

Preparative LC. Eluent PE/EtOAc (75:25). White solid. Yield 22-26%. ^{1}H NMR (400 MHz, DMSO-d_6): δ (ppm) 10.37 (s, 1H), 8.26 (d, J = 1.9 Hz, 1H), 8.01 (dd, J = 8.2, 1.9 Hz, 1H), 7.78 (d, J = 8.2 Hz, 1H), 7.25 (d, J = 1.7 Hz, 1H), 7.14 (d, J = 1.7 Hz, 1H), 6.19 (d, J = 2.7 Hz, 1H), 5.62 (s, 2H), 3.13 (s, 3H), 2.98 (s, 3H); ^{13}C NMR (101 MHz, DMSO-d_6): δ (ppm) 168.3, 168.2, 160.2, 145.2, 133.6, 130.1, 125.8, 125.0, 124.3, 124.1, 116.8, 113.8, 108.2, 78.3, 55.7, 29.4; MS: (ESI) 312.1 [M–H]$^-$
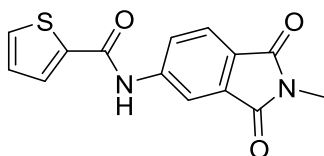
N-(2-Methyl-1,3-dioxoisoindolin-5-yl)thiophene-2-carboxamide (**GP71**)

Crystallization from MeOH. White solid. Yield 74-77%. ^{1}H NMR (400 MHz, DMSO-d_6): δ (ppm) 10.66 (s, 1H), 8.24 (d, J = 1.9 Hz, 1H), 8.07 – 8.00 (m, 2H), 7.89 (d, J = 5.0 Hz, 1H), 7.79 (d, J = 8.2 Hz, 1H), 7.22 (d, J = 5.0 Hz, 1H), 2.98 (s, 3H); ^{13}C NMR (101 MHz, DMSO-d_6): δ (ppm) 168.2, 168.0, 160.8, 144.6, 139.4, 133.6, 133.3, 130.5, 128.6, 126.4, 124.4, 124.3, 114.1, 24.1. MS: (ESI) m/z 284.8 [M–H]$^-$

Chapter 2

BACKGROUND

1. Inosine 5'-Monophosphate Dehydrogenase

Inosine 5'-monophosphate dehydrogenase (IMPDH) is a metabolic enzyme that catalyzes the guanine nucleoside biosynthesis reaction and thus plays a central role in cell growth and proliferation.[53]
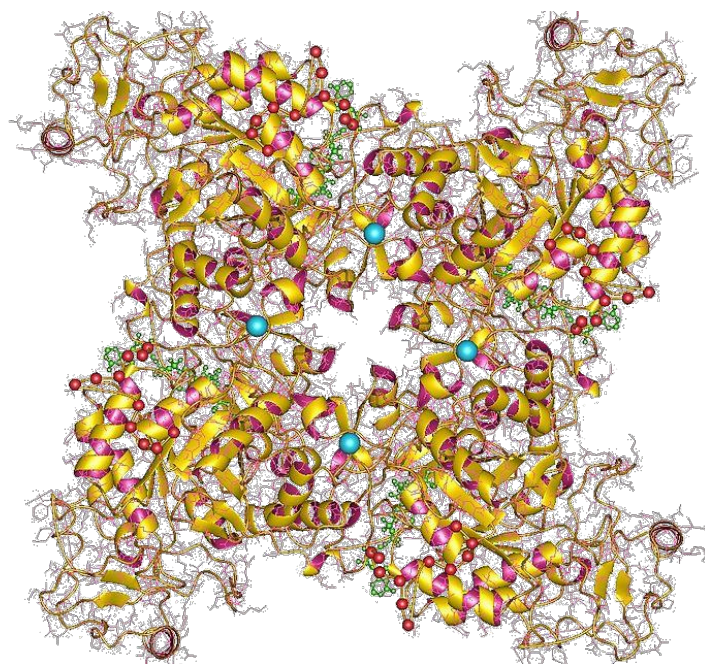
Figure 18. Structure of IMPDH enzyme

It catalyses the NAD^+-dependent oxidation of inosine 5'-monophosphate (IMP) to xanthosine 5'-monophosphate (XMP). This is a rate-limiting step in the de novo synthesis of guanine nucleotides, making it an interesting target enzyme not only for anticancer drug discovery but also for antiviral chemotherapy.[54]

The mechanism of biochemical conversion of IMP to XMP catalysed by IMPDH is initiated by a nucleophilic attack of residue Cys331 on IMP to form a covalent bond between the 2-position of IMP and the sulfhydryl group of Cys331. A hydride ion is then transferred to the cofactor NAD + to generate NADH and the intermediate E-XMP*. Subsequently, E-XMP* is hydrolyzed to release XMP (Figure 18).[55]
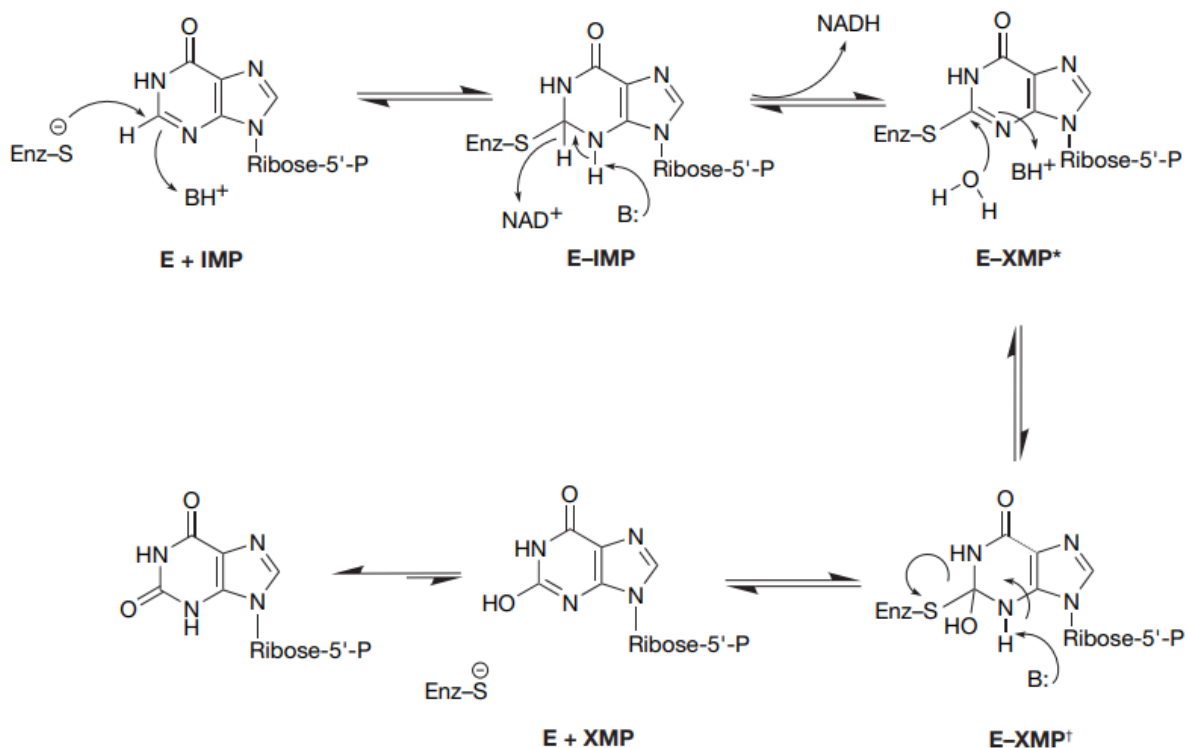
Figure 19. Mechanism of conversion of IMP to XMP by IMPDH

IMPDH is a homotetrameric enzyme consisting of 55 kDa subunits containing 514 amino acids. Two isoforms of human IMPDH have been identified, designated type I and type II. Both contain 514 amino acids and have 84% sequence identity. IMPDH is also found in bacteria and protozoa, and these forms have 30%-40% sequence identity with the human enzyme.[56]

Type I IMPDH appears to be predominant in normal human leukocytes and lymphocytes, whereas the type II enzyme is predominant in tumour and rapidly proliferating cells. However, it is likely that both enzymes contribute to the proliferative responses of lymphocytes.

Experiments have shown that IMPDH is overexpressed in activated lymphocytes and tumour cells. This is not surprising since these cells require large amounts of purine nucleotides to proliferate.

Viral replication also requires sufficient amounts of these nucleotides. It is therefore logical that inhibition of IMPDH has immunosuppressive, anticancer and antiviral properties.[56]

2. Inhibitors of IMPDH

Depending on the binding position and structure, the inhibitors of IMPDH can be divided into three groups:[57]

2.1 Mycophenolic acid and nucleotide-based compounds

Some nucleosides (Figure 19) can inhibit IMPDH as their monophosphates by competing with IMP for binding with IMPDH. Ribavirin is an example: the major event that occurs in cells exposed to ribavirin and structurally related compounds such as 5-ethynyl-1-b-D-ribofuranosylimidazole-4-carboxamide, tiazofurin, and selenazofurin is a depletion of intracellular GTP and dGTP pools as a result of inhibition of IMPDH.[58]

Together with ribavirin, which requires phosphorylation to ribavirin 5'-monophosphate to be active, EICAR (Figure 19) showed similar linear correlations between GTP pool inhibition and antiviral activity against viral RNA synthesis in four flaviviruses (dengue, yellow fever, Modoc virus and Montana myotis leukoencephalitis virus), and some paramyxoviruses.[54,59]

Ribavirin   **EICAR**
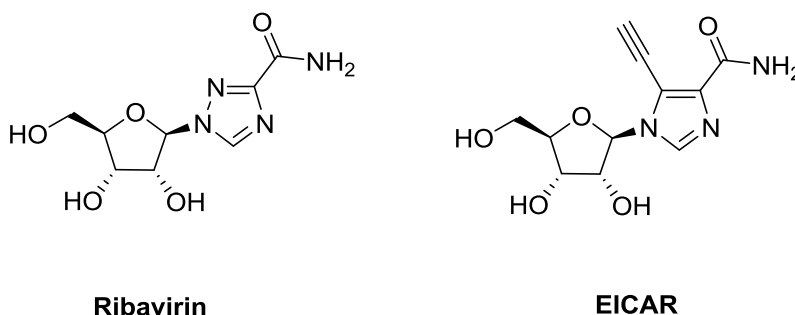
Figure 20. Structure of nucleoside-based inhibitors of IMPDH

Then, the structural modification of NAD^+ has led to the discovery of some NAD^+ site inhibitors of IMPDH. NAD^+ site inhibitors include thiazole-4-carboxamide adenine dinucleotide (TAD, the cellularly active metabolite of tiazofurin) and its analogues, which act like NAD, and mycophenolic acid (MPA). MPA was discovered in 1896 as a fermentation product of various *Penicillium* species. Enzymatic inhibition data suggest that it is a non-competitive inhibitor of IMPDH versus NAD^+: it binds to IMPDH after NADH is released but before XMP is produced. Its structure is related to NAD^+.
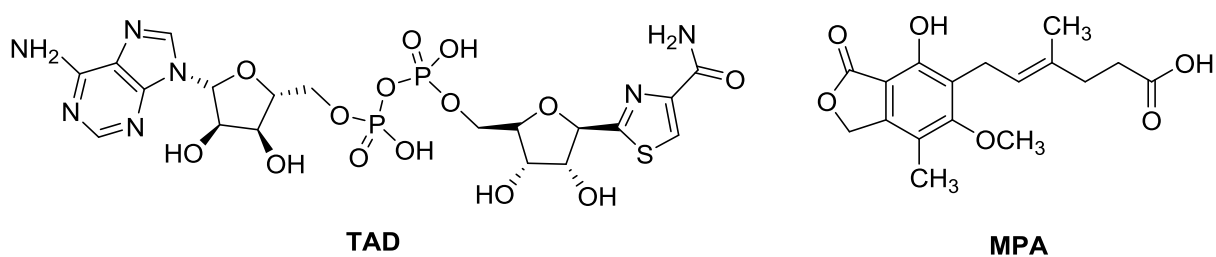
Figure 21. Structure of NAD^+ site inhibitors

MPA inhibits both isoforms of IMPDH with inhibitory rate constants (Ki) of 6±10 nM against recombinant human enzyme type II and 11±37 nM against human enzyme type I.[60] MPA and ribavirin also exhibit a broad spectrum of antiviral activity.[61]

2.2   Urea containing inhibitors

Despite the clinical efficacy of MPA and nucleotide-based drugs, their therapeutic potential has been somewhat limited by their unfavorable gastrointestinal tolerability profile. Moreover, MPA is rapidly converted to an inactive glucuronide in vivo.[62] To overcome the limitations of current IMPDH inhibitors, new IMPDH inhibitors with better tolerability have been developed at Vertex Pharmaceuticals based on the IMPDH crystal structure.

In particular, VX-497 is a small, orally bioavailable molecule that inhibits both isoforms of the IMPDH enzyme, with Ki values of 7±10 nM.
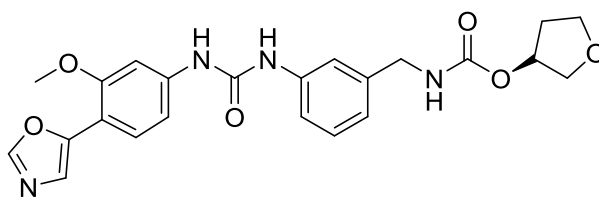
VX-497
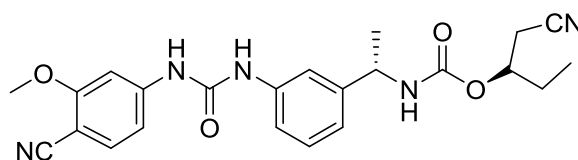
VX-198

Figure 22. Structure of VX-497 and VX-198

Several series of compounds developed by Vertex that are related to VX-497 have also been published in the patent and scientific literature. These compounds, such as VX-148 (Figure 21), are characterised by a modification of the tetrahydrofuran portion of the molecule and a small alkyl substituent with a specific enantiomeric configuration attached to the methylene carbon atom.[63] VX-148 has similar immunosuppressive activity in vivo and in vitro as VX-497 and MPA. It is a potent, specific, and reversible IMPDH inhibitor in vitro.[63]

Another modification that is included in a number of issued U.S. patents for the urea-based IMPDH inhibitors is the introduction of acyl groups into the carbamate that can function as prodrugs. Most of them are prodrugs of VX-497 (Figure 22).
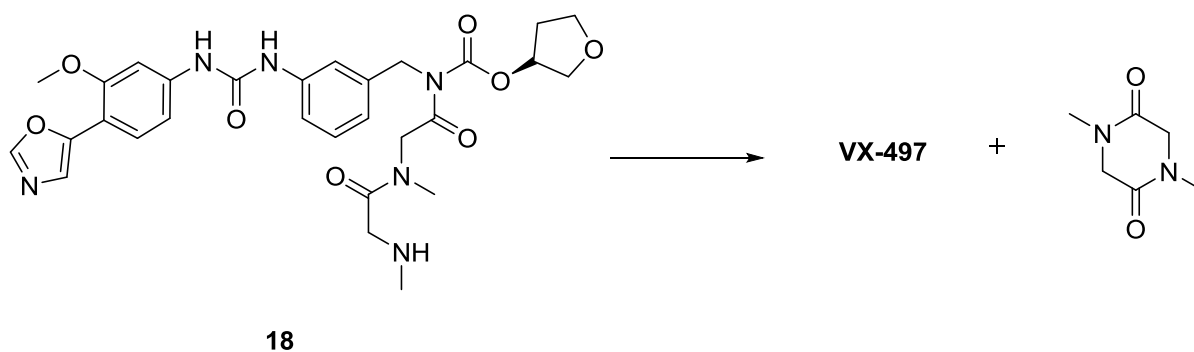
Figure 23. Urea inhibitor of IMPDH **18**, prodrug of VX-497

2.3 Urea bioisosters

The urea-based MPDH inhibitors, such as VX-497, served as the basis for the development of other inhibitors by bioisosteric replacement of urea. In many cases, the 3-methoxy-4-(5-oxazolyl)phenyl group was retained, while in others it was replaced. One of the most common and successful substitutes for urea was an oxazole, and a number of compounds were synthesized. Among them, compound **19** showed good activity: it is a potent, non-competitive inhibitor of the enzyme IMPDH II (IC$_{50}$ = 16 nM).[64]

19
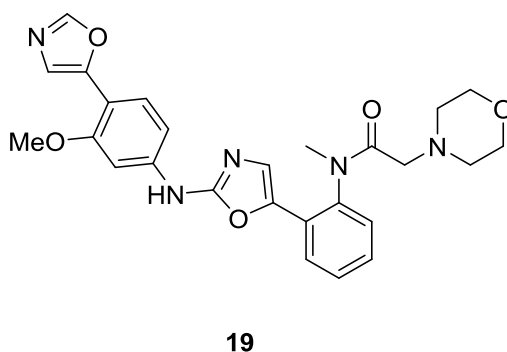
Figure 24. Structure of compound **19**

AIM OF THE WORK
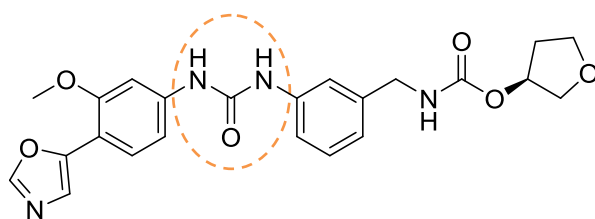
VX-497

BIOISOSTERE
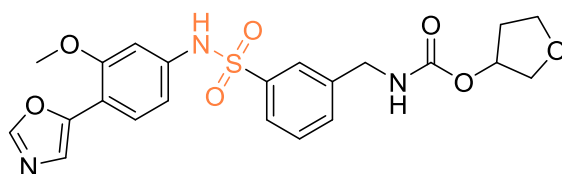
20

The aim of this work was to synthesize a new potential inhibitor of iMPDH, the bioisoster of VX-497, in which a sulfonamide group was introduced instead of urea.

The -SO$_2$NH- group is of great importance in modern medicinal chemistry because sulfonamides can be easily chemically modified and even small changes can lead to an improved version of an existing drug. Sulfonamides can be considered "molecular chimeras" because they can form hydrogen bonds as well as interact with unipolar environments in proteins.[65]

CHEMISTRY

To synthesize the first part of compound **20**, 2-methoxy-4-nitrobenzaldehyde was dissolved in methanol and then toluenesulfonylmethyl isocyanide (TOSMIC) and potassium carbonate were added. The solution was stirred at reflux for three hours to give compound **21** (Scheme 8).
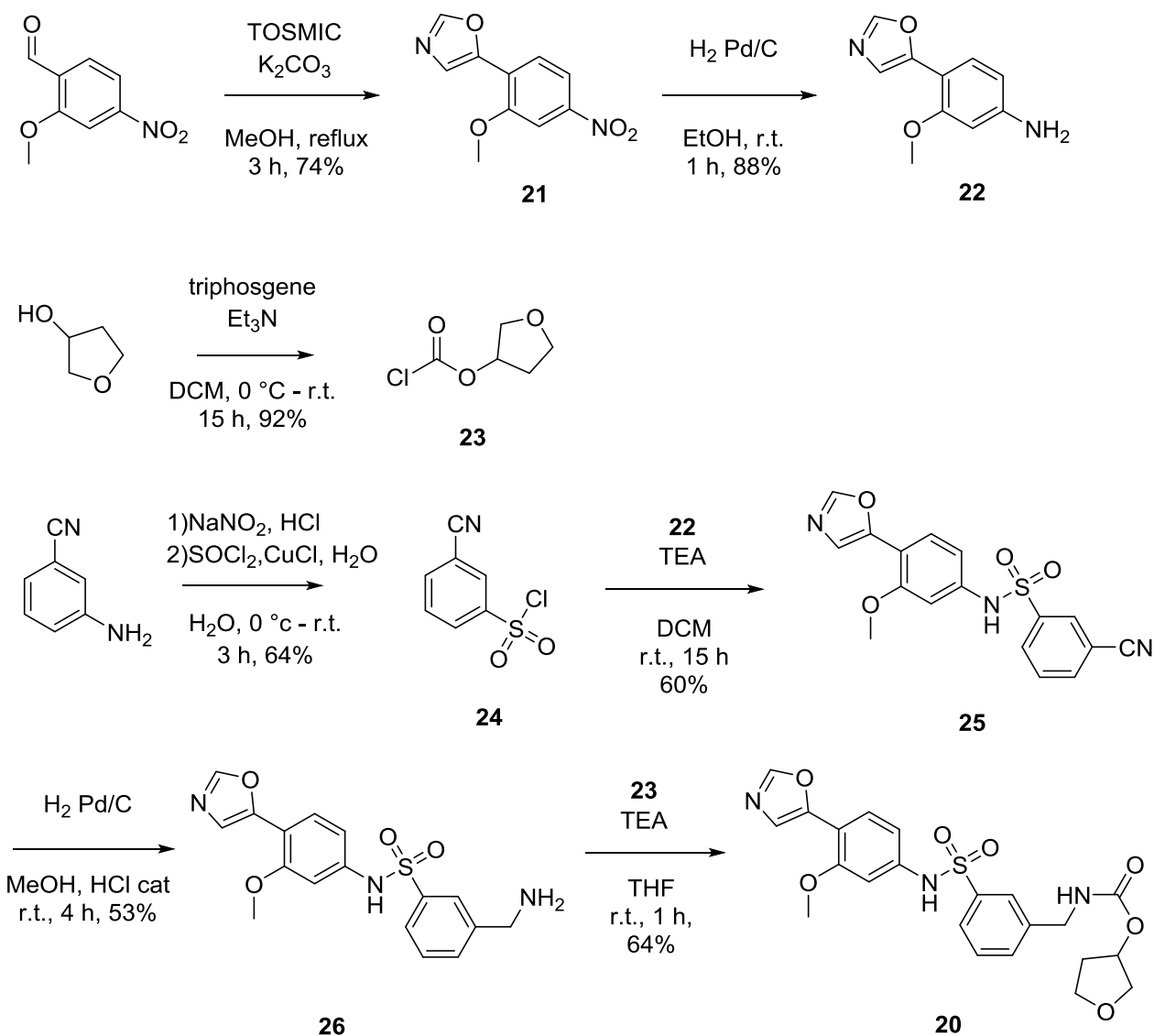
Scheme 8. Synthesis of compound **20**

Compound **21** was then reduced with H₂ and Pd/C in ethanol and the first synthon of the molecule was synthesized.

For the last part of the molecule, tetrahydrofuran-3-ol and Et₃N were dissolved in DCM and, using an ice bath, triphosgene was added dropwise. The solution was then stirred at room temperature for 15 hours to give compound **23**.

For the central core of the molecule, 3-cyanoaniline was used to carry out a variation of the Sandmeyer reaction (Figure 24).[66] The use of fully aqueous acidic conditions for the generation and reaction of the diazonium ion intermediates, combined with the use of thionyl chloride as a source of sulfur dioxide, has been shown to be advantageous for the preparation of a series of

electron-deficient or electron-neutral arylsulfonyl chlorides (Figure 24). The arylsulfonyl chlorides precipitate directly from the reaction mixture in good yield and high purity.
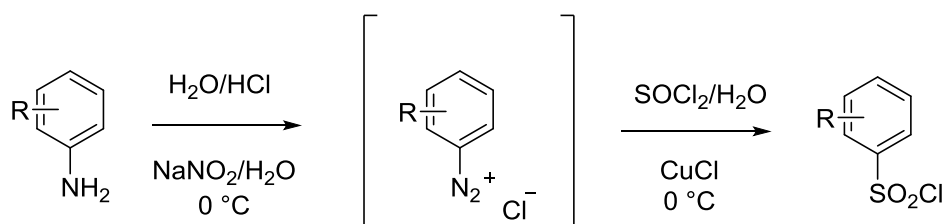
Figure 25. Reaction of transformation of aniline into arylsulfonyl chlorides.

To perform the above reaction, 3-cyanoaniline was dissolved in H_2O/HCl and a solution of $NaNO_2$ in H_2O was added dropwise. The obtained solution was stirred at 0 °C for 30 min to form the diazonium salt. Then CuCl and a solution of $SOCl_2$ in H_2O were added and the reaction mixture was stirred until compound **24** precipitated (Scheme 8).

Compound **25** was obtained from the reaction between compounds **24** and **22** in DCM. The cyano group was then reduced to the amine using H_2, Pd/C and HCl as catalyst and finally the last reaction between compound **26** and **23** led to the desired compound **20**.

CONCLUSIONS

Compound **20** is a bioisoster of **VX-497** and may be a novel inhibitor of the IMPDH enzyme: it will be tested in an in vitro assay as soon as possible. Compared to **VX-497**, compound **20** is a racemic mixture (the tetrahydrofuranol used is not enantiomerically pure), and resolution of the racemate will occur at a later time when assays have shown that the molecule is active. The sulfonamide moiety can establish new interactions and confer good pharmacological properties such as solubility or permeability. Blocking the IMPDH enzyme could be a good strategy to fight viruses and cancer and pave the way for the development of new drugs.

EXPERIMENTAL PROCEDURES

General information

Reagents were purchased from commercial suppliers (e.g., Sigma-Aldrich). All commercially available chemicals were used as purchased and without further purification. DCM was dried over sodium hydride and THF and dioxane were dried over Na/benzophenone before use. The anhydrous reactions were carried out under a positive pressure of dry N_2. TLC was performed using Merck TLC plates on silica gel 60 F_{254}. Chromatographic purifications were performed on columns packed with Merk 60 silica gel, 23-400 mesh, for flash technique. ^{1}H NMR and ^{13}C NMR spectra were recorded at 400 MHz or 100 MHz using a Brucker Avance DPX400. Chemical shifts are given relative to tetramethylsilane at 0.00 ppm. Mass spectra (MS) were recorded using an Agilent 1100 LC / MSD VL system (G1946C) with a flow rate of 0.4 mL/min and a binary solvent system of 95:5 methanol/water. UV detection was performed at 254 nm. MS was recorded in positive and negative modes over the mass range 50-1500. The following ion source parameters were used: drying gas flow rate, 9 mL/min; nebulizer pressure, 40 psig; drying gas temperature, 350 °C.

5-(2-Methoxy-4-nitrophenyl)oxazole (**21**)

To a stirred solution of 2-methoxy-4-nitrobenzaldehyde (100 mg, 0.55 mmol) in 8 mL of methanol, TosMIC (toluenesulfonylmethyl isocyanide) (107 mg, 0.55 mmol) and K_2CO_3 (76 mg, 0.55 mmol) were added and the resulting solution was stirred at reflux for 3 hours. After the completion of the reaction, water (5 mL) was added dropwise while maintaining the pot temperature between 59-69 °C. The resulting slurry was cooled to room temperature and then to 5 °C using an ice bath. After

stirring at 5 °C for 30 minutes, the slurry was filtered and the precipitate (compound **21**) was washed with water and dried.

Yellow solid. Yield: 74%. ^{1}H NMR (400 MHz, chloroform-*d*): δ (ppm) 8.54 (d, *J* = 1.6 Hz, 1H), 8.01 (dd, *J* = 9.1, 1.8 Hz, 1H), 7.96 (d, *J* = 8.9 Hz, 1H), 7.74 (d, *J* = 1.7 Hz, 1H), 7.71, (d, *J* = 13.3 Hz, 1 H), 3.84 (s, 3H); MS: (ESI) m/z 221.7 [M+H]$^+$
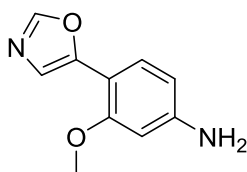
3-Methoxy-4-(oxazol-5-yl)aniline (**22**)

To a solution of compounds **21** (90 g, 0.47 mmol) in ethanol (50 mL) was added Pd/C (4.25 mg, 0.04 mmol) and the reaction mixture was stirred for 1 h under H$_2$ atmosphere. Then the catalyst was filtered off over a Celite pad and the solution was evaporated to give compound **22**.

Yellow solid. Yield: 88%. ^{1}H NMR (400 MHz, chloroform-*d*): δ (ppm) 8.54 (d, *J* = 1.6 Hz, 1H), 7.76 (d, *J* = 1.5 Hz, 1H), 7.68 (d, *J* = 8.1 Hz, 1H), 6.53 (dd, *J* = 8.1, 2.0 Hz, 1H), 6.48 (d, *J* = 1.8 Hz, 1H), 4.50-4.44(m, 2H), 3.82 (s, 3H); MS: (ESI) m/z 191.17 [M+H]$^+$
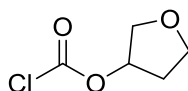
Tetrahydrofuran-3-yl-carbonochloridate (**23**)

3-Hydroxy-tetrahydrofuran (45 μL, 0.56 mmol) was added at 0 °C to a stirred solution of TEA (157 μL, 1.12 mmol) in DCM (2 mL). Then, a solution of triphosgene (498 mg, 1.68 mmol) in DCM (3 mL) at 0 °C was added dropwise to the reaction mixture and this was stirred at room temperature for 15 hour. After the completion of the reaction, the solvent was removed at vacuum and the crude taken up with Et$_2$O (5 mL). Et$_3$N HCl was precipitated and removed by filtration. The filtrate was concentrated at vacuum and compound **23** was purified with flash chromatography.

Eluent: PE:EtOAc (8:2). Colourless oil. Yield: 92%. ^{1}H NMR (400 MHz, chloroform-*d*): δ (ppm) 5.11 (m, 1H), 3.99 – 3.90 (m, 2H), 3.89 – 3.82 (m, 2H), 2.26 (d, *J* = 3.2 Hz, 1H), 2.17 (d, *J* = 3.0 Hz, 1H).
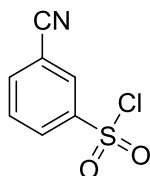
3-Cyanobenzenesulfonyl chloride (**24**)

Solution A: Thionyl chloride (152.3 μL, 2.1 mmol) was added dropwise over 60 min to water (900 μL), cooled to 0 °C, maintaining the temperature of the mixture 0-7 °C. The solution was stirred at room temperature over 3 h. Then, copper(I) chloride (catalytic amount) was added to the mixture, and the resultant yellow-green solution was cooled to -3 °C using an acetone/ice bath.

Solution B: Hydrochloric acid (36% w/w, 462 μL) was added, with agitation, to 3-cyanoaniline (40 mg, 0.21 mmol), maintaining the temperature of the mixture at 5 °C with ice cooling. The reaction mixture was cooled to -5 °C using an ice/acetone bath and a solution of sodium nitrite (16 mg, 0.23 mmol) in water (300 μL) was added dropwise over 30 min, maintaining the temperature of the reaction mixture between -5 to 0 °C: the resultant slurry was stirred at 0 °C for 30 minutes. Solution B was added to solution A over 30 minutes, maintaining the temperature of the reaction mixture at 0 °C. As the reaction proceeded, a solid began to precipitate. When the addition was complete, the reaction mixture was agitated at room temperature for 1 h. The suspended solid was collected by vacuum filtration, washed with water (2 × 5 mL), and dried under vacuum to give compound **24**.

Yellow solid. Yield: 64%. ^{1}H NMR (400 MHz, chloroform-*d*): δ (ppm) 8.24 (t, *J* = 1.8 Hz, 1H), 8.11 (dd, *J* = 7.3, 2.2 Hz, 1H), 7.85 (d, *J* = 6.4 Hz, 1H), 7.64 (d, *J* = 6.3 Hz, 1H); MS: (ESI) m/z 202.7 [M+H]$^+$, MS: (ESI) 200.6 [M–H]$^−$
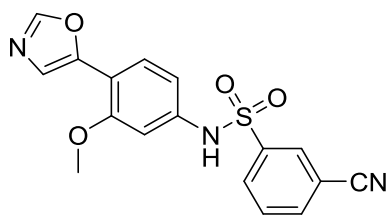
3-Cyano-*N*-(3-methoxy-4-(oxazol-5-yl)phenyl)benzenesulfonamide (**25**)

To a solution of compound **22** (43 mg, 0.23 mmol) and TEA (40 μL, 0.29 mmol) in DCM (3 mL) at 0 °C, a solution of compound **24** (100 mg, 0.45 mmol) in DCM (2 mL) was added dropwise and the reaction mixture was stirred at room temperature for 15 hours. Then, the solution was diluted with water and extracted with DCM (3 x 10 mL). The organic layers were combined, washed with a solution of 5% HCl and dried over Na_2SO_4.

Crystallization from EtOAc. White solid. Yield: 60%. ^{1}H NMR (400 MHz, chloroform-*d*): δ (ppm) 9.90 (s, 1H), 8.42 (d, *J* = 1.6 Hz, 1H), 8.23 (t, *J* = 2.0 Hz, 1H), 8.01 (dd, *J* = 2.2, 1.1 Hz, 1H), 7.86 (dd, *J* = 2.2, 1.1 Hz, 1H), 7.76 (d, *J* = 1.6 Hz, 1H), 7.70 (d, *J* = 8.2 Hz, 1H), 7.65 (d, *J* = 7.6 Hz, 1H), 7.10 (d, *J* = 8.2 Hz, 1H), 6.80 (d, *J* = 1.9 Hz, 1H), 3.84 (s, 3H); MS: (ESI) 354.1 [M–H]⁻
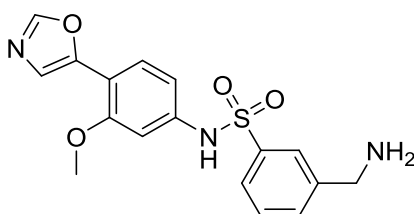

3-(Aminomethyl)-*N*-(3-methoxy-4-(oxazol-5-yl)phenyl)benzenesulfonamide (**26**)

To a solution of compund **25** (35.5 mg, 0.1 mmol) in methanol (30 mL), Pd/C (1.06 mg, 0.01 mmol) and 2 drops of HCl (36% w/w) were added and the reaction mixture was stirred under H_2 atmosphere for 4 hours. Then, the catalyst was filtered off on a celite pad and the filtrate was concentrated at vacuum. Compound **26** was obtained after crystallization.

Crystallization from EtOAc. Yellow solid. Yield: 53%. ^{1}H NMR (400 MHz, DMSO-*d₆*): δ (ppm) 10.02 (s, 1H), 8.53 (d, *J* = 1.6 Hz, 1H), 7.90 (d, *J* = 2.1, 1H), 7.81 (m, 2H), 7.72 (d, *J* = 8.2 Hz, 1H), 7.51 (d, *J* =

8.4 Hz, 1H), 7.41 – 7.35 (m, 1H), 7.04 (d, J = 8.2 Hz, 1H), 6.74 (d, J = 1.9 Hz, 1H), 3.92 (m, 2H), 3.84 (s, 3H), 2.79 (m, 1H), 2.71 (m, 1H); MS: (ESI) 358.0 [M–H]$^-$, 360.1 [M+H]$^+$
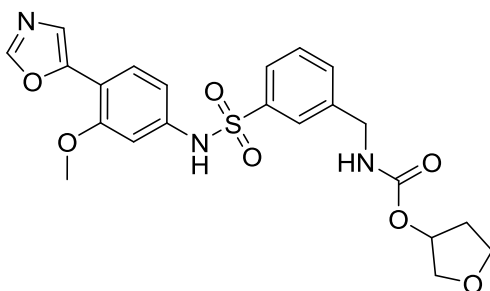
Tetrahydrofuran-3-yl (3-(*N*-(3-Methoxy-4-(oxazol-5-yl)phenyl)sulfamoyl)benzyl)carbamate (**20**)

To a solution of compound **26** (20 mg, 0.05 mmol) in THF (1.5 mL), TEA (11.6 µL, 0.08 mmol) was added: the solution was stirred at room temperature over 5 minutes and then cooled to 0 °C . Then, a solution of compound **23** (12.55 mg, 0.08 mmol) in THF (500 µL) was added dropwise, mantaining the temperature at 0 °C. The reaction mixture was stirred at room temperture for 1 hour and after the completion of the reaction it was diluted with water (10 mL) and extracted with DCM (3 x 10 mL). The organic layers were washed with water, dried over Na$_2$SO$_4$ and evaporated.

Preparative LC. Eluent: DCM/MeOH (98:2). Yellow solid. Yield: 64%. ^{1}H NMR (400 MHz, DMSO-d_6): δ (ppm) 10.61 (s, 1H), 8.34 (s, 1H), 7.83 (t, J = 6.3 Hz, 1H), 7.74 (s, 1H), 7.68 (m, 1H), 7.50 (m, 3H), 7.38 (s, 1H), 6.88 (s, 1H), 6.78 (d, J = 8.6 Hz, 1H), 5.09 (d, J = 5.6 Hz, 1H), 4.20 (d, J = 6.2 Hz, 2H), 3.83 (s, 3H), 3.77 – 3.66 (m, 3H), 3.64 (d, J = 10.3 Hz, 1H), 2.08 (d, J = 7.2 Hz, 1H), 1.84 (d, J = 6.9 Hz, 1H); ^{13}C NMR (101 MHz, DMSO-d_6): δ (ppm) 160.2, 158.5, 150.7, 148.3, 138.3, 137.6, 137.4, 130.9, 128.7, 128.4, 127.3, 126.1, 125.6, 120.5, 118.2, 106.3, 76.0, 72.9, 64.8, 56.1, 41.3, 29.6; MS: (ESI) 472.4 [M–H]$^-$

Chapter 3

BACKGROUND

In modern drug discovery, medicinal chemists face numerous challenges in selecting hits and developing leads. These include issues of affinity/selectivity/toxicity, the need to improve physicochemical and/or ADME properties, or the need for novelty in terms of intellectual property generation. The most widely used lead optimization techniques involve the systematic use of common bioisosteres or scaffolds ("scaffold hopping"). The goal is to discover structurally novel compounds by altering the core structure of known bioactive compounds.[55,67]

Sulfoximines, the monoaza analogues of sulfones, are relevant compounds for science and industry and have found their way into various applications.[68,69] While sulfoximines were absent from medicine and agrochemistry for decades, interest in these fields has only recently awakened, leading to the inclusion of the sulfoximidoyl group in drug and agrochemical discovery programmes.[70,71] A prerequisite for successful use is the availability of a synthetic methodology, the need for which is currently being met by academic research. Satisfying the latter need remains important and aims to establish the sulfoximidoyl group more firmly in the synthetic toolbox of chemists in industry and academia in general.[72]
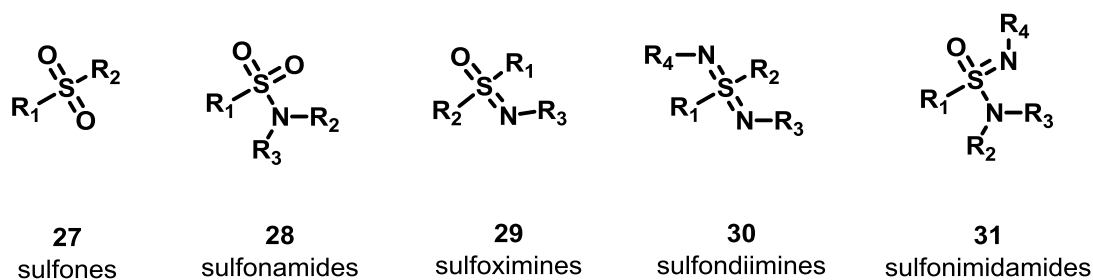
Figure 26. General structures of isosteres of sulfur-containing functional groups

1.1 The Sulfoximidoyl Group

In chemistry, sulfoximines, or strictly according to IUPAC sulfoximides, comprise a class of compounds in which the corresponding molecules have the structure $R_2S(=O)=NR$ (Figure 25).[73] The sulfoximidoyl moiety itself has long been neglected in fields such as medicinal and agricultural chemistry. This neglect is surprising, as the sulfoximidoyl moiety has a number of interesting properties and has generally been shown to be suitable for use in pharmaceuticals and agricultural chemicals.[74] Relevant properties of sulfoximines include constitutional and configurational stability, good water solubility, and, compared to sulfone analogues, the ability to use the sulfoximidoyl nitrogen as an additional substitution point.[75] The stability of the compound class includes chemical and metabolic stability, resistance to hydrolysis, and microsomal digestion.[76] As for the solubility of sulfoximines in water, it has been reported that the replacement of related groups such as sulfonyl and sulfonamidoyl moieties with the sulfoximidoyl moiety tends to increase the solubility of the group containing analogous compounds in aqueous media. Other important properties include the ability of the group to accept hydrogen bonding through the S=O and S=N units and the ability to donate hydrogen bonds through the N-H bond in N-unsubstituted sulfoximines.[67] Metal coordination is also well established at or near the chemical moiety of interest.[77]

As described in a paper by Frings et al, the sulfoximidoyl group has no 'intrinsic shortcomings' as an element that can be integrated for use in drug and agrochemical discovery programs, but instead exhibits a number of interesting properties and great potential for such applications.[76] Given the importance of innovation and expanding the chemical space used for drug and agrochemical development,[78] the problems associated with the lack of attention to the sulfoximidoyl group need to be overcome and are therefore currently being addressed by the academic research community. The lack of synthetic methods, commercial availability, and knowledge of the physicochemical properties of the group is generally associated with the state of neglect described above.[74] Thus, one goal of academic research is to acquire knowledge in this area and establish new or optimized synthetic methods for the preparation of sulfoximines and/or their structural modification.[68,79,80,81] The development of synthetic methods may then, in turn, enable applications in areas beyond basic research that can benefit from the expansion of the chemical space.[82]

1.2 Application of sulfoximines

To date, there are no approved drugs based on sulfoximines/sulfonimidamides, largely due to the limited synthetic methods available to prepare these functional groups and the lack of understanding of their properties in the context of medicinal chemistry.[67] With the advent of increasingly new and safe synthetic methods, interest in the structure of sulfoximines and derivatives continues to grow.[83,84]

Compounds **32** and **33** (Figure 26), obtained by replacing the sulfone group with sulfoximine and sulfondiimide, respectively,[85] were shown to be inhibitors of the Bromodomain and Extra-Terminal (BET) motif in myeloid cell lines and primary cells from patients with acute myeloid leukemia, a heterogeneous disease characterized by differentiation blockade and uncontrolled proliferation of hematopoietic stem and progenitor cells.[86] The BET proteins have multiple functions, including initiation and elongation of transcription and regulation of the cell cycle. Interestingly, BET inhibitors exhibit selectivity for tumor cells by preferentially binding to superenhancers, noncoding regions of DNA that are critical for transcription of genes that determine a cell's identity.[87]

Furthermore, unlike PFI-1, compounds **32** and **33** are chiral, which allows further investigation of the individual enantiomers.[88]
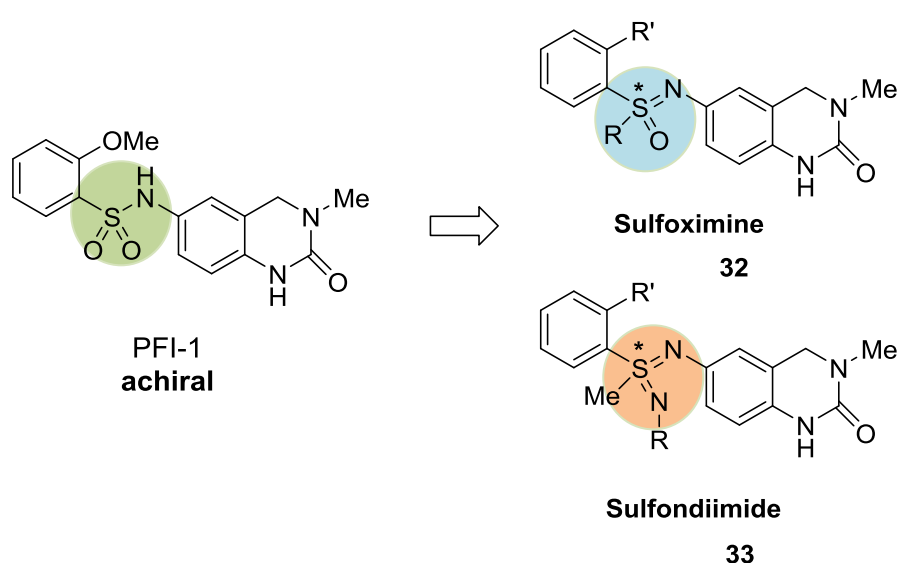
Figure 27. Isosteric replacement of sulfone group with sulfoximine and sulfondiimide moieties in BET inhibitors

In addition to their potential as anticancer agents, sulfoximines have also been used as insecticides.[89,84] Sulfoxaflor (**34**, Figure 27), approved in 2013, was the first commercially available sulfoximine-based insecticide and can therefore be considered a pioneering compound for the use of sulfoximines in medicinal chemistry.[90] It acts as a neonicotinoid by competitively modulating the nicotinic acetylcholine receptor (nAChR), resulting in uncontrolled nerve impulses and subsequently muscle tremors followed by paralysis and death.[91] Sulfoxaflor also has a broader spectrum of control for sap-feeding insects (e.g., aphids, whiteflies, and grasshoppers) than other insecticides, while exhibiting increased UV stability and thus enhanced residual insect control.[92]
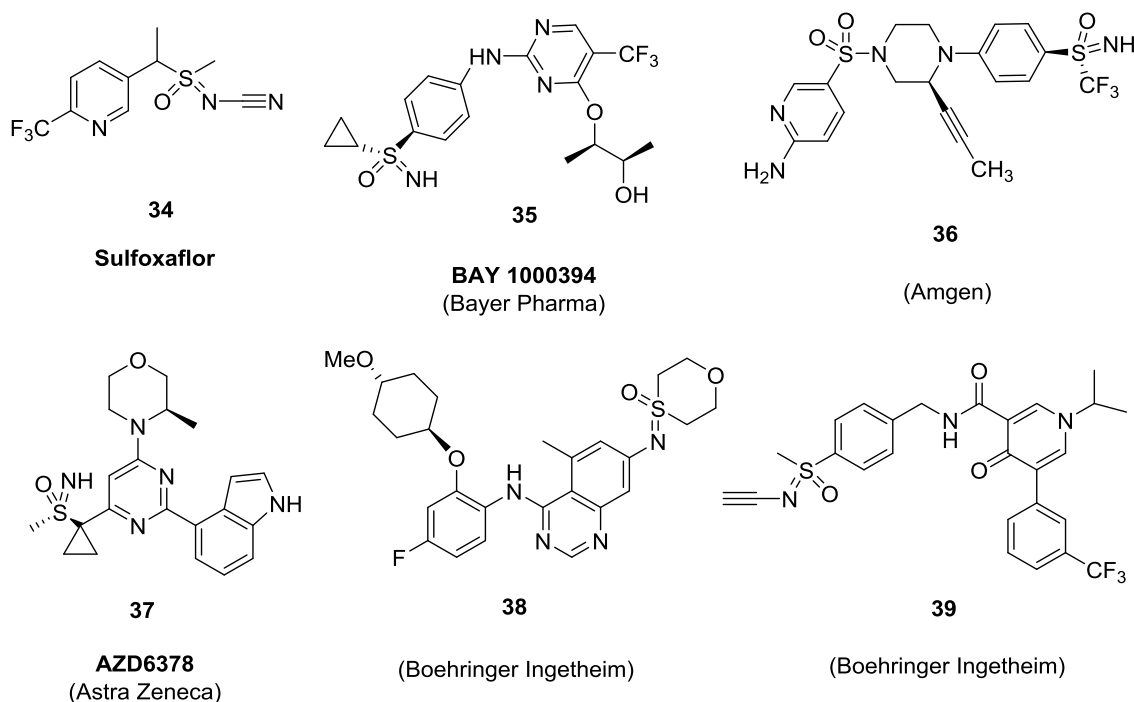
Figure 28. Structure of sulfoximines with potential medical application

.

More recently, other sulfoximins with potential medical applications have been published, such as Amgen's GKRP disruptor **36**,[93] Astra Zeneca's ATR inhibitor **37**,[94] and the MNK inhibitor **38**[95] and human neutrophil elastase inhibitor **39**,[96] both published by Boehringer Ingelheim (Figure 27).

1.3 The allenyl moiety

To date, more than 150 natural products and pharmaceuticals containing an allene component have been identified.[97] In the last two decades, allenes have also proven to be versatile starting

materials for organic synthesis. Structurally, the unit under consideration consists of three carbon atoms lying on one axis and connected by two carbon-carbon double bonds. According to the valence rules, the two outer carbon atoms of the three-carbon axis must bear two additional substituents, so that the two planes containing the terminal atoms and the two respective carbon atoms of the substituents to which they are attached are orthogonal.[98] Compared to the alkenes and alkynes, the allenes are unsaturated hydrocarbons with axial chirality: their unique stereochemistry makes them interesting substrates for stereoselective syntheses or for processes requiring stereocontrol, and the acidity of their hydrogen atoms allows easy functionalization. Moreover, because the allenes are high-energy compounds - their conjugated isomers are much more thermodynamically stable - they can serve very well as intermediates in multistep processes. Their high reactivity also makes them good candidates for use as reactants in multicomponent reactions.[99] The introduction of an allenyl moiety onto an existing molecular scaffold has the potential to improve biological and pharmacological properties. [100]

Due to limitations in synthesis, there are few examples of allene-containing compounds that are biologically active (Figure 28). Derivatives of prostaglandin E are lipid mediators that are converted from arachidonic acid by cyclooxygenase and exert anti-secretory and anti-ulcer gastrointestinal effects. The allenic prostaglandin analogue enprostil **41** proved to be a highly effective inhibitor of gastric acid secretion by selective agonism of prostaglandin E receptor subtype 3 (EP3) in various species. In addition, enprostil has an anti-inflammatory effect by suppressing the production of interleukin 8 in human colon epithelial cell lines.[101] An allene derivative of the neurosteroid allopregnanolone has anticonvulsant and antianxiety effects. Allopregnanolone has been reported to be a potent positive allosteric modulator of the action of γ-aminobutyric acid (GABA) at the GABA-A receptor,[102] and the introduction of an allene group into allopregnanolone (**43**) increased the modulatory activity of the GABA-A receptor with a 70-fold potency than allopregnanolone itself.[100]
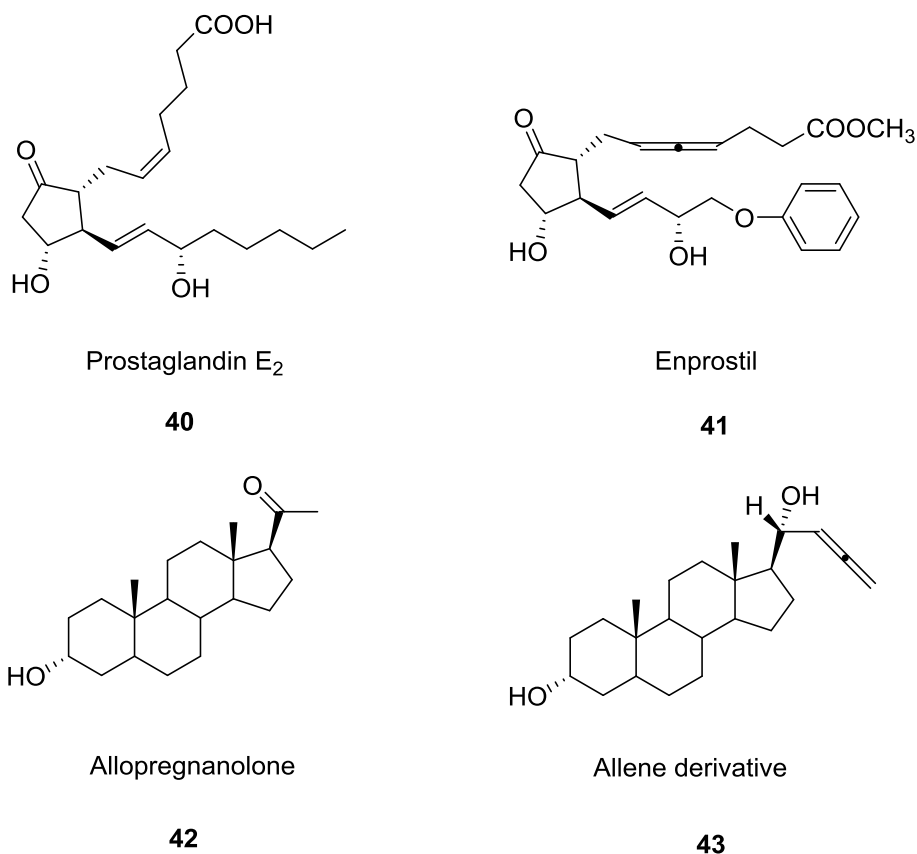
Figure 29. Example of compounds containing allene moiety biologically active

1.4 Synthesis of allenes

As mentioned at the beginning of the chapter, allenyl groups are interesting functional groups in organic chemistry and have gained importance in synthesis.[103] Since the entities under consideration are little-used chemical constituents, novel incorporations of allenyl groups into chemical structures help to expand the chemical space and make previously unknown structural combinations accessible by synthetic means. The latter expansions of the 'chemical frontier' are important drivers of innovation and development in research, industry, and academia.[104] Thus, generally applicable synthetic protocols for the preparation of allenes are needed and have therefore been established by the scientific research community.[105] Selected transformations from existing strategies are discussed in the following section. The starting points are alkynes, which are well-established compounds in organic synthesis and can be used for various transformations, the so-called sigmatropic rearrangements of the -CR_2-C≡C fragment.

.
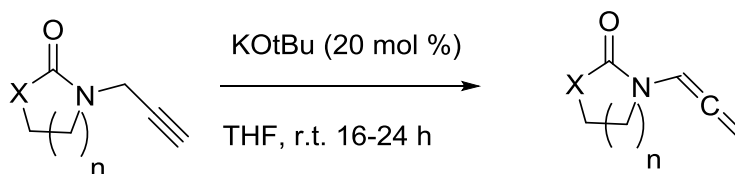
Figure 30. Synthesis of allenes

Figure 29 shows an example of a sigmatropic rearrangement using the method developed by Professor Bolm's group to introduce an allenyl functionality at the nitrogen atom of the sulfoximidoyl group. A base such as potassium tert-butoxide (KOtBu) is commonly used to initiate the reaction described.[106] This specific protocol was developed by Hsung and coworkers and has the added advantage of not requiring heating. Other approaches that have been reported do not rely on the use of a strong base but work well under mildly basic conditions.[107]

To combine the properties of sulfoximines and allenes, Professor Bolm and his colleagues at RWTH Aachen University have synthesised completely new compounds: N-allenylsulfoximine **44** and N-propanedienylsulfoximine **45** (Figure 30).

44   **45**
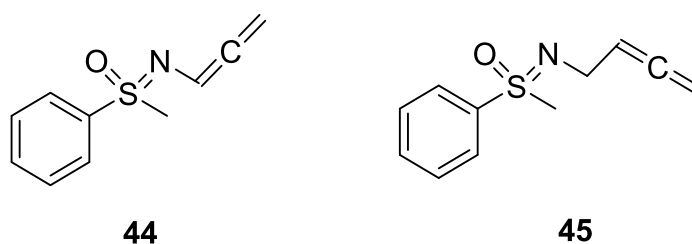
Figure 31. Allene-containing compounds synthesized by Professor Bolm's group

AIM OF THE WORK
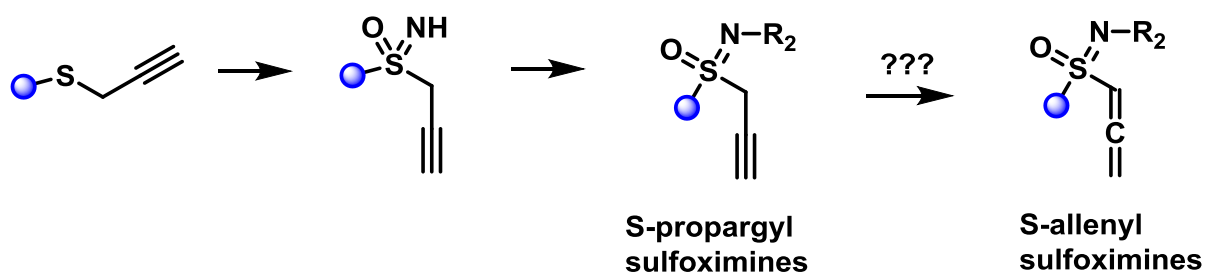
Figure 32. Synthetic strategy for the synthesis of S-allenylsufoximine

The aim of this work was to investigate a possible approach for the synthesis of S-allenylsulfoximines. For this purpose, the same procedure was tried as for the synthesis of S-propargylsulfoximines, which was successfully developed by Bolm and co-workers in Aachen. In the second part, the conversion of S-propargylsulfoximine to S-allenylsulfoximine was studied.

CHEMISTRY

In the first step, 4-chlorothiophenol was reacted with a solution of 80 wt% propargyl bromide in toluene and potassium carbonate in DMF to give compound **46** in good yield (Scheme 9).
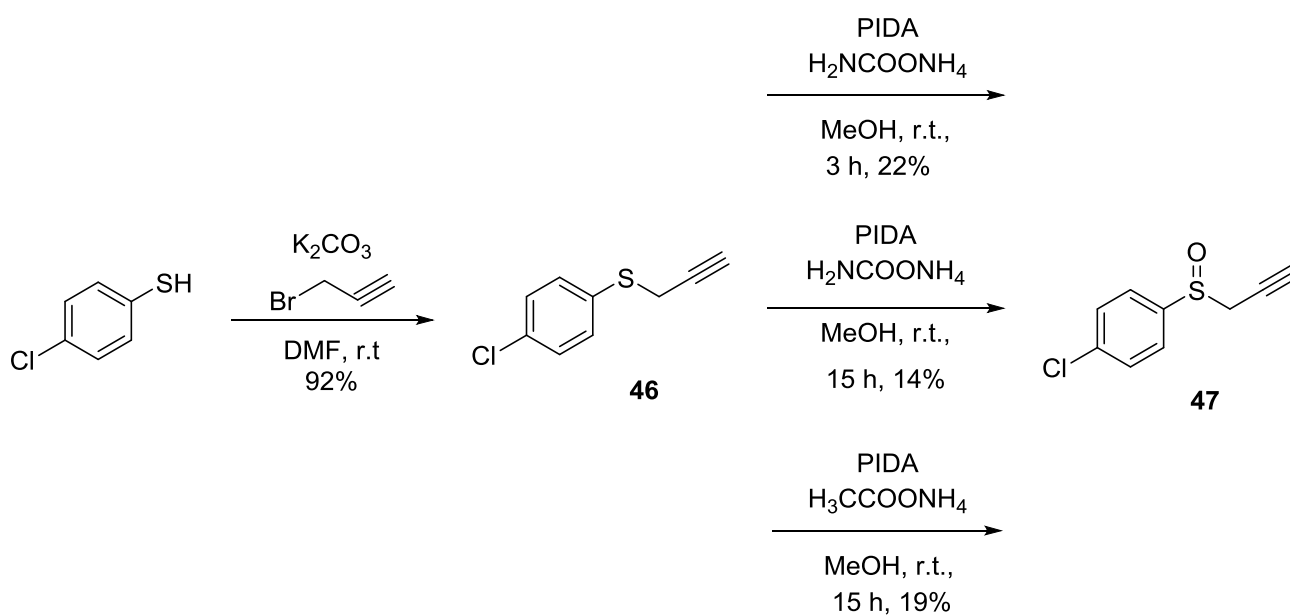
Scheme 9. Synthesis of compound 47

To obtain sulfoximine directly from compound **46**, the method described by Luisi, Bull, and co-workers[81] was tried using (diacetoxyiodo)benzene (PIDA) as the oxidizing agent and ammonium carbamate as the ammonia source. This method is a two-step one-pot reaction that should lead to direct synthesis of sulfoximine from sulfide. Unfortunately, this reaction did not lead to sulfoximine, but only to sulfoxide **47** in low yield, even when attempts were made to increase the reaction time and the ammonia source (Scheme 9).

Because of the difficulty in converting sulfide directly to sulfoximine, sulfone was used as an intermediate step, but to increase the yield, another reaction was attempted to oxidize the sulfide. Reaction of sulfide **46** with sodium metaperiodate in a mixture of H_2O/methanol (1:1) gave the desired sulfoxide **47** in good yield (Scheme 10).[108]
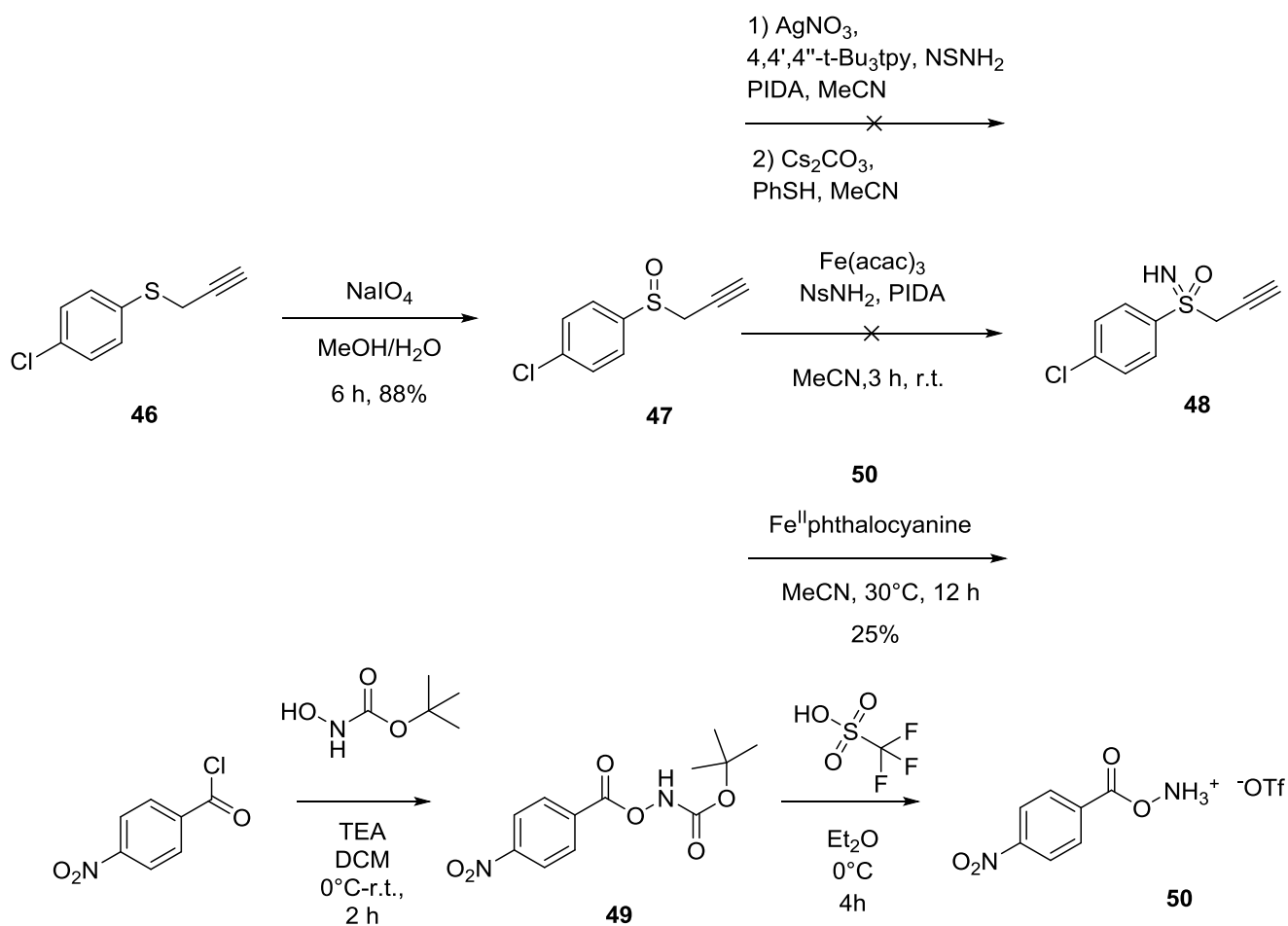
Scheme 10. Trials of synthesis of compound 48

Imination of sulfoxide **47** proved to be difficult. Various procedures were tried, as shown in Scheme 10, using different catalysts such as Ag^+ or $Fe°/Fe^{+2}$, but none of them worked as expected.[104,105] In all reactions, the starting material was recovered.

For the last imination described in Scheme 10, compound **50** had to be synthesised. The reaction between 4-nitrobenzoyl chloride and N-Boc-hydroxylamine with triethylamine in dichloromethane gave compound **49**, which was then deprotected with triflic acid to give the desired product **50** as the triflate salt.

Compound **50** was used in the imination procedure together with iron(II) phthalocyanine in acetonitrile at 30 °C,[109] which gave sulfoximine **48**, but in low yield. Even with increasing duration

of the reaction, amount of iron catalyst and temperature, the reaction always gave low and variable yield (table 11).

Table 11. Experiments on the imination of compound **47**

Entry	50 (eq)	Iron catalyst (eq)	Time	T °C	Yield
1	2.5	0.04	12h	30 °C	25%
2	2.5	0.04	48h	30 °C	11%
3	2.5	0.08	12h	30 °C	n.r.
4	2.5	0.04	12h	45 °C	n.r.

Because of the lack of reproducibility of this procedure and the low yield, other procedures were investigated.

We also tried to change the synthesis strategy: adding the triple bond at a later time, after we had synthesized the sulfoximine, would have been useful to see if the problem of elimination was in the presence of the triple bond. Unfortunately, this did not lead to the desired product: after we synthesized compound **51**, it never reacted with the magnesium bromide compound and product **52** was not obtained.
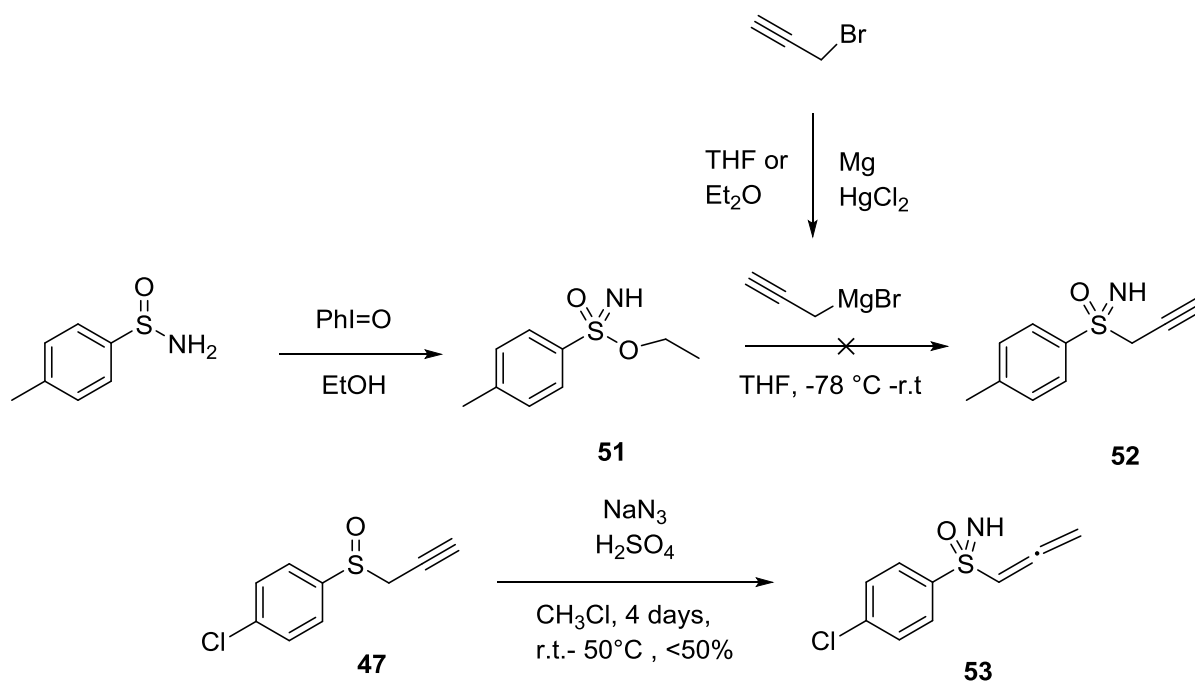
Scheme 11. Trials of synthesis of compounds 52 and 53

At the very least, the reaction described in Scheme 11 resulted not only in the imination of sulfoxide **47** but also in the isomerization of the triple bond, leading to the formation of the allene. The reaction described is a strong and dangerous imination procedure using sodium azide and sulfuric acid as reagents: the reaction must be carried out very carefully by mixing the reagents slowly and cooling the mixture in an ice bath because it is very exothermic. The yield of the reaction calculated from NMR was less than 50%, but purification of **53** was not possible because of the many impurities in the reaction and the low stability of the allene. The allene was clearly identified by NMR, as the ^{13}C NMR spectrum of the internal carbon showed a typical signal at 210 ppm.

Because of the difficulties in purification and the hazardous nature of this reaction, other methods of obtaining the sulfoximine were tried, since it was recognised that the allene compound seemed to be the product of the imination rather than the alkyne compound.

So, the reaction described in Scheme 12 was carried out and in this case also the allene (compound **54**) was obtained. Only a few traces of compound **54a** were observed. In the reaction, rhodium was used as catalyst and a protected sulfoximine was obtained because trifluoroacetamide was used as nitrogen source.

In this case, purification was possible and compound **54** was obtained with a yield of 80%.
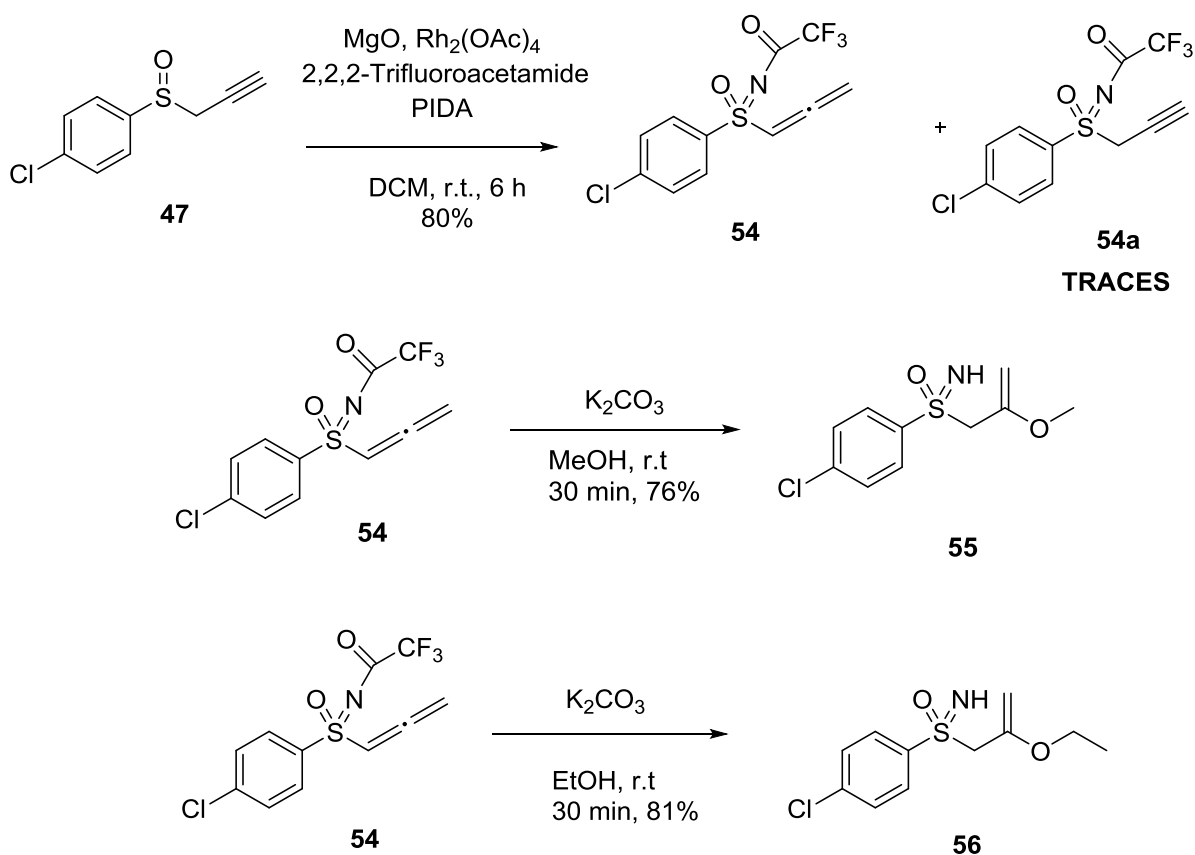
Scheme 12. Synthesis of compound 54, 55 and 56

In the reaction of deprotection of sulfoximine with potassium carbonate in methanol, the allene moiety reacted with the solvent to form compound **55** (scheme 12). This is because allenes are very reactive to nucleophiles and different types of NH sulfoximines can be synthesized with different nucleophiles. When we tried the reaction just described with ethanol instead of methanol, we obtained compound **56** (scheme 12).

Compound **54** can be used as a good starting point for reactions to convert the allene

For example, the reaction of compound **54** with a sulfur nucleophile can lead to new compounds: As shown in scheme 13, the reactive form PhSNa was formed in situ and reacted with the allene.[107] This reaction also led to the deprotection of the sulfoximine, giving compound **57** and

confirming that the N-trifluoroacetyl group can be easily removed to give synthetically useful NH-sulfoximines.
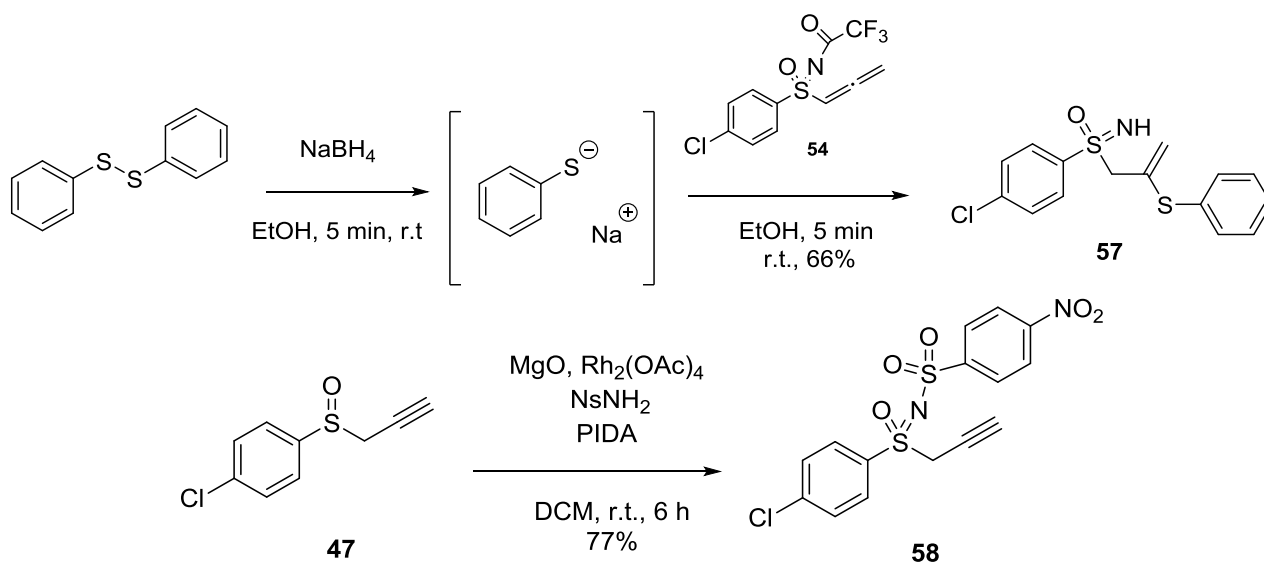
Scheme 13. Synthesis of compound 57 and 58

Finally, an attempt was made to change the protecting group to see if the allene was formed with other groups. The reaction described in Scheme 13 was carried out. The same procedure was used to try to introduce the nosyl group and in this case the isomer is formed with the triple bond instead of the allene. Perhaps the nosyl group stabilizes the triple bond instead of the allene.

CONCLUSIONS

During my stay abroad at the University of Aachen, the reactions leading to the formation of S-allylsulfoximine were studied. Sulfoximine **54** was synthesized, a good starting point for the study of reactions in which allene formation is an intermediate step and which lead to the synthesis of new compounds. The deprotection of compound **54** proves to be very simple and can be carried out as a two-step one-pot reaction. This study confirms that allenes can be very useful in organic chemistry when it comes to the incorporation of new units and that, thanks to research on sulfoximines, they can also be used in pharmaceutical chemistry by taking advantage of their

important properties. In the last part of the work, a new protecting group was studied. The behavior of the triple bond attached to a sulfoximine will be studied in more detail in the future.

EXPERIMENTAL PROCEDURES

General Information

All reagents were obtained commercially unless otherwise indicated, and solvents were taken from a commercial solvent purification system (SPS). Reactions were monitored by thin-layer chromatography (TLC) using Merck silica gel 60 F254 aluminum sheets, and purification was performed by flash column chromatography using Merck silica gel 60 (63-200 µm). Nuclear magnetic resonance (NMR) spectra were recorded using an Agilent VNMRS 600, Agilent VNMRS 400, AVANCE NEO 600, or AVANCE NEO 400. Chemical shifts are in parts per million (ppm) and spin-spin coupling constants (J) are in hertz (Hz). ^{1}H and ^{13}C {1 H} NMR spectra were processed and analyzed using the MestReNova program. 1H NMR spectra were measured with proton broadband decoupling, and the following abbreviations are used: s (singlet), d (doublet), t (triplet), q (quartet), br (broad), m (multiplet). The mass spectra were measured using the Finnigan SSQ Finnigan 7000 spectrometer (EI, 70 eV). High resolution mass spectra (HRMS) were measured using the Thermo Scientific LTQ Orbitrap XL spectrometer. All IR data were recorded with attenuated total reflectance (ATR) and wavenumbers ν are given in cm-1.
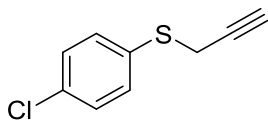
1-Chloro-4-(prop-2-yn-1-ylsulfanyl)benzene (**46**)

To a solution of 4-chlorothiophenol (500 mg, 3.47 mmol) in 8 mL DMF was added potassium carbonate (954 mg, 6.91 mmol) and the reaction mixture was stirred at room temperature for 10 minutes; then propargyl bromide (411 µL, 4.14 mmol) was added and the reaction mixture was stirred at room temperature for 4 h.

At the end of the time, H_2O was added and the reaction mixture was extracted three times with EtOAc. The combined organic layers were washed several times with water, then washed with brine, dried over Na_2SO_4 and evaporated. The product was obtained after purification by flash chromatography on silica gel.

Eluent: Pentane to Pentane/EtOAc (95:5).Yellow oil. Yield 92%. ^{1}H NMR (400 MHz, chloroform-*d*): δ (ppm) 7.43 – 7.36 (d, *J* = 1.0 Hz, 2H), 7.33 – 7.26 (d, *J* = 1.0 Hz, 2H), 3.58 (d, *J* = 0.43 Hz, 2H), 2.24 (t, *J* = 0.24 Hz, 1H); ^{13}C NMR (101 MHz, chloroform-*d*): δ (ppm) 133.4, 131.7, 129.5, 126.0, 79.6, 71.9, 22.9; MS (EI, 70 eV): m/z (%) 45.03 (14), 75.3 (10), 108.2 (57), 125.2 (22), 143.1 (86), 144.1 (30), 145.1 (34), 159.1 (15), 168.1 (21), 169.2 (10), 182.2 [M+H]$^+$ (23), 185.2 (11), 197.2 (14); MS (CI, CH$_4$): m/z (%) 144.7 (31), 147.1 (24), 147.8 (61), 181.8 (64), 182.9 [M+H]$^+$ (100), 184.0 (29), 185.0 (37), 198.9 (53); MS (ESI): m/z 182.9910 [M + H]$^+$
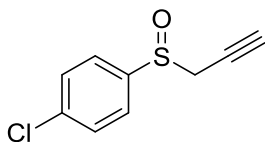
1-Chloro-4-(prop-2-yn-1-ylsulfinyl)benzene (**47**)

To a stirred solution of sodium metaperiodate (196 mg, 0.5 mmol) at 0 °C in 2 mL H_2O was added a solution of compound **46** (100 mg, 0.54 mmol) in methanol (2 mL), and the reaction mixture was vigorously stirred for 4 h at room temperature. After completion of the reaction, the yellow sodium iodate precipitate was filtered off and the filtrate was extracted three times with $CHCl_3$. The organic layers were combined, washed with brine, dried over Na_2SO_4 and evaporated under reduced pressure. Compound **47** was obtained after purification by flash chromatography.

Eluent: Pentane/EtOAc (8:2 to 1:1). Yellow oil. Yield: 88%. ^{1}H NMR (600 MHz, chloroform-*d*): (ppm) δ 7.39 (d, *J* = 8.6 Hz, 1H), 7.29 (d, *J* = 8.6 Hz, 1H), 3.60 – 3.54 (d, *J* = 2.6 Hz, 2H), 2.27 – 2.21 (t, *J* = 2.5 Hz, 1H); ^{13}C NMR (151 MHz, chloroform-*d*): δ (ppm) 141.2, 138.0, 129.3, 125.9, 76.8, 72.3, 47.7; MS (EI, 70 eV): m/z (%) 57.4 (14), 75,3 (16), 85,3 (12), 111.2 (18), 131.2 (19), 149.2 (26), 159.2 (100), 161.2 (36), 169.2 (21); MS (CI, CH_4): 159.0 (93), 160.9 (40), 182.1 (22), 199.0 (100), 201.1 (34), 227.1 (22), 239; MS (ESI): m/z 222.97618 [M+Na][+]
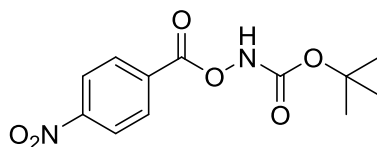
tert-Butyl ((4-Nitrobenzoyl)oxy)carbamate (**49**)

N-BOC-hydroxylamine (200 mg, 1.50 mmol) was dissolved in CH_2Cl_2 (6 mL) and 4-nitrobenzoyl chloride (306 mg, 1.65 mmol) and triethylamine (252 μL, 1.65 mmol) were added at 0 °C. The reaction was stirred for 2 h, then quenched with water (3 mL) and extracted three times with CH_2Cl_2. The organic layers were dried over Na_2SO_4 and the solvent was evaporated at reduced pressure. The residue was purified by flash chromatography on silica gel to give the desired compound.

White waxy solid. Eluent: Pentane/EtOAc (8:2). Yield: 82%. NMR and MS data are in agreement with those reported in the literature.
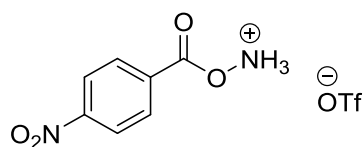
O-(4-Nitrobenzoyl)hydroxylammonium trifluoromethanesulfonate salt (**50**)

To a solution of compound **49** (352 mg, 1.25 mmol) in Et$_2$O (6 mL) at 0 °C, triflic acid (121 μL, 1.38 mmol) was added dropwise to precipitate the final product as the triflate salt. The reaction mixture was stirred for 4 h, then the precipitate was filtered and washed several times with Et$_2$O.

White solid. Yield: 58%. NMR and MS data are in agreement with those reported in the literature.
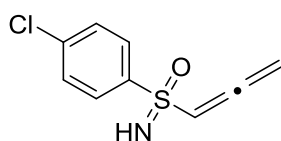
(4-Chlorophenyl)(imino)(propa-1,2-dien-1-yl)sulfanone (**53**)

To a solution of sulfoxide **47** (1.69 g, 8.54 mmol) in CHCl$_3$ (8.5 mL) was added sodium azide (610 mg, 9.39 mmol) and the mixture was cooled to −10 °C with acetone/dry ice bath. Sulfuric acid (42.7 mmol) was added dropwise, taking care to keep the temperature below −10 °C. After addition, the temperature was slowly brought to room temperature and the reaction mixture was stirred at room temperature for 96 h and then at 50 °C for another 8 h. After this time, distilled H$_2$O (6.5 mL) was added with cooling and the phases were separated. The water layer was cooled to 0 °C, made basic with 16 M NaOH, and extracted with CHCl$_3$. The organic layers were dried over Na$_2$SO$_4$ and evaporated under reduced pressure.

^{1}H NMR (600 MHz, chloroform-*d*): δ (ppm) 7.62 – 7.57 (m, 1H), 7.51 – 7.48 (m, 1H), 6.08 – 6.02 (m, 1H), 5.34 (dd, *J* = 13.3, 6.3 Hz, 1H), 5.32 – 5.26 (m, 1H). ^{13}C NMR (151 MHz, chloroform-*d*): δ (ppm) 207.7, 143.1, 141.2, 137.3, 129.5, 129.3, 129.3, 102.0, 82.5; MS (ESI): 214.00889 [M+H][+], 235.99083 [M+Na][+]
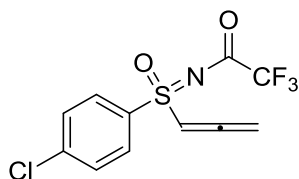
N-((4-Chlorophenyl)(oxo)(propa-1,2-dien-1-yl)sulfaneylidene)-2,2,2-trifluoroacetamide (**54**)

To a suspension of sulfoxide **47** (400 mg, 2.01 mmol), trifluoroacetamide (454 mg, 2.01 mmol), MgO (325 mg, 8.05 mmol), and $Rh_2(OAc)_4$ (22.2 mg, 0.05 mmol) in CH_2Cl_2 (15 mL) was added PIDA (971 mg, 3.01 mmol) and the reaction mixture was stirred at room temperature for 6 h. After completion of the reaction, the catalyst was filtered off over a Celite pad and the filtrate was evaporated under reduced pressure. Compound **54** was obtained after purification by flash chromatography.

Eluent: 1) Pentane/EtOAc (8:2); 2)Pentane/EtOAc (9:1). Yellow oil. Yield: 80%. ^{1}H NMR (600 MHz, chloroform-*d*): δ (ppm) 8.02 − 7.89 (d, *J* = 8.6 Hz, 2H), 7.60 (d, *J* = 8.6 Hz, 2H), 6.60 (m, 1H), 5.60 (dd, *J* = 9.6, 6.3 Hz, 2H); ^{13}C NMR (151 MHz, chloroform-*d*): δ (ppm) 209.6, 163.8, 142.4, 134.9, 129.3, 129.0, 117.1, 86.6, 48.1; MS (EI, 70 eV): m/z (%) 75.1 (49), 76.1 (10), 108.1 (13), 111.0 (69), 112.1 (10), 113.0 (22), 125.1 (55), 127.0 (38), 128.0 (42), 129.0 (10), 130.0 (14), 131.0 (28), 159.0 (100), 160.0 (10), 161.0 (35), 175.0 (32), 177 (11), 185.0 (26), 258.0 (61), 260.0 (23), 308.9 (57), 310.0 (63), 311.0 (28), 312 (23), 327 (33); MS (CI, CH_4): m/z (%) 215.0 (12), 309.9 (100), 311.0 (15), 311.9 (36), 327.9 (45), 329.9 (17); MS (ESI): 309.99306 [M+H]$^+$, 331.9797538 [M+Na]$^+$

General procedure for the synthesis of compound 55 and 56

To a solution of compound **54** (0.13 mmol) in MeOH or EtOH (2 mL) was added potassium carbonate (0.64 mmol) and the reaction mixture was stirred at room temperature for 30 minutes. Then the crude product was purified by flash chromatography on silica gel with a suitable eluent.

(4-Chlorophenyl)(imino)(2-methoxyallyl)sulfanone (**55**)

MeOH as solvent. Eluent: Pentane:EtOAc (1:1). Colourless oil. Yield: 76%. ^{1}H NMR (600 MHz, chloroform-d): δ (ppm) 7.93 – 7.86 (d, J = 3.7 Hz, 2H), 7.51 – 7.44 (d, J = 3.7 Hz, 2H), 4.19 (d, J = 2.8 Hz, 1H), 4.09 (d, J = 2.8 Hz, 1H), 3.93 – 3.81 (m, 2H), 3.41 (s, 3H), 2.97 (s, 1H); ^{13}C NMR (151 MHz, chloroform-d): δ (ppm) 154.1, 140.0, 138.6, 129.5, 129.2, 86.5, 60.0, 54.6; MS (ESI): 246.03459 [M+H]$^+$, 268.01653 [M+Na]$^+$
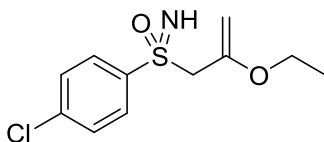
(4-Chlorophenyl)(2-ethoxyallyl)(imino)sulfanone (**56**)

EtOH as solvent. Eluent: Pentane:EtOAc (1:1). Colourless oil. Yield: 81%. ^{1}H NMR (400 MHz, chloroform-d): δ (ppm) 7.91 (d, J =13.3 Hz, 2H), 7.49 (d, J = 13.2 Hz, 2H), 4.17 (d, J = 2.7 Hz, 1H), 4.13 (d, J = 2.7 Hz, 1H), 3.89 (d, J = 6.1 Hz, 2H), 3.57 (m, 2H), 1.08 (t, J = 6.9 Hz, 3H); ^{13}C NMR (101 MHz, chloroform-d): δ (ppm) 151.9, 139.7, 130.4, 128.9, 89.5, 64.6, 63.5, 29.6, 13.9; MS (ESI): 260.05140 [M+H]$^+$
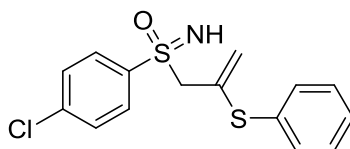
(4-Chlorophenyl)(imino)(2-(phenylthio)allyl)sulfanone (**57**)

A solution of allenylsulfoximine **54** (200 mg, 0.65 mmol) in EtOH (2 mL) was added dropwise to a solution of [PhS]Na prepared in situ by reduction of (PhS)$_2$ (70.96 mg, 0.33 mmol) with NaBH$_4$ (30

mg, 0.77 eq) in EtOH (2 mL) at room temperature under N_2. After completion of the reaction (5 min), the mixture was diluted with brine and extracted with EtOAc. The combined organic layers were dried (Na_2SO_4) and filtered. The solvent was removed in vacuo and the residue was purified by flash chromatography on silica gel.

Eluent: Pentane/EtOAc (4:1 to 1:1). Yellow oil. Yield: 66%. ^{1}H NMR (600 MHz, chloroform-*d*): δ (ppm) 7.94 (d, *J* = 8.6 Hz, 1H), 7.53 (d, *J* = 8.6 Hz, 1H), 7.39 − 7.32 (m, 3H), 7.30 (m, 2H), 5.39 (d, *J* = 7.6 Hz, 1H), 5.23 (d, *J* = 7.6 Hz, 1H), 3.99 (d, *J* = 4.7 Hz, 1H), 3.08 (s, 1H); ^{13}C NMR (151 MHz, chloroform-*d*): δ (ppm) 140.0, 138.9, 133.7, 133.3, 132.6, 131.4, 130.6, 129.5, 129.3, 129.1, 128.6, 127.5, 121.7, 64.2, 29.6; MS (ESI): 324.02773 [M+H][+], 246.00969 [M+Na][+]
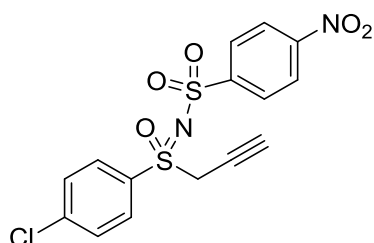
N-((4-Chlorophenyl)(oxo)(prop-2-yn-1-yl)sulfaneylidene)-4-nitrobenzenesulfonamide (**58**)

To a suspension of sulfoxide **47** (100 mg, 0.50 mmol), 4-nitrobenzenesulfonamide (202 mg, 1 mmol), MgO (80.6 mg, 2 mmol), and $Rh_2(OAc)_4$ (5.52 mg, 0.01 mmol) in CH_2Cl_2 (5 mL) was added PIDA (241 mg, 0.75 mmol), and the reaction mixture was stirred at room temperature for 6 h. After completion of the reaction, the catalyst was filtered off on a Celite pad and the filtrate was diluted with H_2O and extracted three times with CH_2Cl_2. The organic layers were combined, dried over Na_2SO_4 and evaporated. Compound **58** was obtained after flash chromatography on silica gel.

Eluent: Pentane/EtOAc (9:1). Yellow oil. Yield: 76%. ^{1}H NMR (400 MHz, chloroform-*d*): δ (ppm) 8.34 − 8.28 (m, 2H), 8.17 − 8.14 (m, 2H), 8.02 − 7.94 (m, 2H), 7.64 − 7.56 (m, 2H), 4.56 (q, *J* = 2.7 Hz, 2H), 2.50 (t, *J* = 2.7 Hz, 1H); ^{13}C NMR (101 MHz, chloroform-*d*): δ (ppm) 149.9, 148.4, 142.6, 137.4, 132.6, 130.3, 129.9, 128.8, 128.2, 127.8, 127.4, 124.3, 69.9, 60.4, 51.0; MS(ESI): m/z 421.96081 [M+Na][+]

BIBLIOGRAPHY

1.   https://www.cdc.gov

2.   Greber, U. F. & Way, M. A superhighway to virus infection. *Cell* **2006**, *124*, 741–754.

3.   Moelling, K. & Broecker, F. Viruses and evolution - Viruses first? A personal perspective. *Front. Microbiol*. **2019**, *10*, 1–13

4.   V'kovski, P., Kratzel, A., Steiner, S., Stalder, H. & Thiel, V. Coronavirus biology and replication: implications for SARS-CoV-2. *Nat. Rev. Microbiol*. **2021**, *19*, 155–170

5.   Römer, C. Viruses and Endogenous Retroviruses as Roots for Neuroinflammation and Neurodegenerative Diseases. *Front. Neuros*. **2021**, *15*, 1–17

6.   Langtry, H. D. & Campoli-Richards, D. Zidovudine: A Review of its Pharmacodynamic and Pharmacokinetic Properties, and Therapeutic Efficacy. *Drugs* **1993**, *45*, 232–258

7.   Zhao, R. Y. & Elder, R. T. Viral infections and cell cycle G2/M regulation. *Cell Res*. **2005**, *15*, 143–149

8.   Modrow, S., Falke, D. & Schätzl, T. Molecular Virology. **2013**

9.   Gelderblom., H. R. Medical Microbiology. 4th edition. **1996**

10. Rey, F. A. & Lok, S. Common Features of Enveloped Viruses and Implications for Immunogen Design for Next-Generation Vaccines. *Cell* **2018**, *172*, 1319–1334

11. Banerjee, N. & Mukhopadhyay, S. Viral glycoproteins : biological role and application in diagnosis. *Virus Disease* **2016**, *27*, 1–11

12. Dimitrov, D. S., Immunovirology, H. & Drive, M. Virus Entry: Molecular Mechanism and Biomedical Applications. *Nat Rev Microbiol*. **2004**, *2*, 109-122

13. Klasse, P. J., Bron, R. & Marsh, M. Mechanisms of enveloped virus entry into animal cells. *Adv Drug Deliv Rev*. **2020**, *34*, 65-91

14. Buchmann, J. P. & Holmes, E. C. Cell Walls and the Convergent Evolution of the Viral Envelope. *Microbiol Mol Biol Rev* **2015**, *79*, 403–418

15. Dick, G. W. A., Kitchen, S. F. & Haddow, A. J. Zika Virus.Isolation and Serological specificity. *Trans. R. Soc. Trop. Med. Hyg*. **1952**, *46*, 509-520

16. Atif, M., Azeem, M. & Rehan, M. Zika virus disease: a current review of the literature. *Infection* **2016**, *44*, 695–705

17. www.who.int.

18. Vodušek, V. F., Vizjak, A., Ph, D., Pižem, J. & Ph, D. Zika Virus Associated with Microcephaly. *N Engl J Med* **2016**, *374*, 951–958

19.   Raper, J. & Chahroudi, A. Clinical and Preclinical Evidence for Adverse Neurodevelopment after Postnatal Zika Virus Infection. *Trop Med Infect Dis* **2021**, *6*, 10

20.   Rojas, M. et al. Molecular mimicry and autoimmunity. *J. Autoimmun* **2018***, 95*, 100–123

21.   Song, H., Qi, J., Haywood, J., Shi, Y. & Gao, G. F. Zika virus NS1 structure reveals diversity of electrostatic surfaces among flaviviruses. *Mol. Biol*. **2016,** *23*, 3–6

22.   Epelboin, S. et al. Zika virus and reproduction: facts , questions and current management. *Hum Reprod Update* **2017***, 23*, 629–645

23.   Musso, D. & Gubler, D. J. Zika Virus. *Clin Microbiol Rev* **2016**, *29*, 487–524

24.   Oliver, M. E. & Hinks, T. S. C. Azithromycin in viral infections **2020**, 29, 1–13

25.   Devillers, J. Repurposing drugs for use against Zika virus infection. *SAR QSAR Environ. Res*. **2018**, *29*, 103–115

26.   Munjal, A., Khandia, R., Dhama, K., Sachan, S. Advances in Developing Therapies to Combat Zika Virus : Current Knowledge and Future Perspectives. *Frontiers in Microbiology*, **2017**, *8*.

27.   Gharbi-Ayachi et al. Non-Nucleoside Inhibitors of Zika virus RNA-dependent RNA polymerase. *J Virol.*, **2020**, *94* (21)

28.   Damiana Antônia de Fátima Nunes et al. NS2B-NS3 protease inhibitors as promising compounds in the development of antivirals against Zika virus: A systematic review. *J Med Virol.*, **2022**, *94*(2), 442-453

29.   Bernatchez, J. A. et al. Drugs for the Treatment of Zika Virus Infection. *J. Med. Chem*. **2020**, *63*, 470–489

30.   Boxiao, W., Thurmond, S., Hai, R. & Song, J. Structure and function of Zika virus NS5 protein: perspectives for drug design. *Cell Mol Life Sci* **2018**, *75*, 1723–1736

31.   Elshahawi, H., Hassan, S. S. & Balasubramaniam, V. Importance of Zika virus NS5 protein for viral replication. *Pathogens* **2019**, 8, 1–12

32.   Pathak, N., Kuo, Y., Ch, T., Huang, C. & Hung, H. Zika Virus NS3 Protease Pharmacophore Anchor Model and Drug Discovery. *Sci Rep.* **2020**, *10*, 8929

33.   Zhao, Z. et al. Nuclear localization of Zika virus NS5 contributes to suppression of type I interferon production and response. *J. Gen. Virol*. **2019**, *102*, 1376

34.   Ferron, F., Decroly, E., Selisko, B. & Canard, B. The viral RNA capping machinery as a target for antiviral drugs. *Antiviral Res* **2020**, *96*, 21-31

35.   Picard-jean, R. I. C. et al. The flavivirus NS5 protein is a true RNA guanylyltransferase that catalyzes a two-step reaction to form the RNA cap structure. *RNA* **2009**, 2340–2350

36.   Dong, H. et al. Rational Design of a Live Attenuated Dengue Vaccine : 2 9 -O-Methyltransferase Mutants Are Highly Attenuated and Immunogenic in Mice and Macaques. *Pathogens* **2013**, *9*, 470

37. Züst, R. et al. Ribose 2'-O-methylation provides a molecular signature for the distinction of self and non-self mRNA dependent on the RNA sensor Mda5. *Nat. Publ. Gr*. **2011**, *12*, 137–144

38. Song, W. et al. Identification and Characterization of Zika Virus NS5 Methyltransferase Inhibitors. *Front. Cell. Infect. Microbiol.* **2021**, *11*, 1–10

39. Coutard, B. et al. Zika Virus Methyltransferase : Structure and Functions for Drug Design Perspectives. *J. Virol*. **2017**, *91*, 1–15

40. Dong, H. et al. Structural and Functional Analyses of a Conserved Hydrophobic Pocket of Flavivirus Methyltransferase. *J Biol Chem* **2010**, *285*, 32586–32595

41. Park, J. et al. Potent Inhibition of Zika Virus Replication by Aurintricarboxylic Acid. *Front. Microbiol. 2019, 10*, 1–10

42. Milani, M. et al. Flaviviral methyltransferase / RNA interaction: Structural basis for enzyme inhibition. *Antiviral Res*. **2009**, *83*, 28–34

43. Benarroch, D. et al. A Structural Basis for the Inhibition of the NS5 Dengue Virus mRNA 2'-O-Methyltransferase Domain by Ribavirin 5-Triphosphate. *J. Biol. Chem*. **2004**, *279*, 35638–35643.

44. Podvinec, M. et al. Novel Inhibitors of Dengue Virus Methyltransferase : Discovery by in Vitro-Driven Virtual Screening on a Desktop Computer Grid. *J. Med. Chem*. **2010**, 1483–1495

45. Benmansour, F. et al. Discovery of novel dengue virus NS5 methyltransferase non-nucleoside inhibitors by fragment-based drug design. Eur. *J. Med. Chem*. **2017**, *125*, 865–880

46. Jain, R., Butler, K. V, Coloma, J., Jin, J. & Aggarwal, A. K. Development of a S-adenosylmethionine analog that intrudes the RNA-cap binding site of Zika methyltransferase. *Nat. Sci. Reports* **2017**, *7*, 1632

47. Hercik, K., Brynda, J., Nencka, R. & Boura, E. Structural basis of Zika virus methyltransferase inhibition by sinefungin. *Arch. Virol.,* **2017**, *162*, 2091–2096.

48. Hamill, R. L. & Hoehn, M. M. A9145, A new adenine-containing antifungal antibiotic. *J. Antibiot.* **1973**, *26*, 8–10

49. Zhang, J. & Zheng, Y. G. SAM / SAH Analogues as Versatile Tools for SAM-dependent Methyltransferases. *ACS Chem. Biol*. **2015**, *11*, 583–597

50. Hercik, K., Brynda, J., Nencka, R. & Boura, E. Structural basis of Zika virus methyltransferase inhibition by sinefungin. *Arch. Virol*. **2017**, *162*, 2091–2096

51. Munjal, A. et al. Advances in Developing Therapies to Combat Zika Virus : Current Knowledge and Future Perspectives*. Front. Microbiol*. **2017**, *8*, 1469

52. SV, L. & AW., T. Modern synthetic methods for copper-mediated C(aryl)[bond]O, C(aryl)[bond]N, and C(aryl)[bond]S bond formation. *Angew Chem Int Ed Engl* **2003**, *42*, 5400–5449

53. Yue, Y., Zheng, Z., Wu, B., Xia, C. & Yu, X. Copper-Catalyzed Cross-Coupling Reactions of Nucleobases with Arylboronic Acids : An Efficient Access to N -Arylnucleobases. *Synthesis* **2011**, *6*, 829-856

54. Jean Fotie. Inosine 5'-Monophosphate Dehydrogenase (IMPDH) as a Potential Target for the Development of a New Generation of Antiprotozoan Agents. *Mini Rev Med Chem* **2018**, 18, 656–671

55. Nair, V. & Shu, Q. Inosine monophosphate dehydrogenase as a probe in antiviral drug discovery. *Antivir. Chem. Chemother.* **2007**, *18*, 245–258

56. Braun-sand, S. B. Inosine monophosphate dehydrogenase as a target for antiviral , anticancer , antimicrobial and immunosuppressive therapeutics. *Futur. Med. Chem* **2010**, *2*, 81–92

57. Cuny, G. D., Suebsuwong, C. & Ray, S. S. Inosine-5 ' -monophosphate dehydrogenase (IMPDH) inhibitors : a patent and scientific literature review (2002-2016). *Expert Opin. Ther. Pat*. **2017,** *27*, 677-690

58. Clercq, E. De.Antiviral Agents: charateristic activity spectrum depending on the molecular target with which they interact. *Adv Virus Res*. **1993**, *42*, 1-55.

59. Nair, V. & Shu, Q. Inosine monophosphate dehydrogenase as a probe in antiviral drug discovery. *Antivir. Chem. Chemother* **2007**, 245–258

60. Cam, S. F., Papp, E., Wu, J. C. & Natsumedas, Y. Characterization of Human Type I and Type I1 IMP Dehydrogenases. *J. Biol. Chem*. **1993**, *268*, 27286–27290

61. W. Sidwelljohn, R. & Huffmann, H Loisb. Allenj, Loisb Rolndand, K. R. Broad-Spectrum Antiviral Activity of Virazole: 1-β-D-Ribofuranosyl-1,2,4-triazole-3-carboxamide. *Science* **1972**, *177*, 705–706

62. Ishikawa, H. Mizoribine and mycophenolate mofetil. *Curr Med Chem* **1999**, *6*, 575–597

63. Jain, J. et al. Characterization of Pharmacological Efficacy of VX-148 , a New, Potent Immunosuppressive Inosine 5-Monophosphate Dehydrogenase Inhibitor. *J. Pharmacol. Exp. Ther.* **2002**, *302*, 1272–1277

64. Dhar, T. G. M. et al. Discovery of N-[2-[2-[[3-Methoxy-4-(5-oxazolyl)phenyl]-amino]-5-oxazolyl] phenyl]-N-methyl-4-morpholineacetamide as a Novel and Potent Inhibitor of Inosine Monophosphate Dehydrogenase with Excellent in Vivo Activity. *J. Med. Chem* **2002**, *45*, 2127–2130

65. Culletta, G., Tutone, M., Zappalà, M. & Almerico, A. M. Sulfonamide moiety as 'molecular chimera' in the design of new drugs*. Curr Med Chem* **2022**

66. Hogan, P. J. & Cox, B. G. Aqueous Process Chemistry: The Preparation of Aryl Sulfonyl Chlorides. *Org. Process Res. Dev*. **2009***, 13*, 875–879

67. Mäder, P. & Kattner, L. Sulfoximines as Rising Stars in Modern Drug Discovery? Current Status and Perspective on an Emerging Functional Group in Medicinal Chemistry*. J. Med. Chem*. **2020**, *63*, 14243–14275

68.   Zhu, Y. et al. Discovery and Characterization of Sulfoxaflor , a Novel Insecticide Targeting Sap-Feeding Pests. *J Agric Food Chem* **2011**, *59*, 2950–2957

69.   Wengner, A. M. et al. BAY 1000394 , a Novel Cyclin-Dependent Kinase Inhibitor , with Potent Antitumor Activity in Mono- and in Combination Treatment upon Oral Application. *Mol Cancer Ther* **2012**, *11*, 2265–2274

70.   Bull, J., Degennaro, L. & Luisi, R. Straightforward Strategies for the Preparation of NH-Sulfoximines: a Serendipitous Story. *Synlett* **2017**, *28*, 2525–2538

71.   Han, Y. et al. Application of sulfoximines in medicinal chemistry from 2013 to 2020. *Eur. J. Med. Chem*. **2021**, *209*, 112885

72.   Foote, K. M. et al. Discovery and Characterization of AZD6738, a Potent Inhibitor of Ataxia Telangiectasia Mutated and Rad3 Related (ATR) Kinase with Application as an Anticancer Agent. *J. Med. Chem.* **2018**, *61*, 9889–9907

73.   Class, G. O. F. & Compounds, O. F. O. Glossary of class names of organic compounds and reactive intermediates based on structure. *Pure &Appl. Chem*. **1995**, *67*, 1307–1375

74.   Lücking, U. Sulfoximines : A Neglected Opportunity in Medicinal Chemistry. *Angew. Chemie* **2013,** 9399–9408

75.   Reggelin, M. & Zur, C. Sulfoximines : Structures , Properties and Synthetic Applications. *Synthesis* **1999**, *6*, 1-64

76.   Frings, M., Bolm, C., Blum, A. & Gnamm, C. Sulfoximines from a Medicinal Chemist's Perspective : Physicochemical and in vitro Parameters Relevant for Drug Discovery. *Eur. J. Med. Chem*. **2017**, *126*, 225–245

77.   Mock, W. L. & Tsay, J. Sulfoximine and Sulfodiimine Transition-State Analogue Inhibitors for Carboxypeptidase A. *J. Am. Chem. Soc*. **1989**, *111*, 149–154

78.   Han, Y. et al. Application of sulfoximines in medicinal chemistry from 2013 to 2020. Eur. *J. Med. Chem.* **2021**, *209*, 112885

79.   Zenzola, M., Doran, R., Luisi, R. & Bull, J. A. Synthesis of Sulfoximine Carbamates by Rhodium-Catalyzed Nitrene Transfer of Carbamates to Sulfoxides. *J. Org. Chem*. **2015**, *80*, 6391–6399

80.   Bizet, V., Hendriks, C. M. M. & Bolm, C. Sulfur imidations : access to sulfimides and sulfoximines. *Chem. Soc. Rev*. **2015**, *44,* 3378

81.   Tota Arianna, Bull James and Luisi, R. Synthesis of NH-sulfoximines from sulfides by chemoselective one-pot N- and O-transfers. *Chem Commun* **2016**, *53,* 348-351

82.   Sirvent, J. A. & Ulrich, L. Novel Pieces for the Emerging Picture of Sulfoximines in Drug Discovery : Synthesis and Evaluation of Sulfoximine Analogues of Marketed Drugs and Advanced Clinical Candidates. *ChemMedChem* **2017**, 487–501

83.   Brosge, F., Lorenz, T., Helten, H. & Bolm, C. BN- and BO-Doped Inorganic–Organic Hybrid Polymers with Sulfoximine Core Units. *Chem. - A Eur. J.* **2019**, *25*, 12708–12711

84.   Prasanjit, G., Bhaskar, G. & Sajal, D. N-H and C-H Functionalization of Sulfoximine: Recent Advancement and Prospects. *Asian J. Org. Chem*. **2020**, *9*, 2035–2082

85.   Dawson, M. A. et al. Inhibition of BET recruitment to chromatin as an effective treatment for MLL-fusion leukaemia. *Nature* **2011**, *478*, 529–533

86.   Altenburg, B. et al. Chiral Analogues of PFI-1 as BET Inhibitors and Their Functional Role in Myeloid Malignancies. *ACS Med. Chem. Lett* **2020***, 11*, 1928–1934

87.   Doroshow, D. B., Eder, J. P. & Lorusso, P. M. BET inhibitors : a novel epigenetic approach. *Ann. Oncol*. **2017**, *28*, 1776–1787

88.   Park, S. J. et al. N -Cyano Sulfoximines : COX Inhibition , Anticancer Activity , Cellular Toxicity , and Mutagenicity. *ChemMedChem* **2013**, *6*, 217–220

89.   Watson, G. B., Siebert, M. W., Wang, N. X., Loso, M. R. & Sparks, T. C. Sulfoxaflor – A sulfoximine insecticide : Review and analysis of mode of action , resistance and cross-resistance. *Pestic. Biochem. Physiol.* **2021**, *178,* 104924

90.   Bacci, L., Convertini, S. & Rossaro, B. A review of sulfoxaflor, a derivative of biological acting substances as a class of insecticides with a broad range of action against many insect pests. *J. Entomol. Acarol. Res* **2018**, *50*, 51-71

91.   Sparks, T. C. et al. Sulfoxaflor and the sulfoximine insecticides: Chemistry, mode of action and basis for efficacy on resistant insects. *Pestic. Biochem. Physiol*. **2013**, *107*, 1–7

92.   Frings, M., Bolm, C., Blum, A. & Gnamm, C. Sulfoximines from a Medicinal Chemist's Perspective: Physicochemical and in vitro Parameters Relevant for Drug Discovery. *Eur. J. Med. Chem*. **2017**, *126,* 225–245

93.   Pennington, L. D. et al. Discovery and Structure-Guided Optimization of Diarylmethanesulfonamide Disrupters of Glucokinase-Glucokinase Regulatory Protein (GK-GKRP) Binding: Strategic Use of a N → S (nN → σ∗ S-X) Interaction for Conformational Constraint. *J. Med. Chem*. **2015**, *58*, 9663–9679

94.   Foote, K. M. et al. Discovery and Characterization of AZD6738, a Potent Inhibitor of Ataxia Telangiectasia Mutated and Rad3 Related (ATR) Kinase with Application as an Anticancer Agent. *J. Med. Chem*. **2018**, **61**, 9889–9907

95.   Abdelaziz, A. M., Yu, M. & Wang, S. Mnk inhibitors: a patent review. *Pharm. Pat. Anal*. **2021**, *10*, 25-35

96.   Kreideweiss, S., Schuler-Metz, A. & Christian Gnamm, Stefan Peters, T. O. In vitro and in vivo characterisation of the novel neutrophil elastase inhibitor BI 1323495. *Eur. Respir. J.* **2020**, *56*, 3303

97.   Huang, X. & Ma, S. Allenation of Terminal Alkynes with Aldehydes and Ketones. *Acc. Chem. Res*. **2019**, *52*, 1301–1312

98.   H. F. Schuster & Coppola, G. M. Allenes in Organic Synthesis. **1984**.

99.   Liu, L., Ward, R. M. & Schomaker, J. M. Mechanistic Aspects and Synthetic Applications of Radical Additions to Allenes. *Chem. Rev***. 2019**, *119*, 12422–12490

100. Ban, H. S., Onagi, S., Uno, M., Nabeyama, W. & Nakamura, H. Allene as an alternative functional group for drug design: Effect of C-C multiple bonds conjugated with quinazolines on the inhibition of EGFR tyrosine kinase. *ChemMedChem* **2008**, *3*, 1094–1103

101. Jones, R. L. Molecular biology of prostanoid receptors; an overview. *J. Lip. Med. and Cell Sign.* **2007**, *21*, 13–34

102. Diviccaro, S., Cioffi, L., Falvo, E., Giatti, S. & Melcangi, R. C. Allopregnanolone: An overview on its synthesis and effects. *J. Neuroendocrinol*. **2021**, *34*, 1–17

103. Brummond, K. M. Allene chemistry. *Beilstein J. Org. Chem*. **2011**, 394–395

104. Schreiber, S. L. & Schreiber, S. L. Target-Oriented and Diversity-Oriented Organic Synthesis in Drug Discovery. *Science* **2000,** *287*, 1964-1969.

105. Brummond, K. M. & Deforrest, J. E. Synthesis. **2007**

106. Krause, N. & Hashmi, A. S. K. Modern Allene Chemistry. **2004**

107. Wei, L. et al. Efficient preparations of novel ynamides and allenamides. *Tetrahedron* **2001**, *57,* 459–466

108. Nocentini, A., Carta, F., Ceruso, M., Bartolucci, G. & Supuran, C. T. Click-tailed coumarins with potent and selective inhibitory action against the tumor-associated carbonic anhydrases IX and XII. *Bioorg. Med. Chem.* **2015**, *23*, 6955–6966

109. Cho, G. Y. & Bolm, C. Silver-Catalyzed Imination of Sulfoxides and Sulfides. *Org Lett.* **2005**, 7, 4983-4985

AKNOWLEDGEMENT